# A NUCLEAR MAGNETIC RESONANCE STUDY OF TELLURIUM DOPED GALLIUM PHOSPHIDE

A. Rogerson

A Thesis Submitted for the Degree of PhD
at the
University of St Andrews

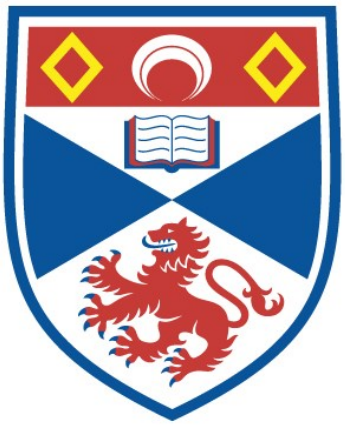

1975

# A NUCLEAR MAGNETIC RESONANCE STUDY OF TELLURIUM DOPED GALLIUM PHOSPHIDE

A thesis

presented by

A. Rogerson B.Sc.

to the

University of St. Andrews

in application for the Degree

of Doctor of Philosophy

Th 8697

## ACKNOWLEDGEMENTS

The author wishes to express his sincere thanks to Dr. D.P. Tunstall for his patient guidance and encouragement throughout this research and for his many stimulating discussions which greatly enhanced the author's understanding, and to the technical and academic staff of the Physics Department of the University of St. Andrews for providing the excellent supporting facilities and funds. He is also indebted to his fellow research workers at St. Andrews for their friendship and good humour, and to Linda McLean for typing this thesis.

ABSTRACT

A study has been made of 7, LEC grown, tellurium doped gallium phosphide samples using pulsed nmr, Hall effect, and related measurements. The results have been correlated with nmr, esr, electron susceptibility, and transport measurements in similar systems, and changes which occur in the donor electron system in the intermediate doping region preceding the metallic transition have been discussed. The effects which these changes have on the nuclear relaxation times of the host nuclei have been discussed in terms of the various stages of nuclear relaxation by spin diffusion to paramagnetic impurities.

In the lightly doped samples, rapid diffusion and diffusion limited relaxation processes have been identified around the minima in the $T_1$:T curves of the $P^{31}$, and two Ga isotopes respectively. The effects on nuclear relaxation of the preferential distribution of the Te donor wavefunction on $P^{31}$ sites have been discussed. Experimental calculations of the $Ga^{69}$ and $Ga^{71}$ spin diffusion coefficients have been made and compared with values derived from spin diffusion theory. $T_1$ results from the more heavily doped samples have been discussed in terms of the various models of the state of the electron system in the intermediate doping region. Evidence of the increasing importance of electron spin-spin interactions and diffusion vanishing relaxation processes have been obtained from the concentration, magnetic field, and temperature dependences of the $T_1$'s of all three isotopes at low temperatures.

Hall and conductivity measurements reflected the reduction in donor ionisation energy with increasing donor concentration in the intermediate doping region, and the observed movement of the position of the $T_1$ minima to lower temperatures in the same samples have been taken as further evidence of this effect. Calculations of the donor ionisation energy have been made from analysis of the temperature dependence of the $Ga^{69}$ and $Ga^{71}$ $T_1$'s around the $T_1$ minima and from the variation of the position of the minimum with frequency. The weakening and eventual disappearance of the $T_1$ minima in the most heavily doped samples have been discussed in terms of the reduction in the effectiveness of nuclear relaxation to single paramagnetic impurities as impurity hopping and spin-spin effects increase. The enhanced magnetic field dependence and increase in $T_1$ observed in the most heavily doped samples at low temperatures have been taken as evidence for the incomplete delocalisation of the donor electron system in these samples.

## CAREER

I first matriculated in the University of St. Andrews in October 1967. I studied Mathematics, Applied Mathematics, and Physics and, in July 1971, graduated with upper second class Honours in Physics. In October 1971, following the award of an S.R.C. Research Studentship, I was enrolled as a research student reading for the degree of Ph.D. under the Resolution of the University Court, 1967, No. 1.

## DECLARATION

I hereby certify that this thesis has been composed by me, and is a record of work done by me, and has not previously been presented for a Higher Degree.

This research was carried out in the Physical Sciences Laboratory of St. Salvator's College, in the University of St. Andrews, under the supervision of Dr. D.P. Tunstall.

## CERTIFICATE

I certify that Allan Rogerson, B.Sc., has spent nine terms at research work in the laboratories of the School of Physical Sciences, University of St. Andrews, under my direction, that he has fulfilled the conditions of the Resolution of the University Court, 1967, No. 1 and that he is qualified to submit the accompanying thesis in application for the Degree of Doctor of Philosophy.

Research Supervisor

CONTENTS

# CHAPTER I

## INTRODUCTION

Much scientific and technological progress has been made through the study of the properties of doped semiconductors, and tellurium doped gallium phosphide is one such system which has received a great deal of attention recently because of its potential as substrate material in light emitting diodes. Of the many different experimental techniques employed in these studies, nuclear magnetic resonance[39] (n.m.r), electron spin resonance[22] (e.s.r), Hall[62], and electrical conductivity measurements have been made extensively to reveal information concerning the electronic nature of the dopant impurities, and their interactions with other impurities, free electrons, nuclei of the host lattice, and phonons.

It has long been known that nuclear relaxation in diamagnetic crystals can be greatly enhanced by the presence of small quantities of paramagnetic impurities[45]. The coupling which exists between the impurity and a nearby nucleus through the dipolar Hamiltonian linking their magnetic moments permits energy transfer between them, induced by the fluctuating magnetic field of the paramagnetic impurity at the nuclear site. The rapid impurity electron relaxation which is the cause of these magnetic fluctuations, also results in transfer of energy to the lattice, and hence results in the impurities acting as sinks for nuclear spin energy. In an initially saturated nuclear spin system, magnetization gradients are soon built up around the impurities due to this relaxation mechanism, and the relaxation rate of the bulk nuclei is increased by the diffusion of nuclear spin energy to these impurities.

Since the early development of the theory of nuclear relaxation by spin diffusion to paramagnetic impurities by Bloembergen[44], many theoretical and experimental studies have been made on the phenomenon. Agreement between theory and experiment is generally good for low impurity concentrations, where one can consider a nucleus interacting with its single nearest impurity only. Under such conditions, one can

distinguish between 'rapid diffusion' and 'diffusion-limited' relaxation processes[47] and also calculate values of the nuclear spin diffusion coefficient of the bulk nuclei.

At higher impurity concentrations, where a nucleus may interact strongly with several paramagnetic impurities[52] and impurity electron spin-spin interactions appreciably affect the electron relaxation rate, the agreement between theory and experiment is less satisfactory. Semiconductors doped with known quantities of paramagnetic donor impurities provide possible systems in which to study these various relaxation regimes further and GaP:Te has certain particular advantages for such a study.

Much current interest has also been directed towards understanding the nature of the metal-nonmetal transition[8] which occurs in doped semiconductors as the doping density is increased beyond some critical concentration. At low concentrations, one can consider each donor as being isolated from the rest and having an energy level structure affected only by its interactions with its immediate surroundings. As the concentration increases and interactions with ionized impurities and other donors increase, the electron energy levels broaden and a gradual reduction in the donor ionization energy takes place. In compensated material, electron hopping between unionized and ionized donor sites occurs, resulting in an increased electrical conductivity and reduction in the effective number of paramagnetic impurities. With further increases in donor concentration, spin-spin interactions, rapid electron hopping, and coulombic shielding effects result in total delocalization of the donor electron system. The semiconductor then displays metallic characteristics at all temperatures.

N.m.r. has proved particularly useful in studying this phenomenon[8], mainly as the nuclear spin-lattice relaxation time is very sensitive to the changing nature of the electron system in the intermediate doping regime preceding the metallic transition. The availability of gallium

phosphide samples with tellurium donor concentrations up to $2.10^{19}$/c.c. prompted an attempt to study this intermediate doping regime and also associated nuclear spin diffusion processes. Gallium phosphide is particularly suited to study by pulsed n.m.r., as all three isotopes ($Ga^{69}$, $Ga^{71}$, and $P^{31}$) are magnetic and abundant, with the two gallium isotopes having differing electric quadrupole moments.

This thesis, therefore, contains a report of an n.m.r. study of seven tellurium doped gallium phosphide samples in which nuclear spin-lattice relaxation times of the $Ga^{69}$, $Ga^{71}$, and $P^{31}$ nuclei were measured at various temperatures and magnetic fields. These results, together with Hall and conductivity measurements and chemical analyses on the same samples, are compared with relevant data from other sources. The discussion is in terms of the current theories of nuclear relaxation in the presence of paramagnetic impurities and the approach to the metallic transition in doped semiconductors.

# CHAPTER II

# PHYSICS OF DOPED SEMICONDUCTORS

## 2.1 Introduction

The most widely used and extensively studied semiconductors to date are the elemental semiconductors, silicon and germanium. Much of our present understanding of the nature of impurity states and the effects of impurities on the electronic and magnetic properties of semiconductors has come from theoretical and experimental studies of these elements doped with various known impurities. Therefore, in outlining some of the important properties of doped semiconductors in this chapter, frequent reference will be made to recent results on Si and Ge, and similar work on doped gallium phosphide.

## 2.2 Basic Theory

The elements Si and Ge are from group IV in the periodic table and hence have four valence electrons, each of which forms part of a covalent bond with a neighbouring atom to make up the diamond lattice structure characteristic of both semiconductors. Foreign atoms of group V and III, when incorporated substitutionally in this lattice, are left with an excess or deficit of one valence electron respectively. The extra electron is bound to the impurity in a hydrogen-like state lying just below the conduction band and is called a 'donor state'. Similarly, for the group III impurity, a bound hole state is formed just above the valence band and is called an 'acceptor state'.

The donor state wavefunction, $\psi(\underline{r})$, satisfies a Schrödinger equation of the form,

$$\left(-\frac{\hbar^2}{2m}\nabla^2 + V(\underline{r}) + U(\underline{r})\right)\psi(\underline{r}) = E\,\psi(\underline{r}) \qquad 2.2.1$$

where $V(\underline{r})$ is the periodic potential of an electron in a perfect Si or Ge lattice, and $U(\underline{r})$ is the additional potential due to the replacement of a host atom by a donor ion. If we choose the donor

nucleus as coordinate origin, then

$$U(\underline{r}) = -\frac{e^2}{kr} \qquad 2.2.2$$

for large r, where k is the dielectric constant of the host material. We can write equation 2.2.1 in the form

$$(-\frac{\hbar^2}{2m^*}\nabla^2 + U(r))\psi(r) = E\,\psi(r) \qquad 2.2.3$$

where $m^*$ is the effective mass of the electron.

If there are several conduction band minima with which the donor may be associated, then Kohn and Luttinger[1] have shown that, except in the immediate vicinity of the donor atom, the wavefunction of the donor electron has the form

$$\psi(\underline{r}) = \sum_i \alpha_i F_i(\underline{r})\psi_i(\underline{k}_i,\underline{r}) \qquad 2.2.4$$

where $F_i(\underline{r})$ are hydrogen-like envelope functions satisfying the effective mass equations i.e. for the ground state,

$$F(r) = (\frac{1}{\pi a^{*3}})^{\frac{1}{2}} \exp(-r/a^*) \; . \qquad 2.2.5$$

$\psi_i(\underline{k}_i,\underline{r})$ are Bloch functions associated with the conduction band minima, $k_i$, and $\alpha_i$ are coefficients in the summation over the various minima. In the case of a semiconductor doped with a single donor impurity, at infinite dilution, the ionization energy, $E_D$, and "effective Bohr radius", $a^*$, of the bound electron are given by the expressions,

$$E_D = -\frac{e^4 m^*}{2\hbar^2 k^2} \qquad 2.2.6$$

and

$$a^* = \frac{k\hbar^2}{e^2 m^*} \qquad 2.2.7$$

respectively.

In the immediate vicinity of a donor the concepts of a dielectric constant and simple coulombic potential $-e^2/kr$ are no longer valid and

the effective mass approximation breaks down. Then the value of $E_D$ calculated from 2.2.6 can differ appreciably from the experimental value, the discrepancy being greatest for deep lying donors since most of their wavefunction is concentrated close to the impurity.

By modifying the expression for the electron wavefunction to take into account the regions close to the impurity, Kohn and Luttinger[1] were able to reduce this discrepancy for shallow donors such as P and Li in Si. This was done by dividing the wavefunction into two parts, an outer region where the effective mass approximation was still valid, and an inner region for which a new wavefunction had to be calculated.

## 2.3 Effects of Heavy Doping

As the impurity concentration is increased, overlap of the donor wavefunctions and their random distribution throughout the lattice produce broadening of the impurity level. Random coulombic fields due to ionized impurity centres also increase the bandwidth[3] of the impurity level and the net effect is a reduction and broadening of the donor ionization energy. Above a certain donor concentration a Mott transition[7,8] occurs and electrons move freely in an impurity band separated from the conduction band.

Several methods have been employed to calculate the critical donor density, $n_c$, at which the transition occurs, and much experimental and theoretical work has been performed to study the transition in a variety of systems. Perhaps the simplest model for describing the transition is that involving the Hubbard[2] approximation in which long range interactions and the random distribution of donors are neglected. When they are taken into account, the Hubbard model can be modified slightly to incorporate them. In a regular crystalline array, the effect of long range interactions leads to an abrupt transition whereas, for the random distribution of donors considered here, it does not.

In the Hubbard approximation, the energy W of a pair of electrons on the same donor is defined by

$$W = \iint \left(\frac{e^2}{kr_{12}}\right) |\psi(\underline{r}_1)|^2 \, |\psi(r_2)|^2 \, dx_1^2 \, dx_2^2 \, .$$

In the low concentration limit, this is the energy required to take an electron from one donor and place it on a distant one. If there is some overlap of donor wavefunctions, the overlap energy integral between adjacent donors i and j, a distance R apart, is given by

$$I = \int \psi_i^* \, H \, \psi_j \, dx^3$$

where H is the Hamiltonian. This leads to broadening of the impurity level resulting in a band of width B, where

$$B = 2zI$$

and z is the number of nearest neighbours of each donor. We can consider the system of singly occupied donors as belonging to one band, the lower Hubbard band, and system of doubly occupied donors as belonging to a higher band, the upper Hubbard band. The bandwidth of each, $B_1$ and $B_2$, increases with increasing donor concentration. When the two bands merge

$$W = \tfrac{1}{2}(B_1 + B_2) \, ,$$

and no activation energy is required to transfer an electron from a singly to doubly occupied donor. A metallic transition then occurs.

## 2.4 Conduction Mechanisms

In the 'low concentration' region, where the Hubbard bands are narrow and far apart, conduction in uncompensated material is dominated by electron excitation from the donor level into the conduction band [Fig. 2.4.1]. In the literature, the activation energy for conduction by this mechanism is referred to as $\varepsilon_1$, which is equivalent to $E_D$, the ionization energy of the donor. If there is some compensation present

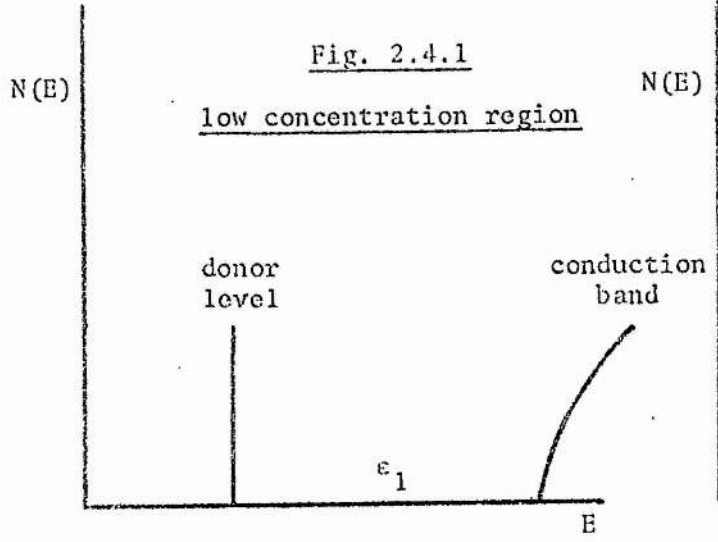


Fig. 2.4.1

low concentration region

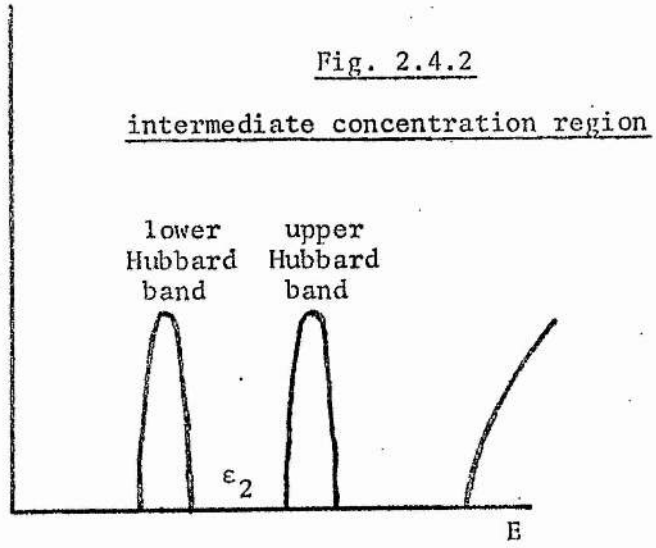


Fig. 2.4.2

intermediate concentration region

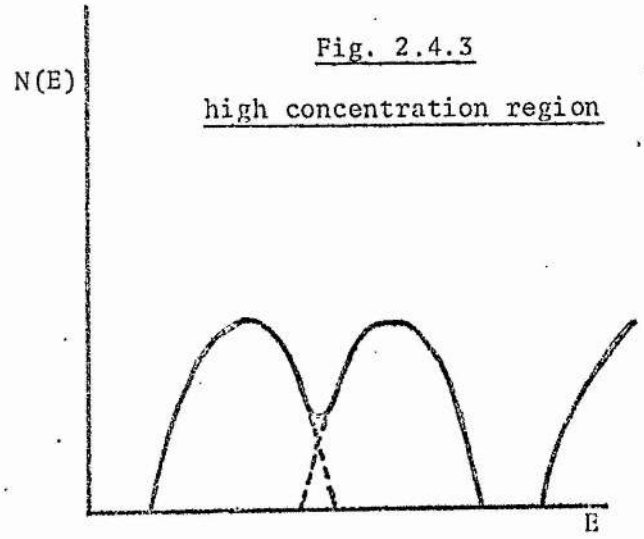


Fig. 2.4.3

high concentration region

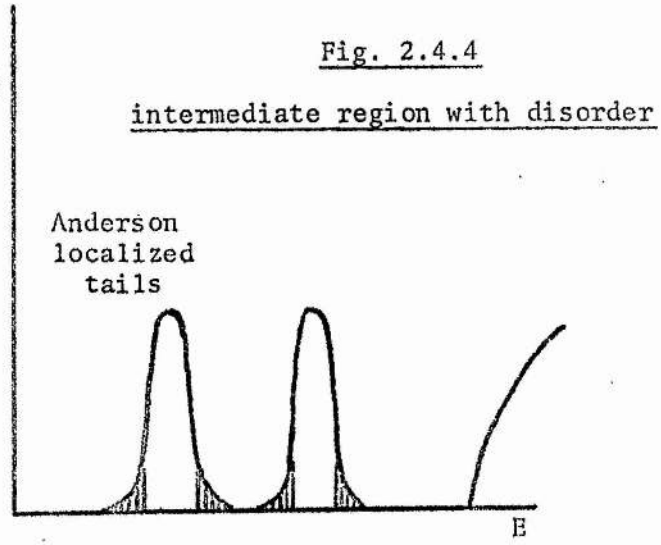


Fig. 2.4.4

intermediate region with disorder

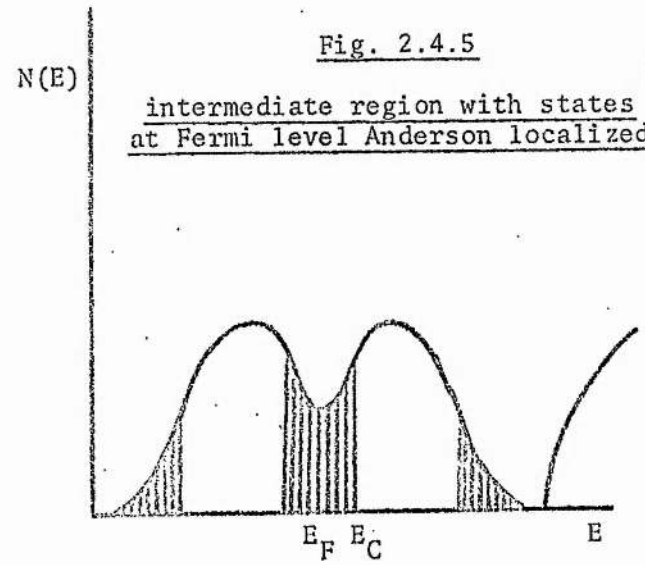


Fig. 2.4.5

intermediate region with states
at Fermi level Anderson localized

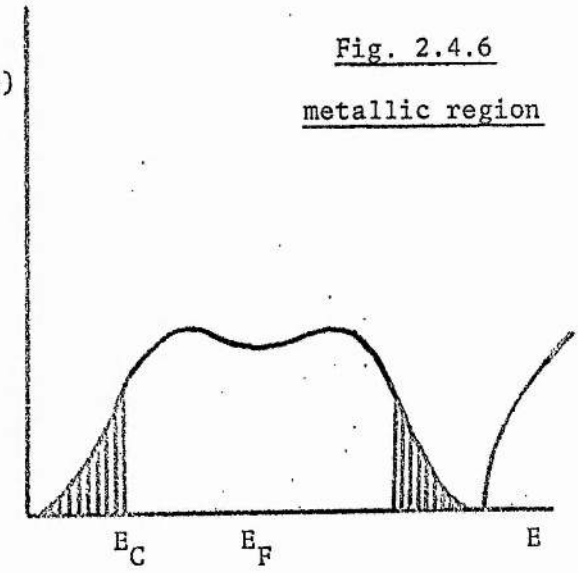


Fig. 2.4.6

metallic region

then, at low temperatures, conduction due to electrons hopping from occupied to unoccupied donor sites with activation energy $\varepsilon_3$ dominates.

We define the 'intermediate concentration' region to be that where the Hubbard bands are broad but do not yet overlap and conduction can occur via electron thermal excitation from the lower to the upper Hubbard band [Fig. 2.4.2]. This corresponds to the excitation of an electron from the ground state of a neutral donor to a bound state of neighbouring neutral donors and can be described by an activation energy $\varepsilon_2$. All three activation energies $\varepsilon_1$, $\varepsilon_2$ and $\varepsilon_3$ have been observed in n-type Ge by Davis and Compton[4], and Allen and Adkins[5]. Identical hole conduction mechanisms have been identified in p-type GaP by Casey et al[6] from Hall and resistivity measurements.

The 'high concentration' region corresponds to those doping densities above which the donor electrons are completely delocalized and move freely in the impurity band at all temperatures [Fig. 2.4.3]. Mott[7] was the first to predict such a transition in an electronic system and various methods used to calculate the critical concentration, $n_c$, have produced values differing only slightly from his original result. The critical concentration $n_c$ is given by

$$n_c^{\frac{1}{3}} a_o \sim 0.25 \qquad 2.4.1$$

where $a_o$ is the impurity Bohr radius. Experimental evidence in a number of systems confirms this to be generally satisfied.

## 2.5 Randomness - Anderson Localization

The Hubbard model does not take into account the effects of the random distribution of donors, compensation, and the presence of the random potentials produced by ionized centres. This randomness causes states in the tails of the Hubbard bands to be localized which result in the transition to metallic conductivity not being abrupt [Fig. 2.4.4]. Because of this localization, it is possible that, even when the two Hubbard bands overlap, the Fermi level $E_F$ may still

be in the localized states below a 'mobility edge' $E_C$, which separates localized and non-localized states [Fig. 2.4.5]. There is still an activation energy to conduction given by $\varepsilon_2 = E_C - E_F$ which goes continuously to zero as the donor concentration is increased [Fig. 2.4.6]. The localized electrons are not bound to single donor centres, but rather, confined by scattering and the random fields to a finite region, away from which their wavefunctions decrease exponentially to zero. The theory of such localization was developed by Anderson[9] and is known as Anderson localization.

## 2.6 Transport Measurements

We have already mentioned in section 2.4 the work of several authors on n-type Ge and p-type GaP. From measurements of the variation of the Hall coefficient $R_H$, the electrical conductivity $\sigma$, and the Hall mobility $\mu_H$ with temperature and impurity concentration they were able to estimate the three activation energies for conduction $\varepsilon_1$, $\varepsilon_2$ and $\varepsilon_3$. Also, they were able to observe the effects of differing amounts of compensation on the dominant conduction mechanisms. Briefly, the temperature dependence of the conductivity may be represented by

$$\sigma = \sum_{i=1}^{3} \left( C_i \, e^{\frac{-E_i}{kT}} \right) \qquad 2.6.1$$

where $C_i$ are constants. Graphs of $\ell n\, \sigma$ against $1/T$ consist of a series of linear regions from whose gradients the dominant activation energies can be calculated. Plots of $R_H$ against $1/T$ are characterized by a series of peaks at temperatures around which a change from one conduction mechanism to another takes place. The temperature dependence of $\mu_H$ gives information relating to the dominant electron scattering mechanisms.

2.7 Electron Spin Resonance Si:P

Paramagnetic resonance of the impurity electron system has proved to be extremely effective in revealing details of the electron environment and relaxation mechanisms. The latter have been of particular interest because of their connection with nuclear polarization schemes in solids. Several authors[10-13] have studied the variation of the e.s.r. linewidth in the regions of low, intermediate, and high doping in Si:P.

At low doping densities ($7.10^{15}$/cc) the e.s.r. spectrum consists of two lines corresponding to the 2I+1 lines resulting from the hyperfine interaction between the donor electron and donor nucleus of spin $I=\frac{1}{2}$. At higher doping levels ($7.10^{16}$/cc) additional lines appear between the two hyperfine lines and have been explained by Slichter[14] in terms of exchange interactions between pairs and small clusters of donors. These lines are superimposed upon a broad line resulting from donor clusters of several atoms and from pairs whose strength of exchange interaction is smaller than, or comparable with, that of the hyperfine interaction with the donor nuclei. Further doping into the 'intermediate' region results in the two hyperfine lines disappearing and the broad line increasing in intensity at the expense of the other exchange lines. Exchange effects and electron hopping produce a narrowing of the line which has a minimum value at approximately $3.10^{18}$/cc, the concentration corresponding to the metallic transition. Above that concentration the linewidth increases again due to lifetime broadening.

Measurements of the relaxation times, $\tau$, of donors in Si:P have been made at low temperatures and at differing concentrations by several authors[15-23]. Pines et al[24] considered a number of possible relaxation mechanisms in Si:P but Feher[22] could only explain two of his experimental results in terms of their theories. He observed at least two distinct concentration dependent relaxation regions at

densities between $10^{15}$/cc and $10^{18}$/cc. The first region, below $10^{16}$ donors/cc, displayed a concentration independent relaxation time and, from its variation with temperature, evidence of three possible mechanisms, each being effective in relatively narrow temperature ranges.

Between 1.25°K and 2.0°K he observed a $\tau \propto T^{-1}$ dependence characteristic of a direct phonon process whilst, between 3°K and 4.2°K, he found $\tau \propto T^{-7}$ indicative of Raman, two phonon relaxation. Above 4.2°K, the temperature dependence of $\tau$ became greater than $T^{-7}$ and evidence of $\tau \propto e^{\Delta/K_b T}$, characteristic of an Orbach[25] or spin exchange process, was obtained. The value of $\Delta$, the energy gap between the electron Zeeman levels and a third excited state, was found to be approximately equal to that of the first excited state of the donor.

Above $10^{16}$/cc $\tau$ became extremely concentration dependent, decreasing from $10^{3}$ seconds at $2.10^{16}$/cc to $10^{-4}$ seconds at $2.10^{17}$/cc. Feher[22] observed the direct phonon relaxation region at low temperatures and noted that the absolute magnitude of $\tau$, at any particular temperature, decreased in more compensated samples. This suggested that an electron hopping mechanism could be responsible for the relaxation. A possible model for this type of relaxation is that in which electrons hop from donor to donor towards clusters of donors which are relaxing to the lattice via some effective mechanism. Increased compensation would increase the hopping process and hence reduce the observed relaxation time. A spin exchange mechanism with the conduction electrons could provide an effective relaxation mechanism, if, as suggested by Anderson[22], this involved a double spin exchange. That is a conduction electron exchanges spin with a bound electron and then repeats the procedure with a second bound electron thus returning to its original state.

Honig[21] suggested a

similar process involving an interchange of bound electrons via extrinsic photoionization into the conduction band. However Castner[23] later observed a resonant Raman relaxation mechanism of the Orbach type in the region 4.2°K to 30°K in Si:P in which the 1s(2) or the 1s(3) states acted as the higher excited states in the process. Finally Roth[19] and Hazegawa[20] independently explained the unusually short electron relaxation times in the direct relaxation region between 1.25°K and 2.0°K in terms of relaxation through time-dependent modulation of the 1s(1) g-factor by the strain associated with a phonon.

## 2.8 E.S.R. in III-V Compounds

Electron spin resonance in the III-V compounds doped with group VI impurities differs from that in the elemental semiconductors in a number of ways. Because practically all the isotopes of the host nuclei, except $P^{31}$, have large magnetic and quadrupole moments, the hyperfine interaction between these nuclei and the donor electrons produce many lines which remain unresolved. The e.s.r. spectrum then consists of a single, inhomogeneously broadened line of between 30 and 150 gauss linewidth.

Title[26] measured the linewidths and g-values of S, Se, and Te donors in GaP at 77°K and observed lines 50 gauss wide for concentrations around $10^{17}$/cc, increasing to 120 gauss at $10^{18}$/cc. The lines were homogeneously broadened however, and this was explained in terms of motional effects caused by electrons hopping between donor sites. He interpreted the measured g-values in terms of the effective mass theory of Kohn and Luttinger. Haroldson and Ribbing[27] obtained similar results for GaP and GaAs doped with group IV and group VI impurities at 4.2°K, again finding homogeneously broadened lines. They suggested that another possible reason for this homogeneity was the high local strains present in all III-V compounds.

Finally Thomson and Lancaster[28] have reported e.s.r. linewidth measurements on GaP:S, GaP:Te, and GaP:Si over the temperature range 4.2°K to 100°K in samples of doping densities between $4.10^{17}$/cc and $10^{19}$/cc. They observed a single line of isotropic g-value. In all samples, the linewidth was independent of temperature below some critical temperature which decreased with increasing impurity concentration. Above this critical temperature the linewidth increased exponentially and they tentatively interpreted this additional width as due to lifetime broadening caused by an electron relaxation mechanism of exponential temperature dependence. An Orbach process, in which the third excited state lay at the conduction band minimum, was suggested as the possible mechanism. The decrease in the ionization energy of the donor level with increasing donor impurity concentration would then explain the concentration dependence of the critical temperature mentioned above. Again the constancy of the linewidth at low temperatures was interpreted as due to unresolved hyperfine interaction with host nuclei.

## 2.9 Incorporation of Impurities in Gallium Phosphide

Gallium phosphide is a III-V, indirect band gap, semiconductor consisting of two interpenetrating, face-centred cubic, Ga and P, sublattices which make up the zinc-blende lattice structure common to most III-V semiconductor compounds. The lattice constant, a, is 5.45Å and the two sublattices are parallel, being displaced from one another by a vector $\underline{r} = (a/4, a/4, a/4)$. The conduction band minima lie along the < 100 > directions at, or very near, the X points where the band gap is 2.24 eV.

Elements of group II form acceptors by substituting in the Ga sublattice while elements of group VI produce donors when substituted in the P sublattice. Foreign atoms from group IV may enter as either donors or acceptors by being incorporated in the appropriate sublattice. Usually, however, group IV elements go preferentially onto one sublattice.

Impurities from other groups in the periodic table may be incorporated substitutionally or interstitially to form deep donor or acceptor levels. Finally elements of group III and V can enter isoelectronically, while Ga and P atoms may occasionally be found on the wrong sublattice thus causing deviations from stoichiometry.

There are several growth parameters which determine the solubility of a given impurity in gallium phosphide and hence place a maximum value on the electrically active concentration of that impurity. The most important of these parameters are growth temperature, impurity size and, of course, growth technique. As this maximum concentration is reached the impurity either ceases to enter the crystal lattice or begins to form electrically inactive complexes, either by self-compensation or segregation. In either case the donor or acceptor concentration as determined from the Hall or Schottky barrier measurements may be only a small fraction of the true impurity concentration.

## 2.10 Liquid Encapsulated Czochralski Crystal Growth

Large single crystals of doped and undoped gallium phosphide, suitable for substrate material in light emitting diodes, have been produced recently by the liquid encapsulated Czochralski [L.E.C.] technique at S.E.R.L., Baldock. The technique has been described extensively elsewhere[29,30]. Briefly, the process involves pulling a single crystal from a silica or boron nitride crucible containing molten GaP and the correct amount of intended dopant material. The surface of the GaP melt and the pulled crystal is covered in a layer of $B_2O_3$ to prevent boil-off of phosphorous from the melt.

During the growth process, however, other impurities enter the crystal in varying amounts. Boron, nitrogen, oxygen and silicon are always present in substantial amounts unless specific precautions are taken to exclude them. Young and Bass[31] have found that supposedly undoped material is usually n-type with room temperature carrier

concentration increasing from seed to tail end of each crystal. They identified the donor impurity as silicon and showed that, in crystals for which $Ga_2O_3$ had been added to the melt to remove the Si, the carrier concentration was reduced considerably. Other impurities such as Al, Cl, Mn, Na and Ca can be present in appreciable amounts but in n-type material, because their levels lie deep in the band gap, the donors amongst them will be neutral and the acceptors ionized.

Young and Bass also found that the dislocation density was low in L.E.C. grown crystals. It increased from about $10^4$ $cm^{-2}$ at the seed end to $10^5$ $cm^{-2}$ at the tail end. Along with Nygren[32], they found that the carrier concentration and dislocation density varied from the centre to the edge of each slice cut perpendicular to the growth axis of the crystal. The amount of variation was dependent on from which part of the crystal the slices were taken, but generally the homogeneity was greatest near the seed end. The maximum variation in doping density in any slice was approximately 20%.

# CHAPTER III

# NUCLEAR INTERACTIONS

## 3.1 Introduction

Before outlining the theory of nuclear relaxation in doped semiconductors it is necessary to describe, in some detail, the fundamental interactions to which magnetic nuclei are subject and which provide nuclear relaxation mechanisms in solids. Having done that, we can introduce the concepts of spin temperature, spin-spin relaxation times and spin-lattice relaxation times, all of which are extremely important macroscopic parameters used in the study of matter by magnetic resonance.

## 3.2 Zeeman Interaction

A nucleus of magnetic moment $\underline{\mu}$, when placed in a magnetic field $\underline{H}$, is described quantum mechanically by the Hamiltonian

$$\mathcal{H} = -\underline{\mu}.\underline{H} \qquad 3.2.1$$

The magnetic moment and angular momentum $\underline{J}$ are parallel vectors and so we can write

$$\underline{\mu} = \gamma\underline{J} \qquad 3.2.2$$

where $\gamma$ is the 'gyromagnetic ratio' of the nucleus.

Defining a spin angular momentum operator $\underline{I}$ in terms of $\underline{J}$, such that

$$\underline{J} = \hbar\underline{I} \qquad 3.2.3$$

and taking the magnetic field $H_o$ to be along the z-direction we can say that

$$\mathcal{H} = -\gamma\hbar H_o I_z \qquad 3.2.4$$

The eigenvalues of this Hamiltonian are multiples of the eigenvalues of $I_z$ and the allowed energies are thus

$$E = -\gamma\hbar H_o m \quad \text{where } m=I, I-1, \text{---} -I \qquad 3.2.5$$

This corresponds to a set of 2I+1 equally spaced energy levels, each separated by $\gamma\hbar H_o$ .

Transitions between adjacent levels can be induced by applying an alternating magnetic field of frequency $\omega$, such that

$$\hbar\omega = \gamma\hbar H_o \qquad 3.2.6$$

perpendicular to $H_o$ [33,34]. This is the coupling most commonly used to produce magnetic resonances and the frequency at which the resonance occurs is known as the Larmor frequency.

When dealing with solids all N spins must be considered and the Hamiltonian which describes their interaction with an external magnetic field is given by

$$\mathcal{H} = -\gamma\hbar H_o \sum_{i=1}^{N} I_z^i \qquad 3.2.7$$

which is the Zeeman Hamiltonian.

## 3.3 Dipole-Dipole Interaction

In the absence of any other interactions the observation of the nuclear energy levels through magnetic resonance would lead to a perfectly sharp absorption line. This is not observed in practice due to the fact that any particular nucleus is not just in a static magnetic field, $H_o$, but also a magnetic field produced by all the neighbouring nuclei. This varies from nucleus to nucleus and hence the absorption frequency varies also, resulting in a broad spectral line.

The classical interaction energy E between two magnetic moments, $\mu_1$ and $\mu_2$, separated by a distance $\underline{r}$ is

$$E = \frac{\mu_1 \cdot \mu_2}{r^3} - \frac{3(\mu_1 \cdot r)(\mu_2 \cdot r)}{r^5} \qquad 3.3.1$$

For a system of N spins, the dipolar contribution to the Hamiltonian becomes

$$\mathcal{H}_{dd} = \frac{1}{2} \sum_{j=1}^{N} \sum_{k=1}^{N} \frac{\mu_j \cdot \mu_k}{r_{jk}^3} - \frac{3(\mu_j \cdot r_{jk})(\mu_k \cdot r_{jk})}{r_{jk}^5} \qquad 3.3.2$$

On transforming to spherical polar coordinates r, $\theta$, and $\phi$ and writing $\mu_j$ and $\mu_k$ in component form, using raising and lowering operators $I_+$ and $I_-$, we can express the dipolar Hamiltonian in the more convenient form for computing matrix elements

$$\mathcal{H}_{dd} = \frac{1}{2} \sum_{j,k} \frac{\gamma_1 \gamma_2 \hbar^2}{r_{jk}^3} [A+B+C+D+E+F] \qquad 3.3.3$$

where

$$A = I_{jz} I_{kz} (1 - 3\cos^2\theta_{jk})$$

$$B = -\tfrac{1}{4}[I_j^+ I_k^- + I_j^- I_k^+](1 - 3\cos^2\theta_{jk})$$

$$C = -\frac{3}{2}[I_j^+ I_{kz} + I_{jz} I_k^+]\sin\theta_{jk}\cdot\cos\theta_{jk}\, e^{-i\phi_{jk}}$$

$$D = -\frac{3}{2}[I_j^- I_{kz} + I_{jz} I_k^-]\sin\theta_{jk}\cdot\cos\theta_{jk}\, e^{i\phi_{jk}}$$

$$E = -\tfrac{3}{4} I_j^+ I_k^+ \sin^2\theta_{jk}\, e^{-2i\phi_{jk}}$$

$$F = -\tfrac{3}{4} I_j^- I_k^- \sin^2\theta_{jk}\, e^{2i\phi_{jk}} .$$

The terms A and B commute with the Zeeman Hamiltonian and hence cannot exchange energy with it. However the term B does connect states $|m_1 m_2>$ with states $|m_1+1, m_2-1>$ or $|m_1-1, m_2+1>$ and hence can induce mutual spin-flips between $\mu_1$ and $\mu_2$. For a system of identical spins this can lead to an efficient mechanism for the transport

of nuclear spin energy.

In the nuclear relaxation of nuclei in diamagnetic crystals containing small quantities of paramagnetic impurities the term C in the dipolar Hamiltonian linking the magnetic moments of the impurities and the nuclei is the dominant cause of such relaxation[36]. This term can induce a flip of the nuclear spin unaccompanied by an electron flip and hence is the most energetically favourable coupling between the impurity and nucleus.

## 3.4 Quadrupole Interaction

Nuclei of spin I greater than $\frac{1}{2}$ can, and usually do possess electric quadrupole moments which interact with electric field gradients to produce a perturbation of the nuclear energy levels.

If the electric field gradient has axial symmetry along the z axis the quadrupole Hamiltonian has the form

$$\mathcal{H}_Q = \frac{e^2 q Q}{4I(I-1)} [3I_z^2 - I^2] \qquad 3.4.1$$

where Q is the electric quadrupole moment of the nucleus and q is the field gradient defined by

$$eq = V_{zz} = \frac{\partial^2 V}{\partial z^2} . \qquad 3.4.2$$

If the quadrupole interaction is weak compared with the magnetic interaction with $H_o$, it may be shown, using first order perturbation theory, that the 2I intervals between successive energy levels are no longer equal. This results in 2I satellite lines being symmetrically placed about the $\frac{1}{2}$ to $-\frac{1}{2}$ line which remains unshifted by the quadrupole interaction. When the lines remain unresolved they produce a

broadening of the resonance.

3.5 Electron Spin Interaction: Knight Shift

The complete Hamiltonian[36] describing the interaction between the electrons and a nucleus can be written as

$$\mathcal{H}_{en} = \gamma_e \gamma_n \hbar^2 \underline{I} \cdot \left( \frac{\underline{\ell}}{r^3} - \frac{\underline{s}}{r^3} + \frac{3\underline{r}\cdot(\underline{s}\cdot\underline{r})}{r^5} + \frac{8\pi}{3}\,\underline{s}\,\delta(\underline{r}) \right) \qquad 3.5.1$$

which includes the coupling between the nucleus and the electron orbital angular momentum $\underline{\ell}$, the dipole-dipole interaction, and the hyperfine scalar contact interaction which is non-zero for s-state electrons. The last term comes into play when the dipole-dipole approximation, assumed to hold for the other terms, breaks down near the nucleus.

In metals, or heavily doped semiconductors, the hyperfine coupling between the nuclei and s-state conduction electrons can lead to a shift in the resonance frequency of the nuclei. This is due to the non-zero magnetic field produced by the polarization of the conduction electrons in the large magnetic field. In a highly degenerate electron gas the spin polarization of the electrons, and hence the resultant magnetic field produced by them, is independent of temperature but directly proportional to applied magnetic field. The ratio of the field shift of the nuclear resonance to the applied field is constant therefore, and called the Knight shift, K.

Electrons with other than s-type character can also produce a Knight shift through their dipolar coupling to the nuclei but only in non-cubic metals. The coupling of the nucleus to the electron orbital motion can also produce a frequency shift and core polarization by the conduction electrons can result in either a positive or negative Knight shift.

Detailed calculations[37] of the Knight shift can be found elsewhere and we shall just state the result for s-state conduction electrons.

If $\Delta H$ is the field shift in an applied field $H_o$, then

$$\frac{\Delta H}{H_o} = \frac{8\pi}{3} < |U_k(o)|^2 >_{E_F} \chi_e^s \qquad 3.5.2$$

where $< |U_k(o)|^2 >$ is the electron density of s-state electrons at the nucleus averaged over the Fermi surface, and $\chi_e^s$ is the Pauli paramagnetic spin susceptibility. The presence and absolute magnitude of a Knight shift in doped semiconductors at low temperatures is a sensitive indication of the onset of impurity banding and the metal-nonmetal transition.

## 3.6 Exchange Interaction

The presence of a nuclear moment on a lattice site has the effect of making that site more favourable to an electron of parallel moment. Because of the presence of electron bonds, the preferred spin orientation of an electron on one site causes an electron on a nearby site to have a preferred orientation in the opposite direction. This results in the nucleus on the nearby site being in the non-zero field of its own electron and, since the field direction would reverse if the nucleus on the original site reversed, an effective nuclear-nuclear exchange coupling results[37]. The Hamiltonian for such an exchange interaction has the form

$$\mathcal{H}_{eff} = A\underline{I}_1 \cdot \underline{I}_2 \qquad 3.6.1$$

where $I_1$ and $I_2$ are the spins of the nuclei linked by the interaction.

For a system of spins

$$\mathcal{H}_{eff} = \sum_{i,j} A_{ij}\, \underline{I}_i \cdot \underline{I}_j \qquad 3.6.2$$

where $A_{ij}$ is a function of $r_{ij}$, the distance between the two nuclei.

In solids the main effect of this exchange interaction is to alter the resonance linewidth and second moment[38]. For interactions

between like nuclei, the linewidth is reduced and the wings of the resonance are enhanced leaving the second moment unchanged. For interactions between unlike nuclei, the linewidth is broadened and the second moment increased. These two effects are known as "exchange narrowing" and "exchange broadening" respectively.

## 3.7 $T_s$, $T_2$, $T_1$

If we have an ensemble of nuclear spins in a magnetic field H, completely isolated from the lattice, then, assuming there exists some mechanism for maintaining internal thermal equilibrium amongst the spins, they will distribute themselves amongst all the available energy levels according to a Boltzmann distribution. We can describe this distribution by a characteristic temperature, $T_s$, called the spin temperature, such that if the equilibrium population of two adjacent levels are $N_1$ and $N_2$ then

$$\frac{N_1}{N_2} = \exp\left(\frac{\gamma\hbar H}{kT_s}\right) . \qquad 3.7.1$$

The spin temperature concept is only valid if internal thermal equilibrium is maintained throughout the ensemble. This necessitates some form of spin-spin coupling such that a disturbance of the populations in one part of the ensemble is quickly transmitted throughout the rest of the ensemble. The dipole-dipole interaction between the magnetic moments of identical nuclei provides such a coupling and it is possible to define a spin-spin relaxation time, $T_2$, which gives a measure of the time required for the system to acquire a uniform spin temperature after a disturbance. In a solid, where dipole-dipole interactions are particularly strong, $T_2$ is usually of the order of tens or hundreds of microseconds.

The ensemble of nuclear spins can never be completely isolated from the lattice and, if the lattice temperature, $T_L$, differs from

$T_s$, a net exchange of energy occurs between them until thermal equilibrium is reached. Usually the heat capacity of the lattice is so much greater than that of the ensemble of spins that we can regard $T_L$ as remaining virtually constant, while $T_s$ changes until $T_s = T_L$. If we disturb the population of the ensemble of spins such that $T_s \neq T_L$ the return to equilibrium will usually take place exponentially and the time constant of this recovery is called the nuclear spin-lattice relaxation time, $T_1$. In a solid $T_1$ can vary from milliseconds to days depending on the strength of the spin-lattice interaction. Our assumption of a single exponential recovery rate of the spin population after disturbance is justified as $T_2 << T_1$ in solids and therefore the ensemble maintains a uniform spin temperature throughout the relaxation process.

There are several methods of perturbing the nuclear energy levels and measuring the spin-spin and spin-lattice relaxation times. In pulsed n.m.r. we observe the variation, with time, of the component of the nuclear magnetization in the magnetic field direction after perturbing the equilibrium magnetization with intense pulses of radio frequency radiation at the nuclear Larmor frequency. We shall discuss this in more detail in chapter 6.

# CHAPTER IV

# NUCLEAR RELAXATION IN DOPED SEMICONDUCTORS

## 4.1 Introduction

In 1954 Bloembergen[39] published a comprehensive survey of the various ways in which nuclear magnetic resonance in diamagnetic crystals could be affected by the presence of imperfections. In that survey he took 'imperfection' to include dislocations, vacancies, foreign atoms in either substitutional or interstitial positions, free electrons and holes, phonons and excitons. In doped semiconductors nuclear relaxation is dominated by three possible mechanisms. They are i) modulation of the quadrupole interaction between the nuclear electric quadrupole moments and electric field gradients by lattice vibrations

ii) modulation of the hyperfine scalar contact interaction with free electrons and holes

iii) the dipole-dipole interaction between the magnetic moments of the nuclei and those of the paramagnetic donor, acceptor or defect centres.

The first mechanism is especially important in III-V semiconductors where, apart from $P^{31}$, all the nuclei have large quadrupole moments. The relative effectiveness of each mechanism may be dependent on a number of physical parameters, such as temperature, magnetic field, or impurity concentration. A study of the dependence of the nuclear spin-lattice relaxation time on these parameters should enable us to determine which, if any, of the above mechanisms are dominant under any particular conditions. The theory relating to the above mechanisms will now be presented along with brief descriptions of recent experimental work in doped semiconductors.

4.2 Nuclear Quadrupole Relaxation

Pound[40] first demonstrated the dominance of nuclear electric quadrupole interactions over magnetic dipole interactions in determining nuclear relaxation times in many solids containing nuclei with spins greater than $\frac{1}{2}$. Fluctuating electric field gradients at the nuclear sites enable the lattice to induce nuclear transitions $m_I = \pm 1$ and $m_I = \pm 2$ even in crystals with cubic or tetrahedral symmetry, where there is no permanent electric field gradient at each site. Van Kranendonk[41] developed a theory in which the lattice interaction was via a two-phonon Raman process and Mieher[42] used a modified version of this theory to explain nuclear relaxation in several III-V compounds. Weber[43] interpreted the temperature dependences of the $Ga^{69}$ and $Ga^{71}$ nuclear spin-lattice relaxation times, $T_1$, in gallium phosphide in terms of Mieher's theory, with relaxation being enchanced by the fluctuating electric field gradients produced by the large amount of covalent bonding in such compounds.

A spatially isotropic $T_1$, given by Mieher, has the form

$$\frac{1}{T_1} = 51 \frac{2I+3}{I^2(2I-1)} \frac{(e^2 \gamma Q)^2}{d^2 v^3 r^{13}} \left(\frac{T}{T_D}\right)^2 E(T/T_D) \qquad 4.2.1$$

where $T_D$ is the Debye temperature, $E(T/T_D)$ is an integral over the Debye spectrum of lattice vibrations, $\gamma$ is an antishielding factor produced by distortions of the electronic cloud around each nucleus, r is the nearest neighbour distance, v is the velocity of sound, d is the density, and Q the electric quadrupole moment.

Weber's results agreed well with theory apart from a small contribution to the nuclear relaxation rate from paramagnetic impurities around 77°K. Relaxation by paramagnetic impurities is likely to be of much greater importance in heavily doped semiconductors and the relaxation mechanisms associated with them are discussed in detail in section 4.4 of this chapter.

## 4.3 Hyperfine Scalar Contact Interaction

Another possible relaxation mechanism in doped semiconductors and metals is that produced by modulation of the hyperfine scalar contact interaction with mobile electrons or holes. This will be of importance at high temperatures in lightly doped samples[44] when most of the impurities are ionized and at low temperatures in heavily doped samples where impurity conduction occurs.

Basically, when an electron passes close to a nucleus, the nucleus experiences a large, time-varying magnetic field which induces mutual spin-flip transitions between it and the mobile charge carrier. The energy quantum, $h\nu_o$, emitted or absorbed by the electron results in a change in its kinetic energy and therefore the exchange can only take place if there is a vacant energy level available for it to move into. Consequently Fermi-Dirac statistics apply and in a highly degenerate electron gas, such as a heavily doped semiconductor at low temperatures or a metal, only those electrons within kT of the Fermi level can take part in the relaxation process.

For conduction electrons the Hamiltonian may be written as

$$\mathcal{H}_1 = -\frac{8\pi}{3}\gamma_e\gamma_n\hbar^2 \sum_{i,j} \underline{I}_i\cdot\underline{S}_j\,\delta(r_{ij}) \,. \qquad 4.3.1$$

On introducing the raising and lowering operators $I^+ = I_x + iI_y$ and $I^- = I_x - iI_y$ we may express this as

$$\mathcal{H}_1 = -\frac{8\pi}{3}\gamma_e\gamma_n\hbar^2 \sum_{i,j} \delta(r_{ij})(I_{iz}S_{jz} + \tfrac{1}{2}(I_i^+S_j^- + I_i^-S_j^+)) \,. \qquad 4.3.2$$

$\gamma_e$, $\gamma_n$ are the electron and nuclear gyromagnetic ratios, $\underline{I}_i$, $\underline{S}_j$ and $\underline{r}_{ij}$ are the $\underline{i}$th nuclear spin, the $\underline{j}$th electron spin, and the distance between them.

The first term in the parentheses was used in the first order calculation to obtain the Knight shift discussed in 3.5. The other terms are similar to the terms in the dipolar Hamiltonian which enable mutual spin-flip transitions and, indeed, they result in similar transitions between nuclei and mobile electrons.

Using the nuclear Zeeman energy as a zero order Hamiltonian $T_1$ may be calculated using standard perturbation theory and Abragam[36] has obtained for non-degenerate electrons in semiconductors,

$$\frac{1}{T_1} = \frac{32}{9} \gamma_e^2 \gamma_n^2 \, n \, V^2 < |U_k(o)|^2 >^2 [2\pi (m^*)^3 kT]^{\frac{1}{2}} \qquad 4.3.3$$

where n is the conduction electron density, V is the sample volume, $m^*$ is an electron effective mass, and $< |U_k(o)|^2 >$ is the electron probability density at the nuclear site averaged over all energy states.

At low temperatures when the electron system is degenerate

$$\frac{1}{T_1} = \frac{64}{9} \pi^3 \gamma_e^2 \gamma_n^2 \hbar^3 < |U_k(o)|^2 >^2_{E_F} \rho^2(E_F) \, kT \qquad 4.3.4$$

where $\rho(E_F)$ is the electron density of states at the Fermi level $E_F$ and $< |U_k(o)|^2 >_{E_F}$ is the electron probability density at the nucleus averaged over states at the Fermi surface.

For free electrons

$$\rho(E_F) = \frac{(3n/8\pi^*)^{\frac{1}{3}} m^* V}{\hbar^3} . \qquad 4.3.5$$

Therefore for non-degenerate electrons $T_1 \propto T^{-\frac{1}{2}}$ and for degenerate electrons $T_1 \propto T^{-1}$.

## 4.4 Nuclear Spin Lattice Relaxation by Paramagnetic Impurities

### 4.4.1 Review

The importance of the presence of paramagnetic impurities on nuclear spin-lattice relaxation was first recognized by Rollin[45] in 1947. In 1949, Bloembergen[35], in developing a theory for such relaxation, introduced the concept of a spin diffusion process by which nuclear spin energy was transported throughout a crystal. He obtained an expression for the nuclear spin-lattice relaxation time, $T_1$, by solving numerically a nuclear magnetization transport equation. Khutsishvili[46] obtained a similar expression by analytical techniques. Blumberg[47] investigated the case where spin diffusion was negligible

and thus distinguished between the so-called "rapid diffusion" and "diffusion limited" cases of nuclear relaxation. The latter case was characterized by a region, a short time after initial nuclear saturation, when the recovery of the nuclear magnetization in the large magnetic field was not a simple exponential in time, t, but proportional to $t^{\frac{1}{2}}$. Tse and Hartmann[48] have generalized Blumberg's work for the case where diffusion is negligible at all times after saturation and find a recovery rate proportional to $\exp(-\frac{t^{\frac{1}{2}}}{T_1})$ which reduces to Blumberg's result when a critical radius, known as the diffusion barrier radius, tends to zero.

Khutsishvili[49], by using the concept of the diffusion barrier radius proposed by Blumberg to fix the correct limits on the solution of the steady state transport equation, was able to obtain a similar expression for the diffusion limited case. Rorschach[50] has derived an expression for $T_1$ which links the two limiting cases and shows that the transition from one case to the other occurs over a small parameter variation. Horvitz[51] has shown that spin diffusion can take place inside the diffusion barrier radius due to the resonant field created by the impurity spins at the frequency necessary to induce mutual spin-flips between adjacent nuclei. Under certain conditions this process can induce more rapid spin diffusion inside the barrier radius than outside but, in systems of fairly high impurity concentration, where spin-spin interactions dominate at low temperatures, it is unlikely to be of importance.

A formal description of the basic theory of nuclear relaxation by paramagnetic impurities will now be presented.

### 4.4.2 Direct Interaction

In a diamagnetic crystal containing a small quantity of paramagnetic impurities, such as a semiconductor containing a low concentration of neutral donors or acceptors, the coupling between the magnetic moment of the paramagnetic impurity, $\mu_e$, and that of a host

nucleus, $\mu_n$, a distance r away is via terms in the dipolar Hamiltonian described in 3.3. Bloembergen[35] has shown that the probability $[T_n^{dir}(r)]^{-1}$ of a nuclear transition being induced by the Fourier component of the fluctuating magnetic field produced by the impurity at a nuclear site is given by

$$[T_n^{dir}(r)]^{-1} = 3\,(\gamma_e\gamma_n\hbar)^2\,\frac{S(S+1)}{r^6}\sin^2\theta\cos^2\theta\,\frac{\tau}{1+\omega^2\tau^2} \qquad 4.4.1$$

where $\theta$ is the angle between the applied magnetic field and the vector joining the nucleus and impurity, S is the spin of the paramagnetic impurity, and $\omega$ is the angular Larmor frequency of the nucleus field H.

$\tau$ is the correlation time of $S_z$, the z-component of the spin S. If we denote $\tau_\ell$ and $\tau_s$ as the correlation times of $S_z$ caused by spin-lattice and spin-spin interactions respectively then we can write approximately that

$$\frac{1}{\tau} = \frac{1}{\tau_\ell} + \frac{1}{\tau_s} \qquad 4.4.2$$

and, in an infinitely dilute spin system, $\tau_s >> \tau_\ell$ therefore $\tau = \tau_\ell$. However, at sufficiently high impurity concentrations and low temperatures, where spin-lattice interaction is weak, it may be true that $\tau_\ell >> \tau_s$ and that $\tau = \tau_s$.

For a random distribution of paramagnetic impurities in the crystal we may average over all $\theta$ and write

$$[T_n^{dir}(r)]^{-1} = \frac{C}{r^6} \quad \text{where} \quad C = \frac{2}{5}\,(\gamma_e\gamma_n\hbar)^2\,\frac{S(S+1)\tau}{1+\omega^2\tau^2} \qquad 4.4.3$$

C being independent of the position of the nucleus in the crystal. As can be seen from the above expression the effectiveness of this relaxation mechanism falls off very rapidly with distance away from each impurity. Unless there existed some mechanism for transporting spin energy from nuclei far away from any impurity to nuclei within the range of influence of that impurity, the direct process would be

ineffective in producing the bulk nuclear relaxation rates observed experimentally. Such a mechanism was first explained by Bloembergen[35] in his original paper and we shall outline it now.

4.4.3 Nuclear Spin Diffusion

The dipolar coupling between identical nuclear spins can induce mutual spin-flip transitions between them and, in the presence of a nuclear magnetization gradient, can provide an efficient transport mechanism for nuclear magnetization describable by a diffusion coefficient D.

If we denote by $W_{ij}$ the probability per unit time of a flip-flop transition of a pair of identical, oppositively directed, nuclear spins i and j then the golden rule states that

$$W_{ij} = \frac{2\pi}{\hbar^2} |(m_i, m_j | V_{ij} | m_i \pm 1, m_j \mp 1)|^2 \frac{T_2}{\sqrt{2\pi}} \qquad 4.4.4$$

where $V_{ij}$ is the term in the dipolar Hamiltonian permitting mutual spin-flips of spins separated by a distance $r_{ij}$ e.g. the term B in equation 3.3.3, $T_2$ is the spin-spin relaxation time of the spins of type i, and $T_2/\sqrt{2\pi}$ is the number of final states per unit frequency interval.

In order to derive the diffusion equation we shall consider initially the simple case of a linear chain of identical spins between which only nearest neighbour interactions are important. If we denote $P_{\pm}(x)$ to be the probability that a spin at point x will be directed upwards (+) or downwards (-) then, for three spins located at positions x+a, x and x-a, the process via which neighbouring spins exchange spin directions can be written as

$$\frac{\partial P_+(x)}{\partial t} = -\frac{\partial P_-(x)}{\partial t} = W P_+(x+a) P_-(x) \qquad 4.4.5$$

and

$$\frac{\partial p(x)}{\partial t} = 2W\{P_-(x)[P_+(x+a)+P_+(x-a)] - P_+(x)[P_-(x+a)+P_-(x-a)]\} \qquad 4.4.6$$

where

$$p(x) = P_+(x) - P_-(x). \qquad 4.4.7$$

Equation 4.4.6 transforms into

$$\frac{\partial p(x)}{\partial t} = W[p(x+a) + p(x-a) - 2p(x)] . \qquad 4.4.8$$

Now, assuming that p(x) varies very little over a distance a, we can expand p(x±a) in terms of a and obtain

$$\frac{\partial p(x)}{\partial t} = Wa^2 \frac{\partial^2 p(x)}{\partial x^2} . \qquad 4.4.9$$

Since we can relate the z-component of magnetization $M_z$ to p(x) by the expression

$$M_z = \tfrac{1}{2} n\hbar\gamma_n p(x) \qquad 4.4.10$$

we can write

$$\frac{\partial M_z}{\partial t} = Wa^2 \frac{\partial^2 M_z}{\partial x^2} \qquad 4.4.11$$

which is a linear diffusion equation for the magnetization $M_z$ with diffusion coefficient $D = Wa^2$.

Taking into account transitions between nuclei other than just nearest neighbours, we obtain

$$\frac{\partial M_z}{\partial t} = \tfrac{1}{2} \sum_n W(na) \, (na)^2 \frac{\partial^2 M_z}{\partial x^2} \qquad 4.4.12$$

where W(na) is the probability of a transition between pairs of spins a distance na apart.

Generalizing for the three dimensional case we can write

$$\frac{\partial M}{\partial t} = D\nabla^2 M \qquad 4.4.13$$

where

$$D = \frac{1}{6} \sum_j W_{ij} \, r_{ij}^2 \qquad 4.4.14$$

D is not a scalar, but a symmetric tensor of second rank and, in a single crystal, may be anisotropic because of the dependence of $W_{ij}$ on $\theta_{ij}$ and $r_{ij}$. This anisotropy is expected to be small in single crystals of cubic symmetry containing only one nuclear spin species although results by Leppelmeier and Jeener[79] in $CaF_2$ indicate that it might be as great as a factor of five between magnetic field directions along the <111> and <100> axes of the crystal. In crystals containing more than one spin ingredient the anisotropy is expected to be greater since, in a detailed calculation, D can be related to the second moment $\langle(\Delta H)^2\rangle$ which is strongly dependent on nearest neighbour interactions. The expression for $\langle(\Delta H)^2\rangle$ for nuclei of type i contains terms corresponding to interactions between like and unlike nuclei with the terms due to unlike nearest neighbour nuclei dominating.

However in a cubic crystal, polycrystalline sample or powder of any crystal system, D reduces to a scalar and the other nuclear spin species have the effect of reducing the isotropic value of D thus obtained by an amount proportional to their effect on the orientational averaged second moment.

On substituting the expression for $W_{ij}$ from 4.4.4 into 4.4.14 and averaging over all $\theta_{ij}$, we obtain an expression for D. For nuclei in a face centred cubic lattice[52] the expression reduces to

$$D = \frac{a^2}{13.5 \, T_2} \qquad 4.4.15$$

where we can relate $T_2$ to the second moment[53] for a Gaussian line by the relation

$$\langle(\Delta H)^2\rangle = \frac{\pi}{2\gamma_n^2 T_2^2} \qquad 4.4.16$$

Lowe and Gade[54] have derived expressions for D by investigating the equation of motion of the density matrix for the spin system.

However this method becomes extremely complex when there is more than one spin species present in other than simple cubic lattices. Considering the status of the experiments from which the spin diffusion coefficients are obtained a knowledge of D to within 50% is adequate, and so the approximate theoretical values obtained using the above method will suffice for this work.

4.4.4 Diffusion Barrier Radius and Pseudopotential Radius

There are three other parameters which need to be defined before deriving expressions for $T_1$ in the limiting cases of nuclear relaxation by paramagnetic impurities. The first is the spin-diffusion barrier radius, b. As the name implies, this is a measure of the distance away from each impurity at which spin diffusion is reduced to zero due to the large differences in Larmor frequencies of neighbouring identical nuclei caused by the inhomogeneous magnetic field of the impurity at the nuclear sites. We define b to be approximately that distance at which the magnetic field inhomogeneity between neighbouring nuclei is equal to the dipolar field produced at one nucleus by its neighbour.

At very low temperatures, and in the absence of any spin-spin interactions, we can consider the impurity to possess a static magnetic moment $\mu_e$. Then for $\tau >> T_2$

$$b = \left(\frac{\mu_e}{\mu_n}\right)^{\frac{1}{3}} a \qquad 4.4.17$$

where a is the distance between like nuclei. However at higher temperatures, the magnetic moment of the impurity may be flipping rapidly in a time shorter than or of the order of $T_2$ due to spin-lattice interaction and then the magnetic field seen by the nearby nuclei will be the time-averaged field of the impurity. Then

$$b = \left(\frac{\mu_e^2 H}{\mu_n kT}\right)^{\frac{1}{3}} a \qquad \tau << T_2 \qquad 4.4.18$$

where H is the large applied magnetic field and T the temperature.

The second parameter is the pseudopotential radius, $\rho$, which is a measure of the distance away from each impurity at which a nucleus has an equal probability of either being relaxed directly by the impurity or engaging in a mutual spin-flip with its neighbour. Khutsishvili[55] defined $\rho$ by the expression

$$\rho = 0.68\ (C/D)^{\frac{1}{4}} \qquad 4.4.19$$

and the name 'pseudopotential radius' was given to it by de Gennes[56] who developed a solution to the diffusion equation using scattering theory.

Finally, in order to solve the nuclear magnetization transport equation successfully, we have to assume that b and $\rho$ are much smaller than the average distance, R, between impurities. R is given approximately by

$$R = \left(\frac{3}{4\pi N}\right)^{\frac{1}{3}} \qquad 4.4.20$$

where N is the paramagnetic impurity concentration.

4.4.5 Derivation of the Nuclear Spin-Lattice Relaxation Time, $T_1$

If we define a function $p(\underline{r},t)$, similar to the $p(x)$ defined in equation 4.4.7, to be the nuclear magnetization density at any point $\underline{r}$, at time t, in a crystal, and assume that all diffusion processes take place over distances much greater than the lattice spacing, a, then we can say that

$$p(\underline{r},t) = \frac{\langle M(\underline{r},t)\rangle}{a^3} \qquad 4.4.21$$

where $M(\underline{r},t)$ is the component of the nuclear magnetization along the applied field direction. Therefore $p(\underline{r},t)$ is the time-dependent three-dimensional equivalent of $p(x)$ in equation 4.4.7.

We are now in a position to set up and solve a differential equation for the rate of change of nuclear magnetization density $p(\underline{r},t)$

with time after initial saturation of the nuclear spin energy levels. Immediately after complete saturation, there is zero resultant magnetization and $p(\underline{r},o) = 0$. The nuclei around each impurity will be relaxed to the lattice via the direct interaction described in section 4.4.2. Therefore the magnetization of those nuclei surrounding each impurity will recover faster than that of nuclei in the bulk material and a magnetization gradient will be set up. We can then consider the contact between the bulk nuclei and the impurity as being the result of a net transport of nuclear spin energy towards the impurity or, equivalently, a net transport of nuclear magnetization away from the impurity. The process via which this transportation is carried out is spin diffusion along the magnetization gradient.

Considering now the direct relaxation process only, the most general expression for the rate of change of nuclear magnetization density $p(\underline{r},t)$ with time is given by

$$\frac{\partial p(\underline{r},t)}{\partial t} = C[p(\underline{r},\infty) - p(\underline{r},t)] \sum_n |\underline{r}-\underline{r}_n|^{-6} \qquad 4.4.22$$

where $p(\underline{r},\infty)$ is the equilibrium nuclear magnetization density, $\underline{r}_n$ is the position of the nth impurity, and C is the factor defined in equation 4.4.3. Combining this with the rate of change of nuclear magnetization density due to spin diffusion we obtain an equation for the net rate of change of the form

$$\frac{\partial p(\underline{r},t)}{\partial t} = D\nabla^2 p(\underline{r},t) + C[p(\underline{r},\infty) - p(\underline{r},t)] \sum_n |\underline{r}-\underline{r}_n|^{-6} \qquad 4.4.23$$

For a sufficiently dilute concentration of impurities we can consider each nucleus as being relaxed by a single impurity and, taking that impurity to lie at the origin of the coordinates, we get

$$\frac{\partial p(\underline{r},t)}{\partial t} = D\nabla^2 p(\underline{r},t) - C(p(\underline{r},t) - p(\underline{r},\infty))r^{-6} \qquad 4.4.24$$

Replacing $p(\underline{r},t)$ by the magnetization $M(\underline{r},t)$ we obtain

$$\frac{\partial M_z(\underline{r},t)}{\partial t} = D\nabla^2 M_z(\underline{r},t) - C\{M_z(\underline{r},t) - M_z(\underline{r},\infty)\}r^{-6} \qquad 4.4.25$$

If we denote M(t) to be the total observed magnetization in a sphere of radius R about a paramagnetic impurity, then

$$M(t) = 4\pi \int_b^R M_z(\underline{r},t)\, r^2\, dr \qquad 4.4.26$$

the lower limit being necessary since those nuclei within the barrier radius are not observed because of the large shifts of their Larmor frequencies. We can then define the nuclear spin-lattice relaxation time $T_1$ by the equation

$$\frac{\partial M(t)}{\partial t} = \frac{M(\infty) - M(t)}{T_1} \qquad 4.4.27$$

where $M(\infty)$ is the total equilibrium magnetization within the sphere of radius R.

De Gennes[56] has shown that, for a sufficiently long time after saturation the magnetization recovery rate given by eqn. 4.4.25 approaches an exponential function of time of time constant $T_1$. In order to solve eqn. 4.4.25 we have to place certain artificial boundary conditions. If we assume a steady state situation, i.e. $\frac{\partial M_z(\underline{r},t)}{\partial t} = 0$, we obtain a time-independent second order differential equation for $M_z(r)$. A second boundary condition is set by placing a magnetization sink at $r = R$ so that $M_z(R)$ has a fixed value $M_1$. $M_1$ eventually cancels in the expression for $T_1$. Without going into further detail, we can obtain expressions for $T_1$ under a number of limiting cases determined by the relative magnitudes of b, $\rho$, and R[57].

## 4.4.6 Diffusion Limited Relaxation

In the case where $b << \rho << R$ nuclear spin energy is being transferred to the lattice faster than spin diffusion can transport it towards the paramagnetic impurities. Khutsishvili[55] and de Gennes[56] have derived expressions for $T_1$ of the form

$$\frac{1}{T_1} = 4\pi N\rho D = 8.5\ N\ C^{\frac{1}{4}}D^{\frac{3}{4}} \qquad 4.4.28$$

The nuclear relaxation rate is limited by the spin diffusion rate and hence this is termed "diffusion limited" relaxation. However in their derivation of the above expression Khutsishvili and de Gennes neglected to consider the behaviour of the system immediately after saturation, when there is zero magnetization gradient and hence no net transportation of energy by spin diffusion. Blumberg[47] considered this problem and obtained an expression for the initial recovery rate of the form

$$M_z(t) = \frac{4\pi^{\frac{3}{2}}}{3}\ N\ C^{\frac{1}{2}}t^{\frac{1}{2}} \qquad 4.4.29$$

This expression holds true for $\frac{b^6}{C} < t < C^{\frac{1}{2}}D^{-3/2}$.
The lower limit is introduced because it gives a measure of the time interval after initial saturation before direct relaxation induced by the impurity begins to affect nuclei outside the barrier radius. The upper limit on equation 4.4.29 gives an estimate of the time interval after saturation after which spin diffusion becomes important.

This is obtained by initially assuming that only the direct relaxation process is important for a time t after initial saturation. Then, during that time, a sphere of radius $r_o$, given by,

$$r_o = (Ct)^{\frac{1}{6}} \qquad 4.4.30$$

around each impurity will have recovered its equilibrium magnetization. For diffusion still to be negligible after that time

$$\frac{r_o^2}{t} > D \quad \text{or} \quad r_o > (Dt)^{\frac{1}{2}} \qquad 4.4.31$$

Therefore from 4.4.30 and 4.4.31 we see that

$$(Dt)^{\frac{1}{2}} < (Ct)^{\frac{1}{6}} \quad \text{or} \quad t < C^{\frac{1}{2}}D^{-3/2}\ . \qquad 4.4.32$$

The existence of this short time non-exponentiality in the magnetization recovery after saturation is one of the identifying characteristics of diffusion limited relaxation.

4.4.7 Rapid Diffusion Relaxation

Blumberg[47] also considered the case in which the diffusion rate is much greater than the direct relaxation rate. This is equivalent to the condition $\rho << b << R$. The nuclear relaxation rate will then be independent of D, but directly proportional to the rate at which the nuclei can be relaxed directly to the lattice by the fluctuating magnetic field of the impurity.

The expression for $T_1$ is found to have the form

$$\frac{1}{T_1} = \frac{1}{p}\frac{dp}{dt} = 4\pi N \int_b^\infty \frac{C}{r^6} r^2 dr = \frac{4\pi}{3} N C b^{-3} \qquad 4.4.33$$

As can be seen from this equation $T_1$ is strongly dependent on the size of the diffusion barrier radius. Because of the comparatively slow direct relaxation rate, the bulk of the nuclear spins will maintain a common spin temperature for all times after saturation, and the magnetization recovery will be a simple exponential in time. For obvious reasons this case of nuclear relaxation by paramagnetic impurities is referred to as the "rapid diffusion" case.

4.4.8 Other Relaxation Cases: Diffusion Vanishing

Lowe and Tse[57] have considered a third limiting case which they describe as the 'diffusion vanishing' case and corresponds to a situation where $R \simeq \rho >> b$. The direct relaxation process should be dominant for all times after nuclear saturation. They use a multi-paramagnetic impurity model to calculate the theoretical values of $T_1$ and obtain single valued exponential recovery rates with magnetic field and concentration dependences differing from the two other limiting cases. They find that

$$\frac{1}{T_1} \propto N^{4/3} H^{-1} \tau^{-\frac{1}{2}} D^{\frac{1}{2}} \qquad 4.4.34$$

The complete expressions for $T_1$ are complicated but they have observed $T_1$'s with the above field and concentration dependences in doped $CaF_2$ crystals.

FIGURE 5.2.1

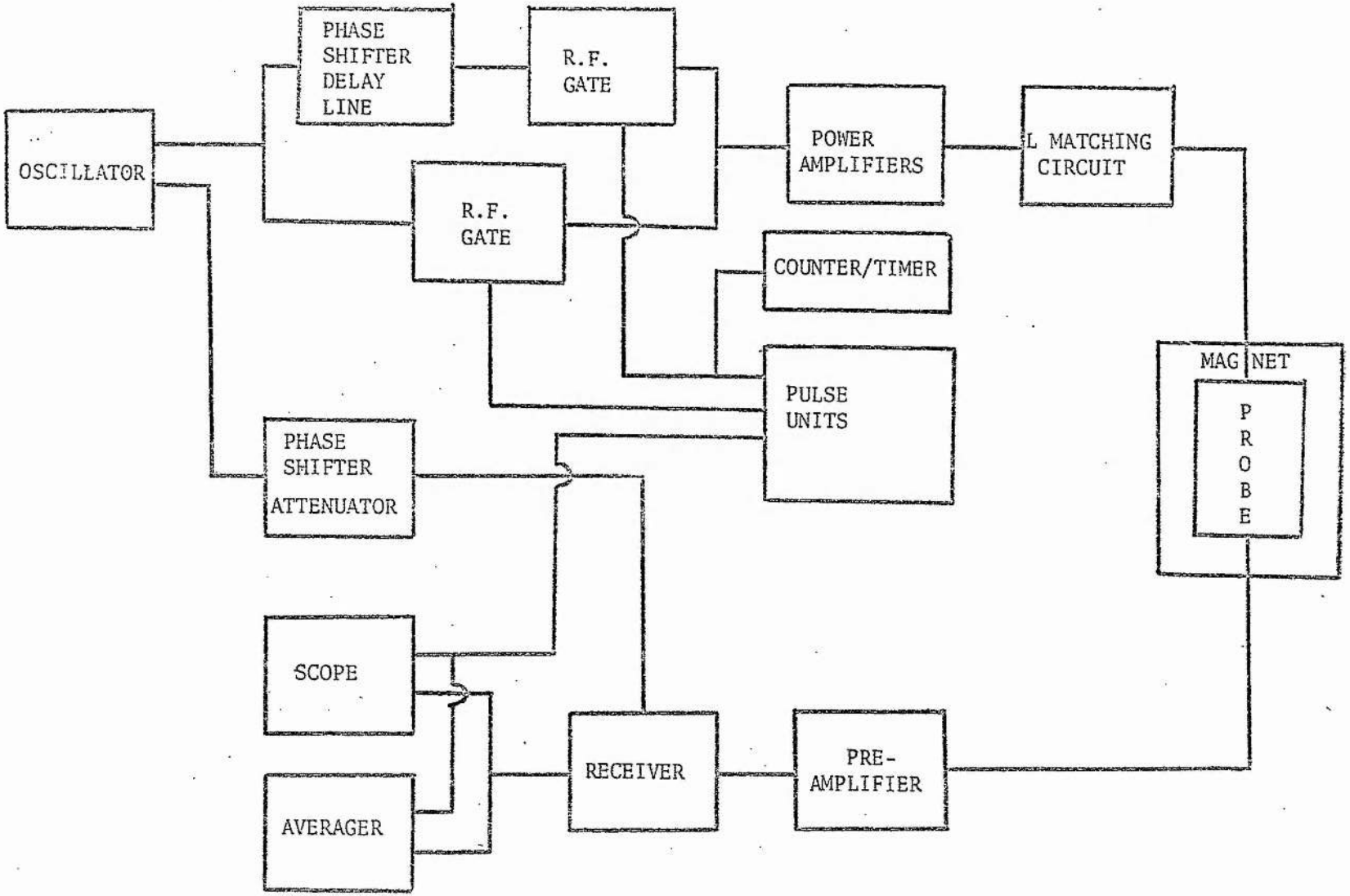
PHASE SHIFTER DELAY LINE
R.F. GATE
OSCILLATOR
POWER AMPLIFIERS
L MATCHING CIRCUIT
R.F. GATE
COUNTER/TIMER
PULSE UNITS
MAG NET
PROBE
PHASE SHIFTER ATTENUATOR
SCOPE
RECEIVER
PRE-AMPLIFIER
AVERAGER

# CHAPTER V

# APPARATUS

## 5.1 Introduction: Pulsed n.m.r. apparatus

In order to measure accurately the various n.m.r. parameters studied during this project certain stringent requirements are placed on the apparatus.

We require a transmitter system capable of producing short, intense pulses of r.f. of variable phase, width and pulse interval. The receiver system must be sensitive to both the phase and amplitude of the small incoming signal and also have high gain stability over long periods. Similar stability requirements are placed on the field produced by the electromagnet and its homogeneity over the sample volume must be good.

Any variation in the above specifications during the course of a measurement can lead to large errors in the measured n.m.r. parameters.

The apparatus employed for this work met all the above requirements. Two separate pulsed n.m.r. systems were used, both of which have been described elsewhere[58-61], and we shall restrict ourselves to brief descriptions of their main features and modifications to the original systems.

## 5.2 Crossed Coil System: 6.5 Mc/s and 10 Mc/s

This system, used to make measurements at 6.5 Mc/s and 10 Mc/s, made use of a crossed coil probe arrangement to isolate transmitter and receiver circuits. A block diagram of the apparatus is shown in Fig. 5.2.1.

Sequences of pulses of variable width and phase at radio frequencies and with amplitudes of 3kV peak to peak could be produced across the transmitter coil resulting in a $90^{o}$ pulse for $Ga^{69}$ nuclei having a width of 5 μsec and rise and fall time of about 1 μsec. Pulses from a bank of Tektronix 162A pulse generators were used to

gate the r.f. output from a free-running crystal oscillator before entering the first of three amplifying stages. These consisted of a 5W amplifier driving a 90W amplifier which, in turn, drove a 1kW amplifier. The high impedance of the transmitter tuned circuit was matched to the 50Ω output impedance of the last amplifying stage by an L matching circuit. A damping resistor, placed across the transmitter coil, prevented excessive ringing of the coil after a pulse and hence reduced the overload time of the receiver to less than 20 μsec. The incorporation of a delay line between the oscillator and one of the r.f. gates enabled pulses of differing phase to be produced.

The preamplifier and receiver for use at 10 Mc/s were identical to those described in reference 58 with phase coherent detection of the signal and automatic gain control in the receiver. Crossed diodes were used in each receiver stage to protect them from overload. For work at 6.5 Mc/s, the Clark receiver was replaced by a Polaron broad-band receiver. The reduced gain available with this receiver necessitated the addition of a Hewlett-Packard 465A amplifier on its output which provided a further gain of 20db for small signals. This was not required at low temperatures, where the n.m.r. signal was large. The maximum signal input to the Polaron was 1v and, at very low temperatures, an attenuator had to be placed between the preamplifier and the receiver to prevent distortion of the signal in the receiver.

The resulting free induction decay (f.i.d.) signal could be displayed directly onto the long-persistence screen of an HP 141A oscilloscope or, as was frequently used under low signal to noise conditions, the signal could be averaged over a set number of consecutive, identical decays using a Data Lab 100 point averager. The DL101 averager had the capability of averaging over 1 to 520 sweeps of the signal, the sweep period being set to span the whole f.i.d. The minimum sweep period available was 200 μsec but, as the

FIGURE 5.2.2

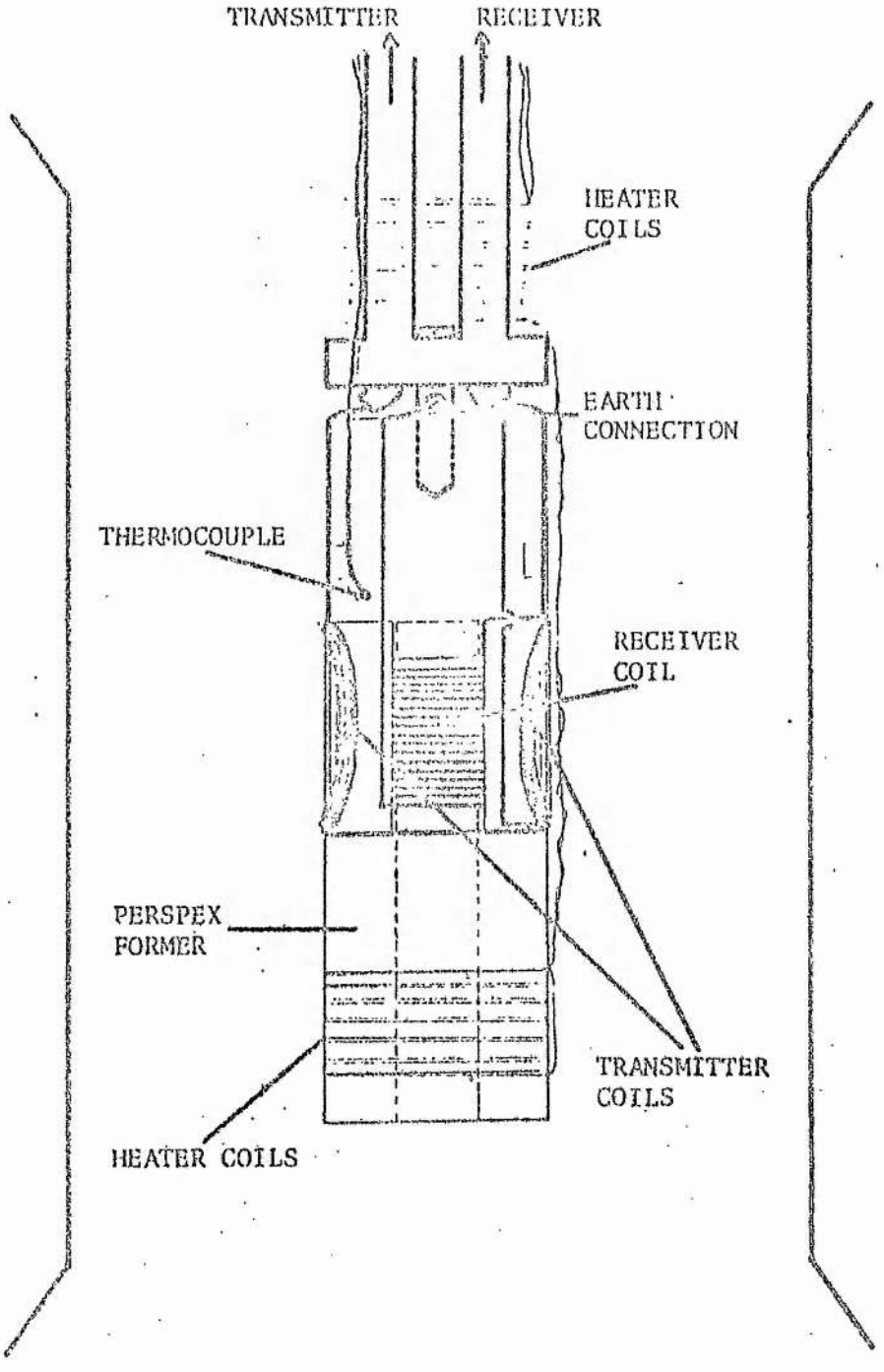
TRANSMITTER
RECEIVER
HEATER COILS
EARTH CONNECTION
THERMOCOUPLE
RECEIVER COIL
PERSPEX FORMER
TRANSMITTER COILS
HEATER COILS

$T_2$'s were not less than 80 μsec, this did not restrict the usefulness of the instrument. Having averaged over a set number of sweeps the f.i.d. was displayed on the oscilloscope in the form of 100 points spanning the whole sweep period.

The electromagnet was a Varian V-3400 Fieldal Mark II type with a VFR 2503 Mark II regulated power supply. After an initial warm up period the field drift was less than 25 milligauss per hour and the homogeneity was greater than 1 part in $10^5$ over a sample volume of $\sim 1cm^3$. With a 9" diameter polecap and 2" pole gap, fields of up to 11 kilogauss could be produced, thus enabling the magnetic resonances of $Ga^{69}$, $Ga^{71}$, and $P^{31}$ nuclei to be observed at 6.5 Mc/s and 10 Mc/s.

The cryostat was an Oxford Instrument liquid helium type with specially designed narrow tail and probe holder for n.m.r. work.

The crossed coil probe, chosen originally to meet the differing requirements of the transmitter and receiver coils independently, was identical in design to that in reference 59. When working at 6.5 Mc/s, new transmitter and receiver coils were set in araldite rather than wound on perspex formers, to increase the filling factor, and hence signal, in the receiver coil. However due to the failure of the araldite to withstand thermal cycling without cracking and because of spurious ringing in the receiver coil off pulse at low temperatures, the coils were rewound again on perspex thus forfeiting a small amount of signal. This set up worked satisfactorily.

The 6.5 Mc/s receiver coil consisted of 17 turns of 38 gauge, cotton-coated, silver wire while the transmitter coil consisted of two sets of 6 turns of 26 gauge enamelled copper wire. A schematic diagram of the probe is shown in figure 5.2.2.

## 5.3 Single-Coil System: 16 Mc/s

The second system, based on a design by Lowe and Tarr [60,61], differed from the first in that the transmitter was untuned, each stage being transformer coupled to the next, and it made use of a

Fig. 5.3.1

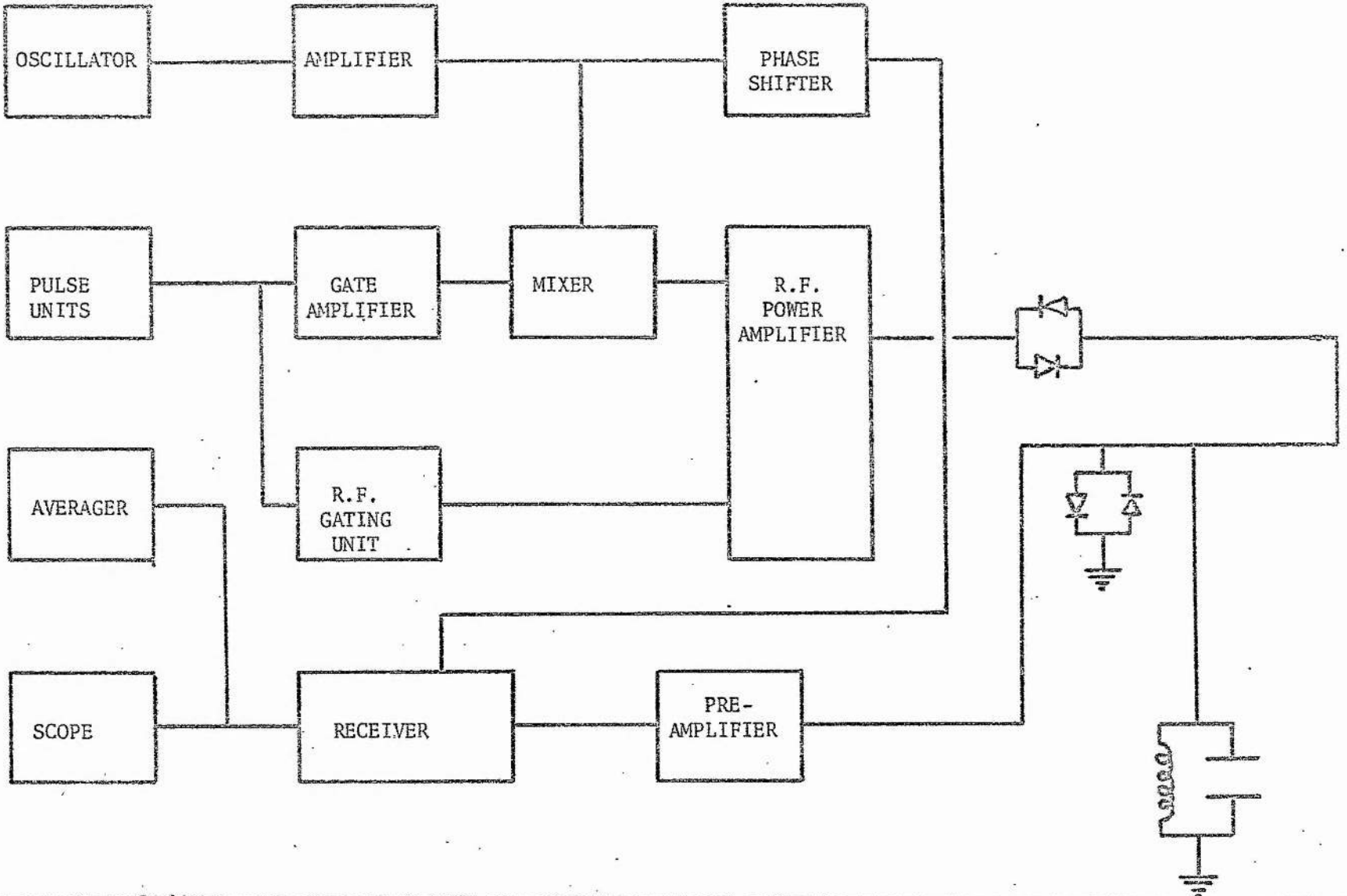
OSCILLATOR
AMPLIFIER
PHASE SHIFTER
PULSE UNITS
GATE AMPLIFIER
MIXER
R.F. POWER AMPLIFIER
AVERAGER
R.F. GATING UNIT
SCOPE
RECEIVER
PRE-AMPLIFIER

single coil arrangement in the probe. A schematic diagram of the apparatus is shown in Fig. 5.3.1. The receiver system was protected from overload on pulse by a diode short to earth which left the pulse across the coil unaffected due to the half wavelength cable between diode and coil. Similarly, off pulse, the transmitter was isolated by a series of crossed diodes between it and the probe. The receiver system off pulse was then matched to the sample tuned circuit. The receiver system consisted of an Arenberg PA-620-B preamplifier and WA-600E wideband amplifier which had a recovery time of less than 5 μsec and gain of 80 to 90db. Weak signals were again averaged using the Data lab averager but this was found unnecessary at most temperatures when the signal was viewed directly on the long persistence screen of an HP 181A oscilloscope.

The electromagnet was a Mullard EE 1035 type with EE4038 current stabilized power supply. With tapered pole pieces of 7½" diameter and 2½" pole gap, fields of up to 16.7 kilogauss could be produced with a maximum field inhomogeneity across the sample of 0.25 gauss. Field stability was better than 40 milligauss per hour and only after running for over eight hours at the highest field setting did heating of the coils begin to cause a slight field drift.

A second Oxford Instrument liquid helium cryostat, differing from the first by the absence of an internal probe holder and having a different tail width, was used.

The coil consisted of two turns of flat copper strip of width 0.4 cm and its overall dimensions were 1 cm in length and 0.7 cm in diameter. It tuned at 16 Mc/s with approximately 3000 pF placed directly across it. Dipped silver mica capacitors were used because of their low capacitance variation with temperature. A small length of manganin wire, placed in series with the coil in the tuned circuit, reduced the Q to around 17 and matched the impedance of the tuned circuit to the 50Ω output impedance of the transmitter.

Fig. 5.4.1

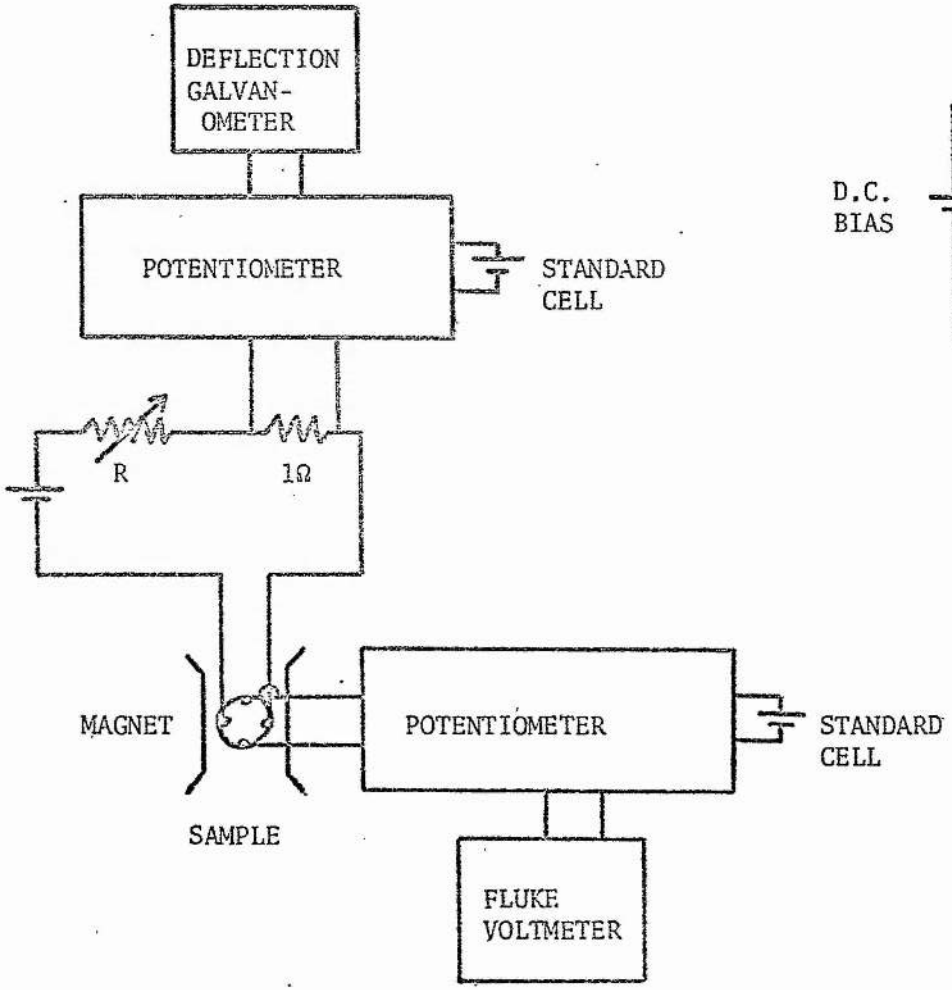


Fig. 5.5.1

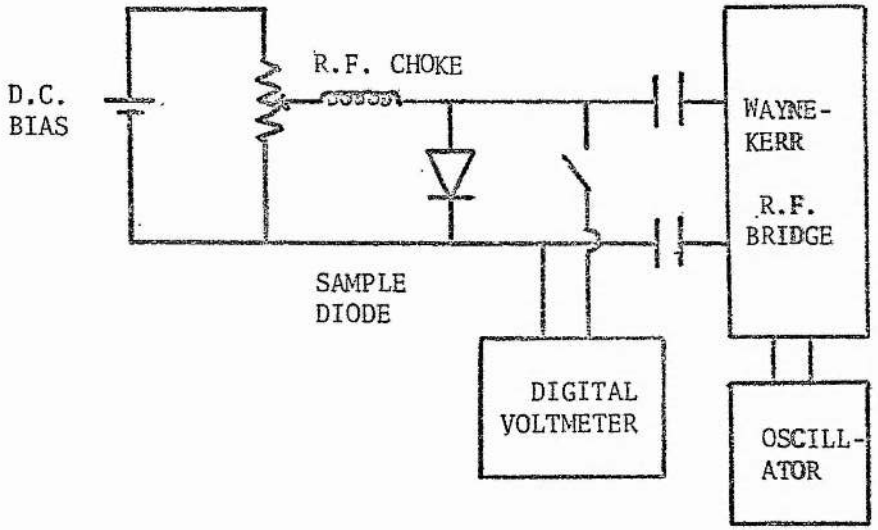

In both systems the exact time intervals between pulses were measured on a Racal SA535 1.2 Mc/s Counter-Timer which was triggered off the leading edge of the two pulses in question.

## 5.4 Hall Apparatus

A diagram of the apparatus used to make Hall and resistivity measurements is shown in Fig. 5.4.1.

Hall voltages were measured to within 1μV on a Tinsley 4025 potentiometer using a Fluke high impedance null-deflection voltmeter to monitor the balance position. The current through the sample was determined by using a Tinsley 3387B potentiometer to measure the voltage across a 1Ω standard resistor placed in series with the sample in the current circuit. Magnetic fields of up to 7500 gauss were obtained using a Newport 4" type A electromagnet and, for higher fields, the Mullard electromagnet described in section 5.3 was employed.

## 5.5 Schottky Barrier Capacitance Apparatus

A diagram of the apparatus used to make Surface Barrier capacitance measurements is shown in Fig. 5.5.1.

The sample is represented by the diode in the diagram and a Wayne-Kerr B601 R.F. Bridge was used to measure its capacitance and impedance. The bias voltages applied to the diode were measured on a DMM2 digital voltmeter.

The choke was used to prevent the 1 $MH_z$, 200mV peak to peak, r.f. from an AIRMEC type 399 video oscillator from interfering with the d.c. bias. Similarly, the 1μF capacitance prevented the d.c. voltages entering the r.f. bridge.

## 5.6 Samples

Seven gallium phosphide samples were studied during this project. Six of these were taken from slices cut normal to the (111) growth axis of L.E.C. grown crystals obtained from S.E.R.L., Baldock.

Each crystal was intentionally doped with tellurium, a group VI element, and it was hoped that the donor concentration range covered by these samples might span the intermediate doping region described in section 2.4. The seventh sample was made up of platelets from a tellurium doped sample grown at Ferranti and, because of the powdered nature of this sample, no Hall or Schottky barrier measurements could be taken to check its tellurium concentration.

Each of the L.E.C. grown crystals was initially labelled with standard S.E.R.L. furnace and slice numbers. We state these numbers here as they are required to check the expected unintentional impurity content from mass spectrographic data obtained from similar grown samples. For convenience we will relabel the samples A,B,C,D,E,F and G so that

A corresponds to the Ferranti platelet sample

B corresponds to the S.E.R.L. sample PEO 175/1

C corresponds to the S.E.R.L. sample PEO 175/24

D corresponds to the S.E.R.L. sample PEO 175/32

E corresponds to the S.E.R.L. sample PEO 175/36

F corresponds to the S.E.R.L. sample PEO 113/52

G corresponds to the S.E.R.L. sample PEO 175/(44-44).

The letters and numbers preceding the stroke refer to the furnace number while the numbers following the stroke refer to the slice numbers. Low numbers correspond to the seed end of the crystal, whereas high numbers are cut from near the tail end.

# CHAPTER VI

# EXPERIMENTAL TECHNIQUES

## 6.1 Hall and Conductivity Measurements

### 6.1.1 Introduction

As mentioned in section 2.6, a good general picture of the electrical conduction mechanisms in a doped semiconductor can be obtained from measurements of the electrical conductivity $\sigma$ and Hall coefficient $R_H$ as functions of temperature and impurity concentration[62]. If measurements are made over a wide enough temperature range actual values can be attached to the donor concentration $N_D$, acceptor concentration $N_A$, activation energies $\varepsilon_1$, $\varepsilon_2$, and $\varepsilon_3$, and mobility $\mu$. By tacitly equating Hall mobility with the drift mobility we obtain an expression for the carrier concentration n in terms of $R_H$

$$n = \frac{1}{e R_H} \quad \text{and} \quad \mu = \frac{\sigma}{ne} . \qquad 6.1.1$$

Assuming only one donor and acceptor level and negligible occupancy of their excited states then

$$n = \frac{2(N_D - N_A - n)}{N_A + n} \left(\frac{(2\pi m^* kT/h^2)^{3/2}}{D}\right) \exp\left(-\frac{E_D}{kT}\right) \qquad 6.1.2$$

where D is the degeneracy factor of the donor level, $m^*$ is the density of states effective mass, and $E_D$ is the donor ionization energy which is the activation energy for conduction in the low doping region.

Therefore, in order to estimate the tellurium concentration in each of our L.E.C. grown crystals measurements of $\mu_H$ and $\sigma$ were made using the van der Pauw technique[63]. This technique provides a method of measuring the electrical conductivity and Hall effect of discs of arbitrary shape.

### 6.1.2 Sample Preparation

Initially samples B to F consisted of thin slices from single GaP crystals. Each slice was 0.05 cm thick and of varying size depending on which part of the crystal it had been taken from.

A circular disc of 0.5 cm diameter was cut from the centre of each slice using an M.E.L. ultrasonic cutter. The disc was etched in Bromine-Methanol (1% Bromine, 99% Methanol) for 2 minutes to remove surface contamination, washed in methanol, and kept under propanol until the next stage of preparation.

The disc was removed from the propanol and four small indium dots pressed onto the dry surface of the disc as near to the circumference as possible. The dots were then fused to the surface by heating the disc, under vacuum, in an r.f. heater. The heater consisted of a carbon sample holder eddy-current heated by an r.f. coil surrounding it. The sample was placed on the carbon holder and a glass vacuum jacket placed over it. This was evacuated using a backing pump and the r.f. power applied to the coil. After 90 seconds the r.f. was switched off and, after waiting 10 minutes for the sample and holder to cool down, the sample was removed. Each indium contact was checked for ohmicity by measuring the d.c. resistance across any pair in both directions. Occasionally ohmicity was checked by displaying the V-I characteristic across a pair of contacts on an oscilloscope when a sinusoidal voltage, such as that from a waveform generator, was applied across them. Linearity of the trace indicated ohmic behaviour. It was found experimentally that good ohmic contacts were produced consistently when the r.f. heating lasted 90 seconds.

Tin contacts were tried initially but, perhaps because of tin's high melting point, it was found that it was much more difficult to ensure that all four contacts were ohmic.

Having placed four indium contacts on the disc it was necessary to solder copper leads directly onto them. This was done using 38 gauge enamelled copper wire after the sample had been rigidly attached to the head of the Hall probe. Nail varnish was found to be a sufficiently temperature resistant adhesive for this task and it had the advantage of being removed easily under the action of acetone.

6.1.3 van der Pauw Method

In order to calculate the electrical conductivity $\sigma$, Hall mobility $\mu_H$, and hence n, we use the result derived in van der Pauw's original paper[63]. That is

$$\frac{1}{\sigma} = \frac{\pi d}{\ell n\ 2} \left(\frac{R_{AB,CD} + R_{BC,DA}}{2}\right) f\left(\frac{R_{AB,CD}}{R_{BC,DA}}\right) \qquad 6.1.3$$

where d is the thickness of the disc, $R_{AB,CD}$ is the potential difference $V_D - V_C$ between contacts D and C per unit current through A and B, and $f\left(\frac{R_{AB,CD}}{R_{BC,DA}}\right)$ is a function which, for a disc shaped sample with contacts placed symmetrically around the circumference, is approximately unity. The exact value of $f\left(\frac{R_{AB,CD}}{R_{BC,DA}}\right)$ for a given ratio $\frac{R_{AB,CD}}{R_{BC,DA}}$ is obtained from a graph in the original paper. The contacts A,B,C,D are placed at any points around the circumference of the disc in a clockwise or anticlockwise direction.

The quantities $R_{AB,CD}$ and $R_{BC,DA}$ were obtained from graphs of $V_D - V_C$ against $I_{AB}$, and $V_A - V_D$ against $I_{BC}$ respectively. Currents up to 20 μA were passed through the sample. Measurements were taken at room temperature and at 77°K by immersing the Hall probe in liquid nitrogen.

The Hall mobility and carrier concentration were measured from the change, $\Delta R$, in the resistance $R_{BD,AC}$ when a magnetic field, B, was applied perpendicular to the sample. Then

$$\mu_H = \frac{d\sigma \Delta R_{BD,AC}}{B} \qquad 6.1.4$$

and

$$n = \frac{B}{de\Delta R_{BD,AC}} \qquad 6.1.5$$

$\Delta R_{BD,AC}$ was found from the change in the gradient of the graph of $V_C - V_A$ against $I_{BD}$ when the field B was applied. Currents up to 40 mA were passed through the samples and normal precautions were taken to eliminate thermal e.m.f.'s.

The main errors introduced in the measurement of σ and n were due to the finite contact sizes and distance away from the disc circumference of each contact. Methods of determining these errors, described in van der Pauw's original paper, led to a calculated error of about 5% in both σ and n.

## 6.2 Surface Barrier Capacitance Measurements

### 6.2.1 Introduction

If it is not possible to take Hall and resistivity measurements over a sufficiently wide temperature range to allow the determination of $N_D$, $N_A$ and $E_D$ explicitly, then a measurement of the surface barrier capacitance permits an estimate of the quantity $N_D - N_A$ to be made. This technique was first suggested by Schottky[64] in 1942 in connection with the height of the potential barrier at metal-semiconductor boundaries and is commonly referred to as the Schottky barrier technique.

If a metal contact is deposited on the surface of an extrinsic semiconductor, and a voltage applied across the junction, then a depletion region forms beneath the contact. The width and capacitance of this region varies with applied voltage and acts as a barrier to the flow of mobile carriers from the metal to the semiconductor. The capacitance C is proportional to the excess of ionized centres of a given type in the depletion region and hence it is possible to determine the density of ionized centres $N_D - N_A$ from a variation of C with applied voltage V. Assuming that all the shallow donors are thermally ionized at room temperature or, as is certainly true in the depletion region, stripped of loosely bound electrons by the strong electric fields, then $N_D - N_A$ is given by

$$N_D - N_A = -2\left[ek\frac{d(A/C)^2}{dV}\right]^{-1} \qquad 6.2.1$$

as derived by Goldman[65] where A is the area of the metal contact, k the dielectric constant, and e the electronic charge.

Therefore $N_D - N_A$ beneath the metal contact can be found from the gradient of $1/C^2$ against V.

6.2.2 Sample Preparation

Unlike the Hall measurements, we do not require any restrictions on the shape of the sample. Each sample was etched and washed in bromine-methanol just as for the Hall measurements. Two indium dots were then fused to one surface of the sample in the r.f. heater and their ohmicity checked in the usual way. The sample was re-etched without the necessity of protecting the indium contacts and stored under propanol.

When contacts had been placed on all of the samples, they were placed under masks of known cross-sectional area, A, in a Nanoteck evaporating chamber. A small amount of gold was then deposited on each sample, thus forming the metal rectifying contact. The gold contact was deposited on the opposite surface to the one on which the indium dots had been placed. The thickness of the gold film was not critical.

6.2.3 Measurements

Having placed ohmic and rectifying contacts on all samples the surface barrier capacitance measurements could be performed. Each sample was placed in a spring clip sample holder with the indium dots placed in contact with a copper strip, while the gold contact was held firmly by a german silver pressure contact.

An initial check was made to ensure that the V-I characteristics of the diode displayed the correct behaviour in both forward and reverse bias. Currents increasing in decade steps between 1 μA and 10 mA were passed through the diode in both directions and the voltage measured on a digital voltmeter. Having applied a small oscillating voltage of about 1 Mc/s the capacitance C and impedance R of the diode at that frequency were balanced on a Wayne-Kerr r.f. bridge for reverse bias voltages between 0 and 4v. The balance condition was

monitored on a FARNELL A.C. millivoltmeter.

The values of $N_D - N_A$ obtained by this method give only the values immediately beneath the metal contact and, because of the random distribution of impurities in the sample, this may differ from the average impurity concentration throughout the sample. In order to obtain a statistically accurate assessment of the average value of $N_D - N_A$, measurements must be taken at a number of points over the sample surface. Any gross inhomogeneities in the doping throughout the sample would also show up using this technique.

We were unable to perform the many different measurements necessitated by this technique but we did take measurements from the centre and edges of the same disc where the doping inhomogeneities were expected to be greatest and from these measurements we were able to obtain an average value of $N_D - N_A$ for each sample.

## 6.3 Other Analytical Techniques

In performing the Hall and Surface Barrier capacitance measurements we assumed that the samples were free of all other impurities other than the one species accounting for the shallow donor level of concentration $N_D$ and the one species making up the total ionized acceptor concentration $N_A$. This was certainly not the true situation for the L.E.C. grown samples studied in this project and, although the above techniques provided reasonably good estimates of $N_D$, $N_A$ and $E_D$, a further detailed spectroscopic analysis was made to determine the exact nature and concentrations of all the impurities in our samples. This was done by D.C. arc excitation of the impurity energy levels and, although the technique was not sensitive to several rather important known impurities, it did provide us with a more realistic appraisal of the impurity content of our samples.

For reasons of sample and financial shortage no mass spectrographic analysis was made on our samples. However there was available, data[31,66] of m.s. analyses carried out on samples grown by similar

techniques at S.E.R.L. and, from this data, we could make reasonable estimates of impurity concentrations not revealed by D.C. arc excitation.

## 6.4 N.M.R. Techniques

### 6.4.1 Set Up Procedure

Before making any n.m.r. measurements on the 6.5 Mc/s and 10 Mc/s equipment, it was necessary to tune each stage of the transmitter for maximum power output. This was done by maximizing the voltage across a 50Ω dummy load placed across the output of each stage in turn. Having done this the tuning capacitors in the L matching circuit were adjusted for maximum voltage across the transmitter coils as measured on a high voltage probe placed directly across them. A small reference signal from the oscillator was applied to the transmitter coil and the resulting signal pick-up in the receiver coil permitted the tuning of the preamplifier and receiver for maximum gain.

Because of the phase coherent detection in the receiver, it was possible to observe beats on the scope between the reference signal into the receiver and an n.m.r. signal which had Larmor frequency close to that of the reference as the magnetic field approached the resonance condition. By adjusting the magnetic field and phase of the reference signal until a condition of zero beat and signal was obtained, the field could be set exactly on resonance, with the reference $90^{\circ}$ out of phase with the n.m.r. signal.

The techniques we used to measure $T_1$ required sequences of pulses of sufficient size to tip the nuclear magnetization through exactly $90^{\circ}$ or $180^{\circ}$. The $90^{\circ}$ pulse was obtained by adjusting the reference phase and pulse width until the size of the free induction decay on the scope was a maximum. The $180^{\circ}$ pulse was obtained by increasing the width of the $90^{\circ}$ pulse until zero signal was again observed. The time interval between pulses during this procedure was kept at approximately $5T_1$ so as to allow all of the nuclear magnetization to return to the field direction before the application of another pulse.

6.4.2 Measurement of $T_1$

Two methods for measuring the nuclear spin-lattice relaxation time were employed throughout this work. The first method involved the application of a $180^o$ pulse to invert the equilibrium nuclear magnetization, followed by a $90^o$ pulse at some time $\tau$ later when the magnetization in the field direction had grown back to zero resultant amplitude. At this one time $\tau$ the free induction decay following the $90^o$ pulse was zero and

$$\tau = T_1/\ell n\ 2\ . \qquad 6.4.1$$

The second method[67] consisted of applying a series of around ten $90^o$ pulses spaced by approximately $5T_2$ which, due to the lack of any appreciable coherence effects between pulses, saturated the nuclear spin system. At any time t after saturation by this 'pulse train' the free induction decay magnitude S(t) following a $90^o$ measuring pulse was proportional to the amount of nuclear magnetization which had returned to the field direction in that time. The equilibrium magnetization $S_o$ was found by waiting a time equal to approximately $5T_1$ before applying the $90^o$ pulse. Then, assuming that for all times after saturation the recovery of the nuclear magnetization follows a simple exponential relationship, the following equation holds

$$S(t) = S_o(1-e^{-t/T_1})\ . \qquad 6.4.2$$

Therefore, having taken measurements of S(t) at several values of t up to $3T_1$ after saturation, a semilogarithmic plot of $\ell n(S_o - S(t))$ against t should be a straight line of gradient $-1/T_1$. This behaviour was observed at all times after saturation except in a number of special cases described in chapter 8.

The latter method was preferred to the former despite the longer time required to measure any particular $T_1$ by this method, and the $180^o \sim \tau \sim 90^o$ method was only used infrequently to check the validity

of the experimental technique. The reasons for this preference were two-fold. Firstly, in spin systems in which quadrupole effects perturb the Zeeman resonance, a 180° pulse may only invert the $m_I = \pm\frac{1}{2}$ levels for all spins, and only some of the spins in the other levels due to the first order shift in the resonant frequency of these satellite levels[68]. This incomplete inversion of the nuclear magnetization would result in a non-exponential recovery of S(t) and an erroneous measurement of $T_1$. Hence this method could not be used for the two Ga isotopes in GaP since both have spins 3/2 and electric quadrupole moments. Secondly, short-time nonexponentialities in the nuclear magnetization recovery is a characteristic of diffusion limited relaxation to paramagnetic impurities described in section 4.4.6 and, of the two methods, only the pulse train method unambiguously revealed this feature.

### 6.4.3 Measurement of Dipolar Relaxation Times $T_{1dd}$

Several measurements of the dipolar relaxation times of the $P^{31}$ spins were made in the heavily doped samples to see if they revealed any further information on the nature of the electron system in these samples. Although the theory behind the concept of the dipolar relaxation time has not been developed in chapter 3 its significance can be understood from a number of references[59,69,70]. $T_{1dd}$ is essentially the nuclear relaxation time in zero field or, more precisely, in the dipolar fields produced by neighbouring spins. In order to measure $T_{1dd}$ in a high field experiment we have to transfer energy initially from the large Zeeman reservoir to the dipolar reservoir. The way this was performed experimentally was through the application of a 90° pulse followed by a 45° pulse which was 90° phase shifted with respect to the first. The phase shifting capability described in section 5.2 allowed this to be carried out and, at any time t after transfer into the dipolar reservoir, the magnitude of the signal $S_{dd}(t)$ following a 45° pulse was given by

$$S_{dd}(t) = S_{dd}(o)\, e^{-t/T_{1dd}} . \qquad 6.4.3$$

Hence $T_{1dd}$ could be calculated in a similar way to $T_1$.

6.4.4 Measurement of Knight Shift

As mentioned in section 3.5, the Knight shift is a very sensitive parameter for the study of the metal-nonmetal transition in doped semiconductors and, as it was possible that impurity banding effects might be quite large in our most heavily doped samples, it was decided to attempt to measure the shift of the resonance line of sample G, the most heavily doped sample relative to sample A, the most lightly doped sample. The method used for measuring the linewidth was that suggested by Clark[58], using a pulsed n.m.r. apparatus and a P.A.R. Boxcar Integrator.

Basically, we used the boxcar to integrate the total free induction decay signal following a $90^{\circ}$ pulse, applied every $5T_1$'s, as the magnetic field was slowly swept through resonance. Because of the beating of the reference r.f. with the signal, only when the magnetic field passed through the resonance was the integrated output of the boxcar non-zero. With the correct boxcar gate width, time constant, and field sweep rate, as calculated from Clark's paper, the output from the boxcar was proportional to either the absorption or dispersion curve of the resonance depending on whether the reference r.f. into the receiver was in phase or out of phase with the signal respectively. By connecting the boxcar output to the Y axis of an X-Y recorder while the X axis was connected to a d.c. voltage proportional to the magnetic field variation, traces of the absorption or dispersion curves could be obtained.

Two methods were used for comparing the two lines. The first involved placing both samples within the coil and observing the combined lines as the field was swept through resonance. The second method involved the construction of a sample changer so that, having obtained the absorption line of one sample the second sample was moved

into the coil while the probe remained in situ. A simple mechanical device for raising and lowering the samples into the n.m.r. coil sufficed. On sweeping through the resonance again any shift in the resonant field of the two samples could be detected by the shift in the position of the absorption peak on the X-Y plot.

6.4.5 Temperature Control

In order to compare the experimental values of the many physical parameters described above with the various theories concerning their behaviour in doped semiconductors, and hence deduce some knowledge of the physical processes occurring in our samples, it was necessary to be able to take measurements of these quantities at a number of different temperatures. Methods therefore had to be devised for achieving, maintaining and measuring these temperatures.

Temperatures between 25°K and 300°K were measured using a copper-constantan thermocouple placed as near to the sample as was possible without interfering with other measurements. This restricted the placing of the thermocouple in the crossed coil n.m.r. probe to 0.5 cm away from the sample since placing it any closer affected the coupling between the transmitter and receiver coils. Temperatures between 77°K and 63°K were achieved to a stability of $\pm\frac{1}{2}$°K by filling the helium space in the cryostat with liquid nitrogen and using controlled pumping with a rotary pump to reduce the vapour pressure. Similarly, temperatures between 4.2°K and 1.6°K could be produced by pumping on liquid helium with a large capacity pump. The temperature was measured from the helium vapour pressure as given by a mercury barometer connected between the helium pumping line and the cryostat.

In order to obtain a complete set of $T_1$ data at 6.5 Mc/s, it was found necessary to be able to control the temperature some way above 77°K and below 63°K. The first system devised to attain the high temperature range involved the filling of the probe holder with helium exchange gas while the remainder of the helium chamber contained liquid

Fig. 6.4.1

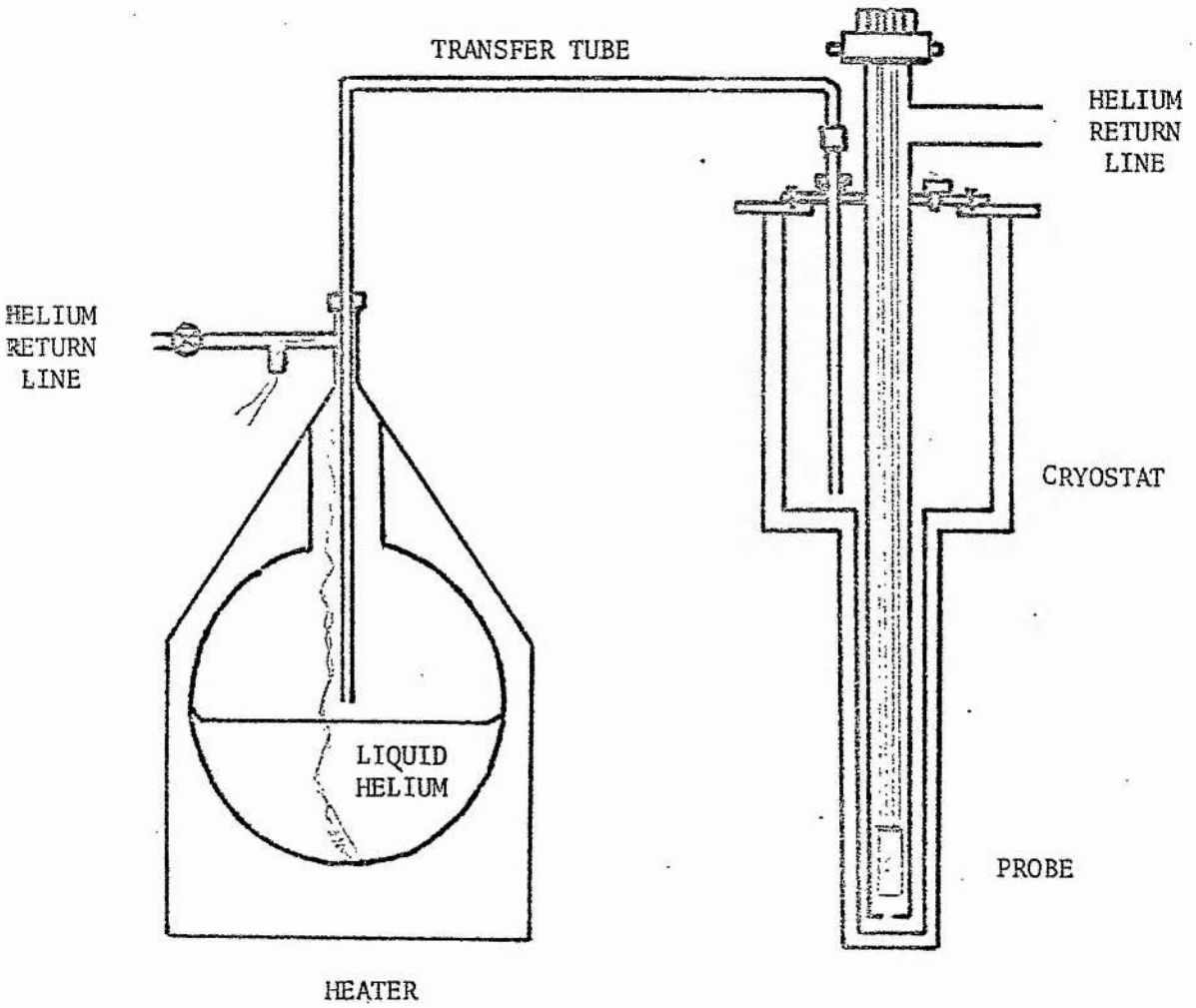
TRANSFER TUBE
HELIUM
RETURN
LINE
HELIUM
RETURN
LINE
CRYOSTAT
LIQUID
HELIUM
PROBE
HEATER

nitrogen. By attaching non-inductively wound heater coils to the n.m.r. probe, above and below the sample, and dissipating up to 20 watts in the heaters, temperatures up to 100°K were possible before local heating in the coils, and rapid nitrogen boil-off, necessitated a more efficient control system being devised.

6.4.6 Helium Gas-Flow System

A helium gas flow system was set up which enabled stable temperatures between 25°K and 63°K to be reached with an accuracy of measurement from the copper-constantan thermocouple of ±1°K. The system, shown diagrammatically in Fig. 6.4.1, forced cold helium gas to flow passed the sample and hence cool it. A 1kΩ wire-wound resistor placed inside the liquid helium vessel, below the liquid level, caused helium gas to flow along the transfer tube into the cryostat. The gas was then forced to flow passed the sample by having a small hole at the base of the probe holder and the only outlet from the cryostat to the helium return line at the top of the holder.

The temperature could be changed by varying either the flow rate or the power dissipation in the heater coils around the sample. The minimum stable temperature possible with this system was 25°K as the path taken by the helium gas after leaving the helium vessel was lengthy, and a certain amount of heating on the way was inevitable. Temperatures took less than 30 minutes to stabilize and this was sufficiently short to make the system operable. It was found also that temperatures between 63°K and 200°K could be achieved with this system but the stabilization time became prohibitively long at the high temperature end of this region. The optimum power dissipation in the 1kΩ resistor was about 2 watts, which corresponded to a helium boil-off rate of 2 litres/hour, while the maximum power required in the sample heating coils was about 18 watts.

Fig. 7.1.1

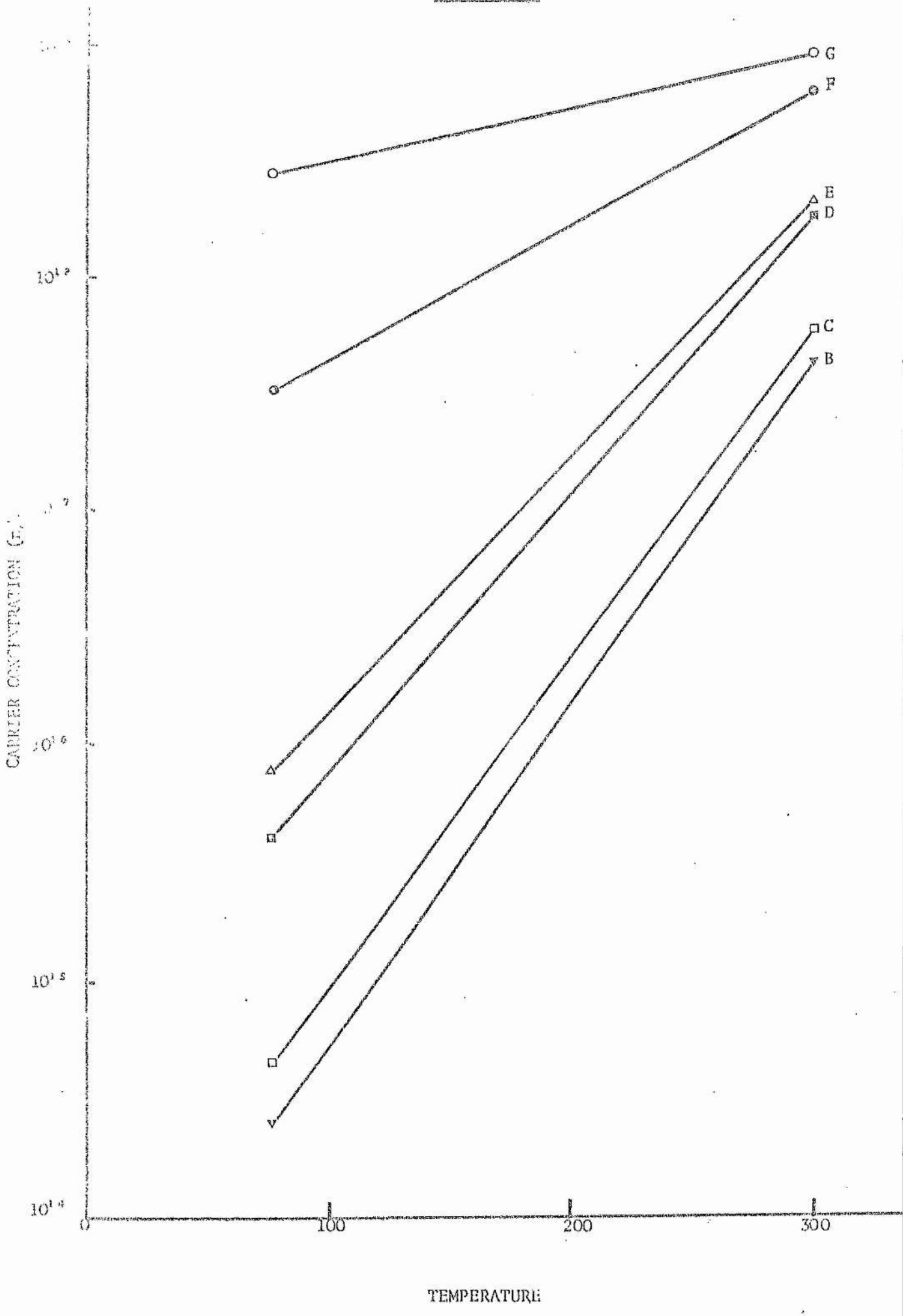

# CHAPTER VII

# RESULTS AND DISCUSSION

## 7.1 Hall and Conductivity Measurements

Hall and electrical conductivity measurements were made in samples B to G at 295°K and 77°K. All samples were n-type and the measured values of carrier concentration n, conductivity σ, and Hall mobility $\mu_H$ are listed below.

| Samples | (Carrier Concentration) n/c.c. | | (Electrical ) σ (Conductivity) $(\Omega\ cm)^{-1}$ | | (Hall Mobility) $\mu_H (cm^2\ V^{-1} sec^{-1})$ | |
|---|---|---|---|---|---|---|
| | 295°K | 77°K | 295°K | 77°K | 295°K | 77°K |
| B | $4.2.10^{17}$ | $2.5.10^{14}$ | 7.87 | 0.013 | 115 | 330 |
| C | $6.0.10^{17}$ | $4.6.10^{14}$ | 11.90 | 0.019 | 124 | 256 |
| D | $1.8.10^{18}$ | $4.0.10^{15}$ | 23.81 | 0.069 | 83 | 112 |
| E | $2.1.10^{18}$ | $7.6.10^{15}$ | 26.32 | 0.135 | 78 | 113 |
| F | $6.0.10^{18}$ | $3.4.10^{17}$ | 55.56 | 1.429 | 59 | 26 |
| G | $9.0.10^{18}$ | $2.8.10^{18}$ | 71.43 | 13.158 | 46 | 29 |

The estimated experimental errors in the values of n and σ were 5% while those in $\mu_H$ were 10%. No Hall or conductivity measurements were made on sample A as it was in powdered form. Its room temperature carrier concentration, measured at Ferranti Ltd., lay between $2.10^{17}$/c.c. and $4.10^{16}$/c.c. Due to the high resistivity of samples B to F at liquid helium temperatures no measurements were possible on them below 77°K. A single conductivity measurement was possible at 4.2°K in sample G and it produced a value of 0.08 $(\Omega\ cm)^{-1}$. These results are presented diagrammatically in Figs. 7.1.1 and 7.1.2.

The rapid variation of n and σ with temperature between 295°K and 77°K in samples B, C, D and E is indicative of conduction dominated by excitation of electrons from the Te donor level into the conduction band. The

Fig. 7.1.2

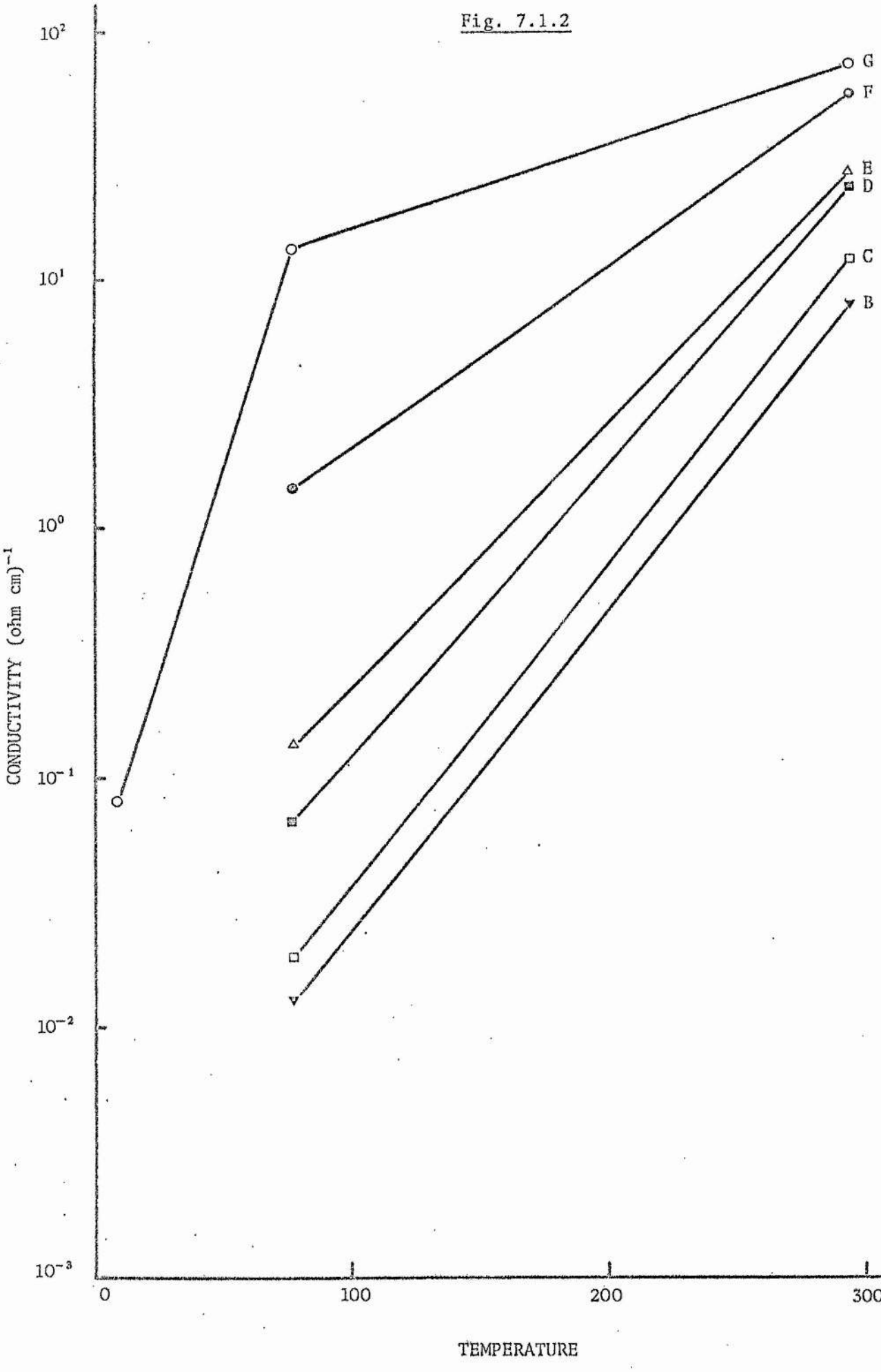
$10^2$
$10^1$
$10^0$
$10^{-1}$
$10^{-2}$
$10^{-3}$
CONDUCTIVITY (ohm cm)$^{-1}$
G
F
E
D
C
B
0
100
200
300
TEMPERATURE

weakening of this temperature dependence with increasing donor concentration resembles that observed by several authors[6,31,71,72,80] in doped gallium phosphide in this concentration range and is the result of a reduction in the donor ionization energy and the onset of impurity conduction.

Samples F and G display a marked weakening in the temperature variation of n and σ and the measurement of σ in sample G at 4.2°K is itself evidence that the donor concentration in this sample is very near that at which metallic impurity conduction takes place. We can obtain a useful estimate of just how close sample G approaches the metallic transition by comparing its Hall and conductivity behaviour with that obtained in other doped semiconductors around the metallic transition.

Yamanouchi et al[80] have obtained the most comprehensive set of transport data in Si:P and sample G has a resistivity over the temperature range 295°K to 4.2°K which closely resembles their sample no. 5 for which they estimate the total uncompensated donor concentration to be $2.69.10^{18}$/c.c. As they estimate that metallic impurity conduction occurs at donor concentrations between 3 to $4.10^{18}$/c.c. in Si:P the donor concentration in sample 5, and consequently in our sample G, is approximately 10% to 30% below that critical value.

The theoretical critical concentration $n_c$ for metallic conduction in GaP:Te can be found by substituting for the Te impurity Bohr radius, $a_H = 7\text{Å}$, in equation 2.4.1. However it has been found empirically by Alexander and Holcomb[85] that in doped Ge and Si $n_c^{1/3} a_H$ varies between 0.20 and 0.25 at the transition and if we assume that a similar variation is possible in GaP:Te then the value of $n_c$ lies between 2.3 and $4.5.10^{19}$/c.c.

Comparing our conductivity and mobility measurements with those obtained by Casey et al[6] in GaP:Zn, we find that our sample G lies somewhere between their samples 6 and 7 which have total uncompensated acceptor concentrations of 1.2 and $2.1.10^{19}$/c.c. respectively, the latter sample displaying complete metallic behaviour. Therefore, from a comparison with

Casey's results, we can say that the donor concentration in sample G appears to be within 50% of the critical concentration for metallic conductivity. Further correlation between the conductivity behaviour in our samples and Casey's was not made as the difference in ionization energies of the Zn acceptors in his samples and the Te donors in our samples makes such a comparison difficult and of dubious value.

The mobility measurements are of interest as they display the remarkably different temperature dependences in the six samples. The values obtained at room temperature agree well with the concentration dependent mobilities observed by Nygren et al[32] in Te doped L.E.C. material. The decrease in $\mu_H$ at low temperatures can be explained in terms of scattering by ionized impurities. Substantial compensation, necessary for such a scattering mechanism, is expected in these samples[31], and similar mobility behaviour has been observed by several authors[31,32,71,73] in doped GaP.

Dean et al[74] have found $E_D$ to be 93 meV for Te donors in GaP at infinite dilution and Montgomery[72] has shown that $E_D$ decreases to about 40 meV for donor concentrations of about $8.10^{18}$/c.c. Therefore, in the concentration range covered by our samples, it is unlikely that all of the donors are ionized at room temperature. However it is true that the difference between the measured value of n and the actual value of $N_D - N_A$ will decrease as the ionization energy decreases. Without taking measurements of n and $\sigma$ over a wide temperature range the determination of $N_D$, $N_A$, $E_D$ and $m^*$ is difficult and we have to make a number of assumptions in order to obtain reasonable estimates of the above quantities from the data available.

## 7.2 Schottky Barrier Capacitance Measurements

Before analysing the Hall data any further we will present the results from the Schottky barrier measurements. Measurements were made at room temperature in samples B to F. In samples C, D, E, and F

measurements were made on a number of different pieces of the same sample and an average value of $N_D - N_A$ obtained. The results are shown in table 7.2.1.

Table 7.2.1

| Sample | B | C | D | E | F | G |
|---|---|---|---|---|---|---|
| $N_D - N_A$ $cm^{-3}$ | $5.10^{17}$ | $9.6\pm0.5$ $.10^{17}$ | $2.3\pm0.8$ $.10^{18}$ | $2.6\pm0.5$ $.10^{18}$ | $1.07\pm0.13$ $.10^{19}$ | $9.5\pm0.65$ $.10^{19}$ |

As mentioned in 6.2.3, the values of $N_D - N_A$ obtained by this method are strictly values of the density of ionized impurities in the depletion region immediately beneath the metal rectifying contact. As such, therefore, the method does not give an accurate indication of the average value of $N_D - N_A$ unless measurements are taken at many points throughout the sample. This was not possible, even in samples C, D, E and F for which measurements were made on more than one piece of each sample. However the results do show that, in general $N_D - N_A \geq n$ as we would expect from the previous discussion of the Hall data.

## 7.3 Mass spectrographic data

Mass spectrographic data for doped crystals grown by the L.E.C. technique at S.E.R.L. are given in appendix I.

These data indicate that as well as the intended dopant there might be substantial concentrations of B, C, O, N, Al and Si unintentionally added to our samples. Of these elements B, N, and Al enter GaP isoelectronically and so do not affect the electrical properties directly. C and O form deep donor levels and will be electrically neutral in n-type GaP:Te. Only Si forms a shallow donor level, lying at 82 meV below the conduction band at infinite dilution, and Young and Bass[31] have found that its concentration increases towards the tail end of each pulled crystal.

The maximum donor concentration calculated by them from Hall data in undoped material was $8.10^{18}$/c.c. and, due to the large amount of compensation, the maximum room temperature carrier concentration was $2.10^{18}$/c.c. The minimum donor concentration in undoped material, grown in a silica crucible without the addition of $Ga_2O_3$ to remove the Si contaminant, was calculated to be $6.10^{16}$/c.c. The room temperature carrier concentration in this sample was $4.10^{16}$/c.c. When a BN crucible was used instead of silica the measured Si content was much lower.

The mass spectrographic data from S.E.R.L. indicates that the majority of our samples were grown in a BN coated graphite crucible. Thus the Si concentration should be low compared with the concentration of the intentionally added dopant Te in our samples. From the results stated in the last paragraph concerning the room temperature carrier concentrations in undoped material, the fact that the room temperature carrier concentrations in all but two of our samples is greater than $1.8.10^{18}$/c.c. is further evidence that the Si concentration is small compared with the Te donor concentration.

Confusion should not be aroused by the large Si concentration found in the mass spectrographic data in Appendix I for the crystal grown in a C/BN crucible since, for that particular crystal, Si was the intentionally added dopant.

## 7.4 D.C. Arc excitation analysis

The results of the d.c. arc excitation analysis of all our samples are presented in appendix II. These measurements were made near the end of the project without the direct supervision of the author and, although the results for the Te concentrations are in reasonable agreement with results from other techniques, there are good reasons for questioning the validity of the concentration values obtained for the unintentionally added impurities. None of the sets of mass

spectrographic data from crystals grown in the furnaces at S.E.R.L. by the L.E.C. technique show the exceptionally large concentrations of impurities indicated by these results. It may be possible that some of the elements detected in this analysis were due to surface contamination of the samples after long periods of handling in the laboratory. Several experiments were performed on the samples which could have resulted in such contamination although, of course, such surface contamination would not affect the n.m.r. or Hall measurements. The Te concentrations as obtained from the d.c. arc excitation measurements are given in table 7.4.1.

Table 7.4.1

| Sample | A | B | C | D | E | F | G |
|---|---|---|---|---|---|---|---|
| Te /c.c. | $<6.10^{18}$ | $<6.10^{18}$ | $<6.10^{18}$ | $<6.10^{18}$ | $6.10^{18}$ | $1.2.10^{19}$ | $2.4.10^{19}$ |

The technique was not sensitive to the elements Si, O, N and C. The sensitivity of the technique was approximately $6.10^{18}$/c.c. for Te, and so it does not provide any information on the Te concentrations in samples A to D other than that they are less than $6.10^{18}$/c.c. The precision of the measurements in samples E to G was 25%. The rather high values for Te concentrations in samples E to G could be indicative of the presence of substantial segregation and self compensation in these highly doped samples.

## 7.5 Determination of $N_D - N_A$

It is clear that none of the above techniques has provided explicit values for $N_D - N_A$ in our samples. By making certain assumptions about the effective mass, ionization energy and degree of compensation it is possible to obtain estimates of $N_D - N_A$ from the Hall measurements at $295^{\circ}K$ and $77^{\circ}K$ in samples B and C, where the difference between n and

$N_D - N_A$ are expected to be greatest.

From equation 6.1.2 we have that

$$\frac{n(N_A+n)}{N_D - N_A - n} = \left(\frac{2\pi m^* kT}{h^2}\right)^{3/2} \exp\left(-\frac{E_D}{kT}\right) \qquad 7.5.1$$

and at 77°K in samples B and C $n << N_D - N_A, N_A$. Therefore we can write

$$\frac{N_A}{N_D - N_A} = \frac{1}{n}\left(\frac{2\pi m^* kT}{h^2}\right)^{3/2} \exp\left(-\frac{E_D}{kT}\right) . \qquad 7.5.2$$

By substituting various trial values of $E_D$ into this equation we can obtain possible compensation ratios corresponding to each value of $E_D$. On substituting these values into 7.5.1 for T = 295°K we can then obtain a series of possible $N_D$ and $N_A$ values for both samples. We expect large compensation ratios of around 30% in these L.E.C. samples and so this helps to fix the value of $E_D$. A complication arises due to the fact that $E_D$ may decrease with increasing temperature above a certain temperature due to ionized impurity screening effects. This mechanism was suggested by Neumark[6,75] to explain the discrepancy between the values of $N_D$ and $N_A$ calculated by Hall and neutron activation measurements in zinc doped gallium phosphide. We made a correction for this effect by substituting values of $E_D$ in 7.5.1 which were 10% smaller, than the value used in 7.5.2 to obtain $N_A/N_D$, this percentage being the observed reduction in GaP:Zn.

For semiconductors with silicon type band structure the density of states effective mass is given by

$$m^* = M^{2/3} (m_t^2 m_\ell)^{1/3} \qquad 7.5.3$$

where M is the number of conduction band minima and $m_t$ and $m_\ell$ are the transverse and longitudinal effective masses. In GaP, Orton and Taylor[76] have measured $m_t$ and $m_\ell$ to be 0.18 $m_o$ and 1.5 $m_o$ respectively

and if we assume there are only three conduction band minima then $m^* = 0.76\ m_o$. Our assumption of only three minima is equivalent to saying that the minima occur at, or very near, the X points in the reduced Brillouin zone. Recent neutron scattering measurements[77] indicate that this is indeed so. The approximate values of $N_D - N_A$ and $E_D$ obtained from this rather crude analysis are given below.

| Sample | $N_D - N_A$/c.c. | $E_D$ meV |
|---|---|---|
| B | $6.8 \pm 0.3 . 10^{17}$ | 60 |
| C | $9.8 \pm 0.3 . 10^{18}$ | 60 |

Samples D to G could not be analysed by this method as impurity conduction at low temperatures affected the value of n at 77°K and hence equations 7.5.1 and 7.5.2 are not valid. However the Schottky barrier measurements give reasonable estimates of the values of $N_D - N_A$ in these samples. The exceptionally high value of $N_D - N_A$ obtained by the Schottky barrier technique for sample F may be indicative of the presence of substantial concentrations of deep lying unionized donors in this one sample.

The best estimates of $N_D - N_A$ derived from the above calculations and analyses in each of our samples are given below in table 7.5.1.

Table 7.5.1

| Sample | A | B | C | D | E | F | G |
|---|---|---|---|---|---|---|---|
| $N_D - N_A$ /c.c. | $2.10^{17}$ | $6.8 \pm 0.3 . 10^{17}$ | $9.8 \pm 0.3 . 10^{17}$ | $2.3 \pm 0.8 . 10^{18}$ | $2.6 \pm 0.5 . 10^{18}$ | $1.07 \pm 0.13 . 10^{19}$ | $9.5 \pm 0.65 . 10^{19}$ |

## 7.6 Discussion

There still remains some uncertainty surrounding the purity of our samples and only a thorough, carefully controlled, analysis would clear

away this uncertainty. However as mentioned in chapter 2, the problem of unintentionally added impurities is not just one concerning our seven samples but a general problem in the growth of large single crystals of III-V compounds.

The effects that these unintentional impurities will have on the n.m.r. results to be discussed in the next chapter will depend on a number of factors which will be revealed during the discussion of the n.m.r. results. However as the only controlled variable in our samples is the Te donor concentration, and as the main features of the n.m.r. results show a dependence on this concentration which in general can be interpreted quite satisfactorily neglecting the effects of other impurities, it seems reasonable to assume that the Te concentration, and not that of other impurities, determines the majority of the n.m.r. features found in our results.

FIGURE 8.1.1

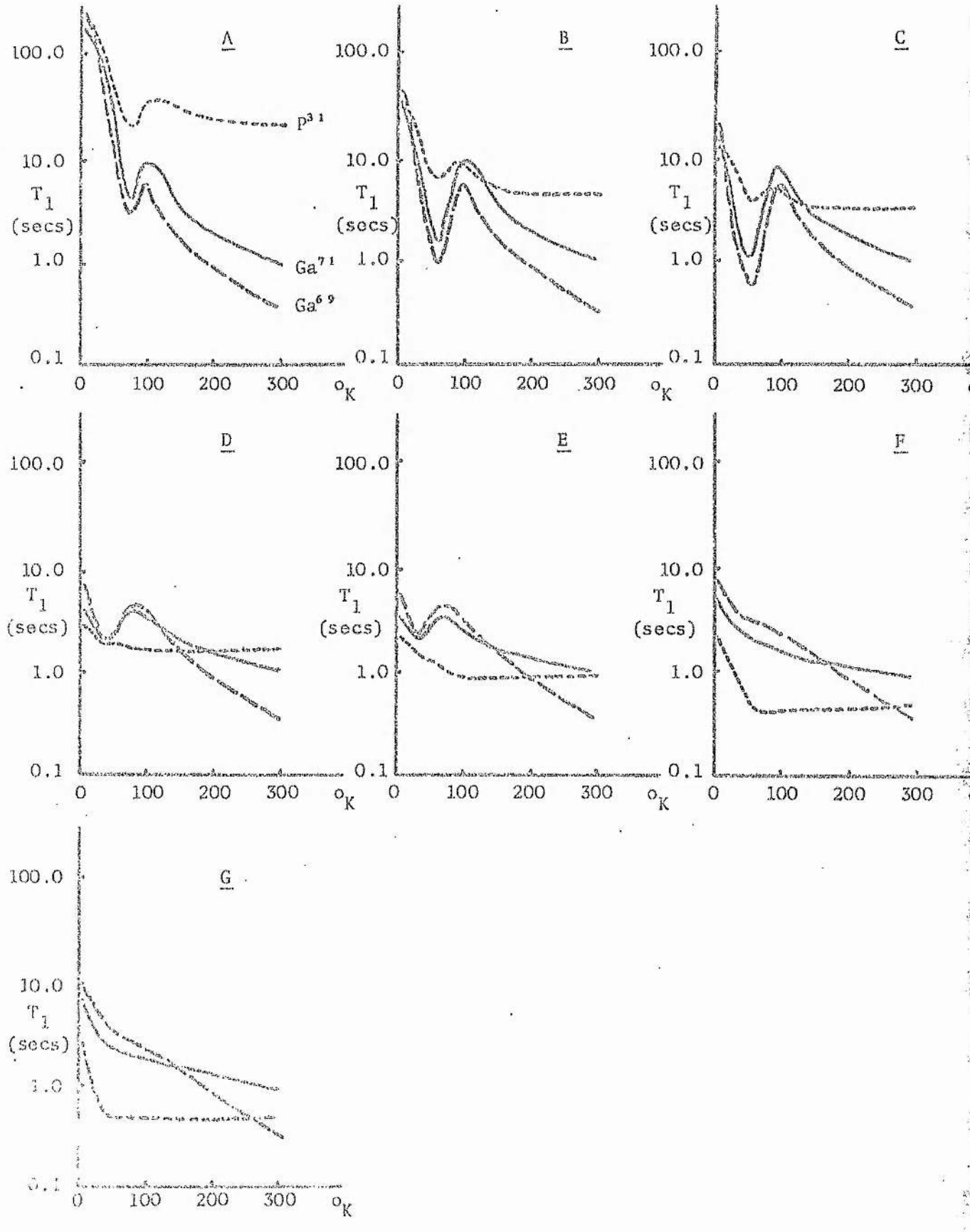

# CHAPTER VIII

# N.M.R. RESULTS

## 8.1 $T_1$ measurements at 6.5 Mc/s

Measurements of the nuclear spin-lattice relaxation times, $T_1$, of the $P^{31}$, $Ga^{69}$ and $Ga^{71}$ isotopes in samples A to G were made at 6.5 Mc/s between 1.8°K and 295°K. The results are shown in Fig. 8.1.1 and the main features of the $T_1$:T curve for each sample is described below.

In all but the most heavily doped samples, each $T_1$:T curve is characterized by a minimum which occurs at the same temperature for all three isotopes in the same sample, and which is shifted to progressively lower temperatures in samples A to E [Figs. 8.1.2, 8.1.3, 8.1.4]. On moving to lower temperatures the minimum broadens and the value of $T_1$ at the minimum, $T_1$ min, decreases with increasing donor concentration in samples A to C but increases again in samples D and E. The behaviour of $T_1$ min for the $P^{31}$ nuclei in samples A to C follows that of the two Ga isotopes but in samples D and E no discernable minima are observed. In samples F and G no distinct minima are observed in the $T_1$:T curves of any of the isotopes.

Short-time non-exponentialities, lasting for as long as one second after initial saturation of the spin system by the pulse train, are observed in the magnetization recoveries of the $Ga^{69}$ and $Ga^{71}$ nuclei at temperatures around the $T_1$ minimum. The percentage of the equilibrium magnetization that recovers during this period varies from around 25% at the $T_1$ minimum in sample A to less than 5% at the minimum in sample E. The length of the non-exponentiality is greater for $Ga^{71}$ nuclei (1 second) than $Ga^{69}$ nuclei ($\frac{1}{2}$ second) in the same sample. No such non-exponentialities are observed in the $P^{31}$ recovery in any samples.

For the two Ga isotopes, the minima are superimposed upon an additional inverse temperature dependence of the $T_1$'s characteristic of the quadrupolar relaxation $T_1$:T curves obtained by Weber[43] in undoped gallium phosphide. Above the minima, the almost temperature independent $T_1$'s of the $P^{31}$ nuclei

Fig. 8.1.2

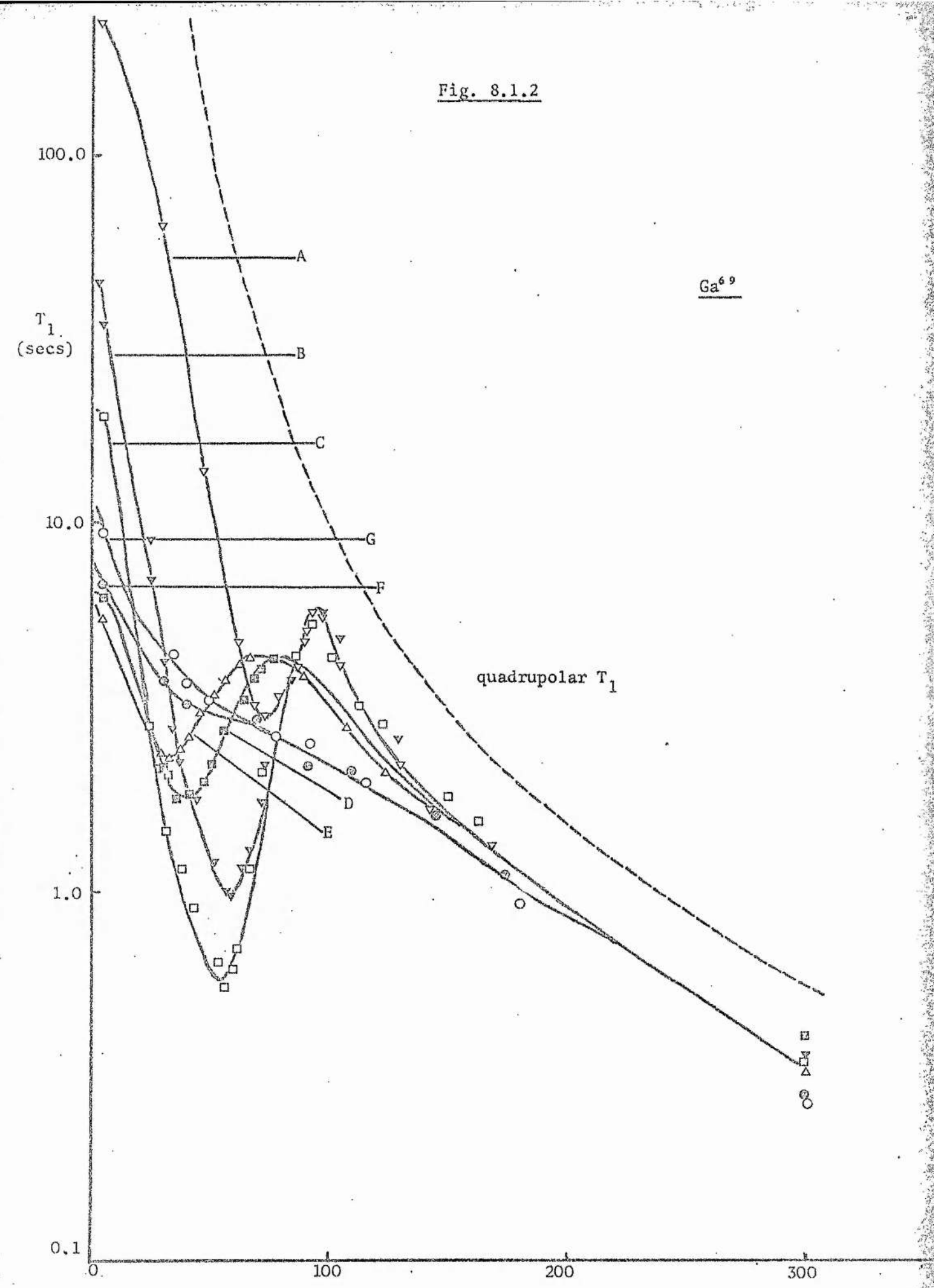
100.0
10.0
1.0
0.1
$T_1$ (secs)
A
B
C
G
F
D
E
$Ga^{69}$
quadrupolar $T_1$
0
100
200
300
TEMPERATURE

Fig. 8.1.3

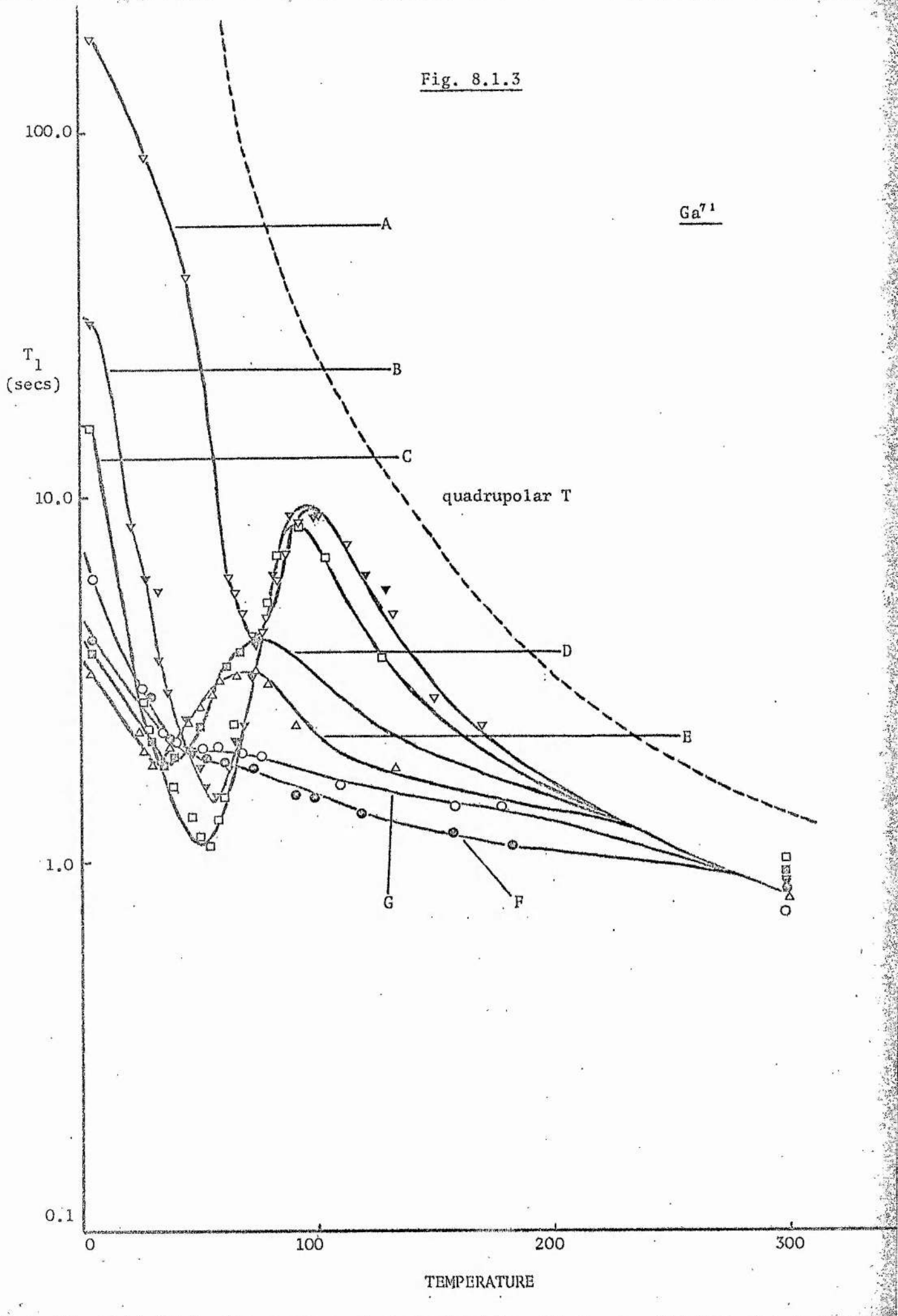
100.0
10.0
1.0
0.1
$T_1$ (secs)
A
B
C
D
E
F
G
quadrupolar T
$Ga^{71}$
0
100
200
300
TEMPERATURE

Fig. 8.1.4

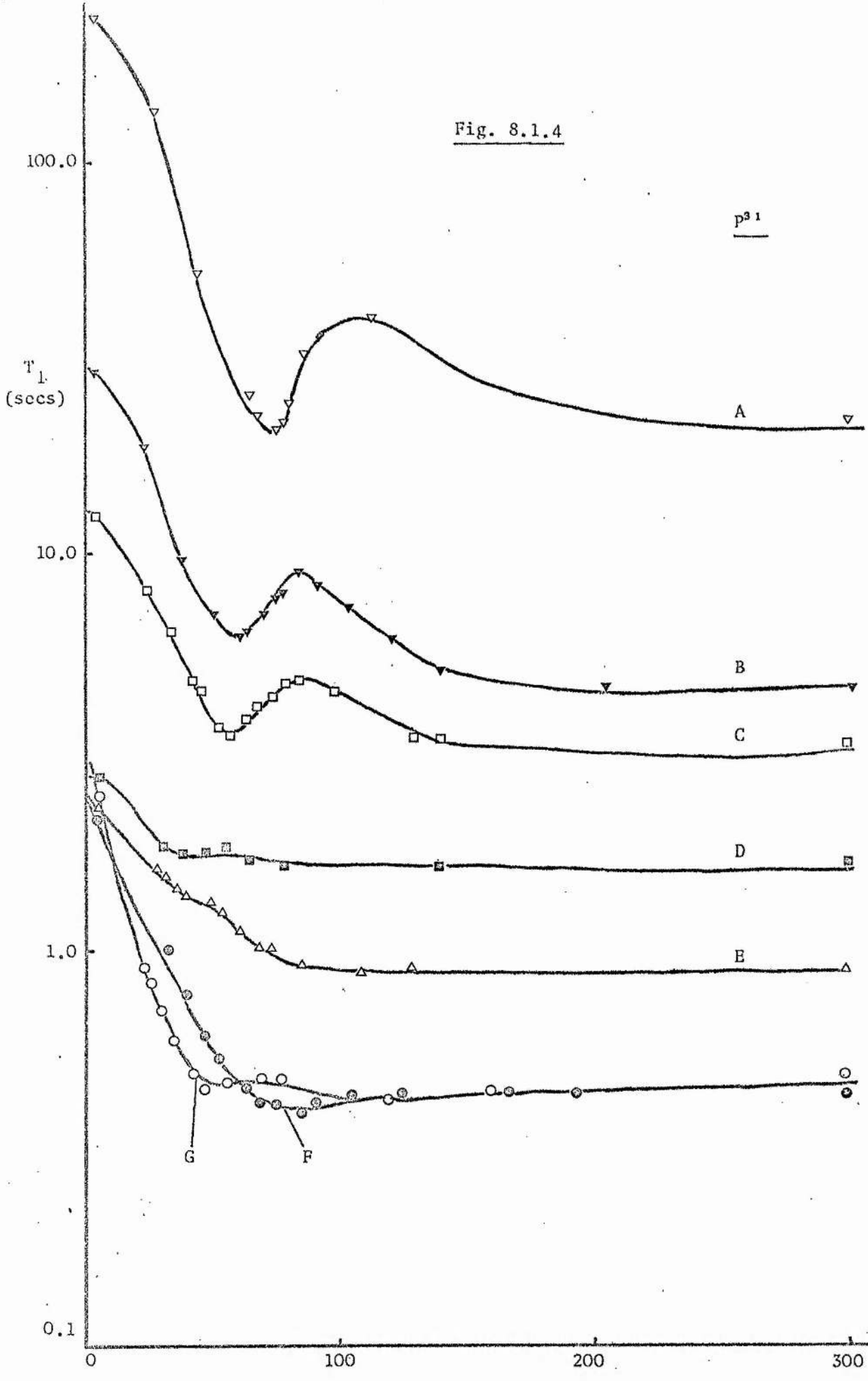

are again similar to the high temperature results of Weber. Below the minima in samples A to C the $P^{31}$ relaxation times increase with decreasing temperature while similar low temperature behaviour is observed in samples E, F and G below a temperature which has a minimum value, of around $50^{\circ}K$, in sample G.

Below $4.2^{\circ}K$ the $T_1$'s of all three isotopes in samples B to G display only weak temperature dependences [Fig. 8.11.1]. The largest percentage variation in $T_1$ between $1.8^{\circ}K$ and $4.2^{\circ}K$ is observed for the $P^{31}$ nuclei in sample G where a $T_1 \propto T^{-\frac{1}{2}}$ relationship appears to hold. The absolute values of the $T_1$'s at $4.2^{\circ}K$ decrease by about two orders of magnitude in going from sample A to E. However for all three isotopes in sample G there is a marked increase in the $T_1$ at $4.2^{\circ}K$ and below compared with sample F.

Finally, in samples A to D, $T_1(Ga^{69}) \leqslant T_1(Ga^{71})$ at all temperatures except $4.2^{\circ}K$ and below whereas, in samples E to G, $T_1(Ga^{69}) > T_1(Ga^{71})$ below a temperature which varies from around $130^{\circ}K$ to $180^{\circ}K$ in these three samples.

Temperatures were measured to within $\pm 1^{\circ}K$ using a copper-constanton thermocouple and Doran potentiometer. The weakness of the n.m.r. signal restricted the accuracy of the $T_1$ measurements to about 5% in most samples.

Having briefly outlined the main features of the 6.5 Mc/s $T_1$ results, we now proceed to discuss each feature in more detail and attempt an explanation in terms of the relaxation mechanisms discussed in chapter 4.

## 8.2 $Ga^{69}$, $Ga^{71}$ quadrupolar relaxation

The two Ga isotopes, $Ga^{69}$ and $Ga^{71}$, both have spin 3/2 and electric quadrupole moments, $Q_{69}$ and $Q_{71}$, of $0.2318.10^{-24}$ $cm^2$ and $0.1461.10^{-24}$ $cm^2$ respectively. As mentioned in section 4.2, quadrupolar relaxation is expected to provide the dominant relaxation mechanism in undoped material at high temperatures and, superimposed on Figs. 8.1.2 and 8.1.3, we have

Mieher's[42] theoretical quadrupolar $T_1$:T curves for undoped GaP.

Despite the low signal to noise ratio at high temperatures, it can be seen that our experimental results for the $Ga^{69}$ $T_1$'s above 100°K follow the quadrupolar curve quite well. There is an overall shift to lower $T_1$ values however, and the $T_1$'s of the more highly doped samples deviate from the 'all samples common' curve at a higher temperature. Similar behaviour is observed in the $Ga^{71}$ curves but the deviation from the purely quadrupolar curve at higher doping densities is more pronounced.

The general discrepancy between the experimental and theoretical $T_1$ values can be explained in terms of the general reduction in $T_1$ values due to nuclear relaxation via interaction with paramagnetic impurities or free electrons. The strength of both these interactions depends on the size of the nuclear gyromagnetic ratio $\gamma$ and, as $\gamma(Ga^{71}) > \gamma(Ga^{69})$, we would expect the $Ga^{71}$ $T_1$:T curve to deviate from the quadrupolar curve at a higher temperature than that of the $Ga^{69}$ nuclei in the same sample. This is indeed observed.

For purely quadrupolar relaxation $1/T_1 \propto Q^2$ from equation 4.2.1 and hence, for $Ga^{69}$ and $Ga^{71}$ nuclei in the same sample

$$\frac{T_1(Ga^{71})}{T_1(Ga^{69})} = \left(\frac{Q_{69}}{Q_{71}}\right)^2 = 2.52 \; . \qquad 8.2.3$$

The mean ratio $T_1(Ga^{71})/T_1(Ga^{69})$ at 295°K in our samples is $2.41 \pm 0.14$ which is in good agreement with this purely quadrupolar value.

A complication arises when we wish to separate the quadrupolar contribution to the relaxation rate from the other contributions. If we assume that at room temperature the relaxation is purely quadrupolar, we can obtain $T_1$'s due to the other mechanisms by subtracting the theoretical quadrupolar curve which passes through our room temperature $T_1$ measurements from the experimental $T_1$:T curve. At the

temperatures around which the $T_1$ minima occur the quadrupolar relaxation rate, $1/T_{1quad}$, is much smaller than that due to paramagnetic impurities, $1/T_{1para}$, and so we can write

$$\frac{1}{T_1} = \frac{1}{T_{1quad}} + \frac{1}{T_{1para}} \qquad 8.2.4$$

and hence obtain values of $T_{1para}$ in that region. The corrected $T_1$:T curves for $Ga^{69}$ and $Ga^{71}$ so obtained are presented in Figs. 8.2.1 and 8.2.2. In any future discussion relating to the non-quadrupolar nuclear relaxation in the two Ga spin systems, we shall use the corrected values of $T_1$, that is $T_{1para}$ above, obtained from equation 8.2.4.

## 8.3 Existence of a $T_1$ minimum

It can be deduced from the temperature dependence of the Hall coefficient in samples B to E that, at the temperatures at which the $T_1$ minima occur, practically all of the uncompensated donors in our lightly doped samples are electrically neutral. They each have an unpaired orbital electron bound to them and are therefore paramagnetic. We have discussed the theory of nuclear relaxation by paramagnetic impurities in ch.4 and it is to this relaxation mechanism that we turn for an explanation of the existence of the minima in our $T_1$:T curves.

In the rapid diffusion and diffusion limited cases of nuclear relaxation by paramagnetic impurities, $T_1$ is inversely proportional to C and $C^{\frac{1}{4}}$ respectively, where C is the factor defined in section 4.4.2. Now C is proportional to $\tau/1+\omega^2\tau^2$ where $\tau$, the electron spin-lattice relaxation time of the paramagnetic donor in our lightly doped samples, may be dependent on a number of physical parameters.

The e.s.r. linewidth measurements of Thomson and Lancaster[28] on a Te doped GaP sample of donor density $4.10^{17}$/c.c. indicate that $\tau$ is strongly temperature dependent in the range $50^{\circ}K$ to $100^{\circ}K$. If we consider their measured linewidths as being made up of a constant,

Fig. 8.2.1

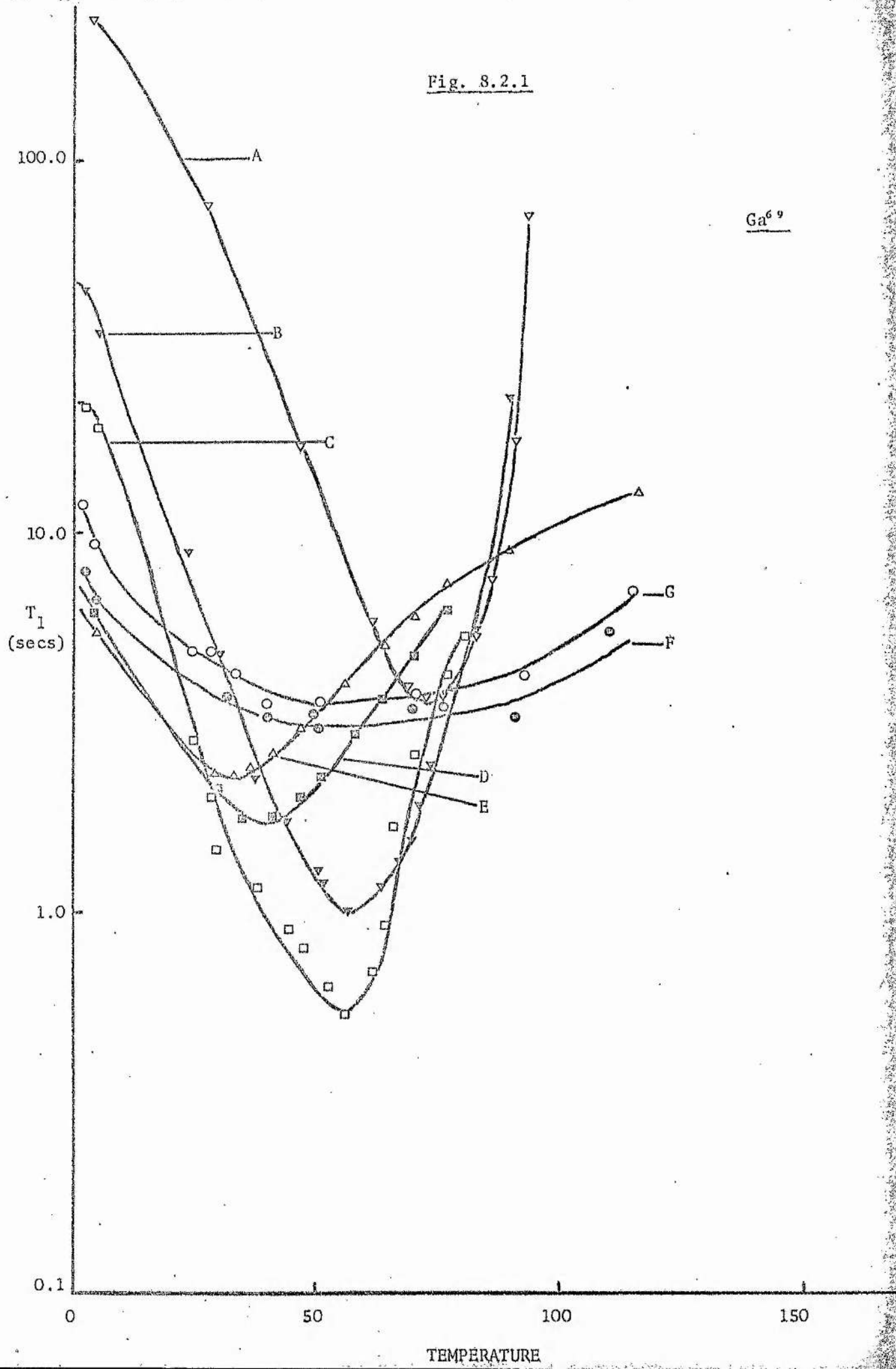

Fig. 8.2.2

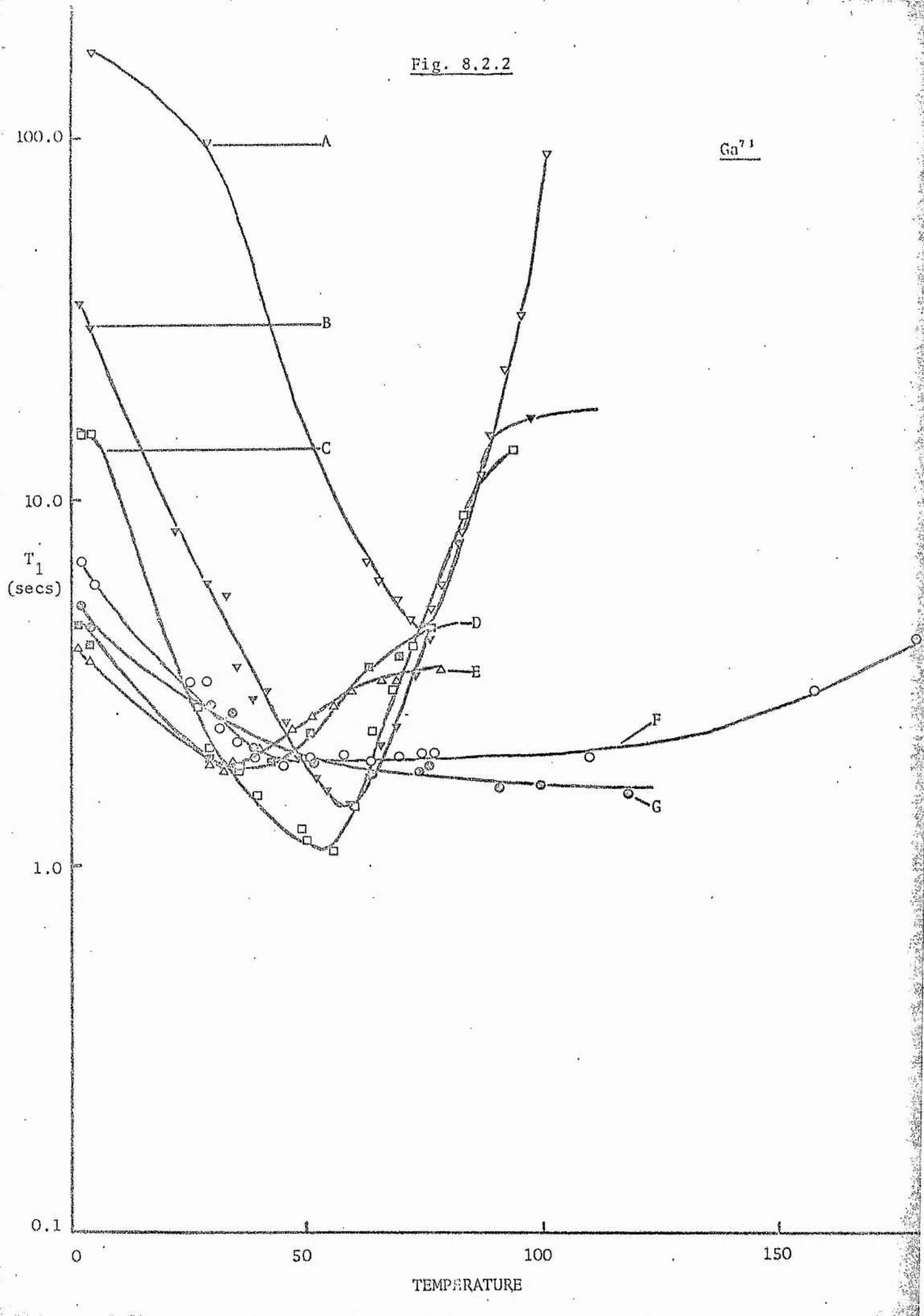

low temperature component $\Delta H(T = 0)$ and a component $\Delta H_1$ due to lifetime broadening then, at $60^{\circ}K$, $\Delta H_1 \simeq 2$ gauss. Now since $\Delta H_1 = 1/\gamma\tau$ for lifetime broadening, we can deduce that, at $60^{\circ}K$, $\tau = 3 \pm 1.10^{-8}$ seconds and is varying rapidly with temperature.

As our $T_1$ measurements were made at 6.5 Mc/s, $1/\omega = 2.44.10^{-8}$ seconds and in the temperature range in which the $T_1$ minima occur, the condition $\omega\tau = 1$ will occur. When this happens the factor C has a maximum value and $T_1$ has a minimum. Therefore we can reasonably conclude that, in samples A to C at least, the minima are the result of the resonant condition latent in the expressions for nuclear relaxation to the paramagnetic Te donors. It is not obvious at the moment whether we can apply the simple theory of nuclear relaxation by paramagnetic impurities to explain the minima in the two Ga resonances in samples D and E since no corresponding minima are observed in the $P^{31}$ $T_1$'s in these samples. We shall expand on this in more detail later.

Using equation 4.4.3 we can now calculate the orientational average values of the factor C at the $T_1$ minima for all three isotopes in samples A to C and obtain that

$$C(Ga^{69}) = 5.3.10^{-41} \quad \text{c.g.s. units}$$
$$C(Ga^{71}) = 8.4.10^{-41} \quad " \quad "$$
$$C(P^{31}) = 1.46.10^{-40} \quad " \quad "$$

## 8.4 Identification of relaxation cases ($Ga^{69}$, $Ga^{71}$)

Proceeding with the theory that nuclear relaxation by Te donors is the cause of the $T_1$ minima, we now attempt to determine which, if any, of the limiting cases of such a relaxation mechanism, described in 4.4.6 and 4.4.7, is applicable in our samples.

The existence of short-time non-exponentialities in the magnetization recovery of the two Ga resonances around the minima after

saturation is evidence for the diffusion limited case (Figs. 8.4.1, 8.4.2). However, the absence of any such non-exponentialities in the $P^{31}$ magnetization recovery (Fig. 8.4.3) in the same samples suggests initially that those observed in the Ga resonances might be due to other effects, such as the incomplete saturation of the Ga nuclear energy levels. This situation has been studied previously[68], showing that non-exponential recoveries can be expected provided the quadrupole interactions are much greater than the dipole-dipole interactions in the rotating frame. Under these conditions, the dipolar interactions are unable to maintain a Boltzmann distribution between the energy levels and, in general, nuclear relaxation is described by 2I relaxation rates.

However in our case, quadrupolar interactions are much weaker than magnetic interactions at the temperatures at which the $T_1$ minima occur and, under such conditions, the magnetization recovery rate, for a spin system with I = 3/2, follows a simple exponential provided the energy levels are initially saturated. The pulse train method was chosen specifically to ensure complete saturation and, as evidence that this occurred, no change was observed in the asymptotic recovery rate when the number of pulses in the train was increased from ten to fifty. In comparison, the value of $T_1$ obtained using the $180^\circ \sim \tau \sim 90^\circ$ pulse sequence was approximately two-thirds that obtained by the above method, thus revealing the former method's unsuitability for measuring $T_1$'s of the two Ga isotopes in our samples.

Another cause of non-exponentiality in the observed $T_1$'s could be the existence of macroscopic doping inhomogeneities in our samples. However, the failure to observe such non-exponentials in the $P^{31}$ recovery or in the two Ga recoveries far away from the $T_1$ minima rule out this possibility.

Hence we take the existence of short-time non-exponentialities in the two Ga $T_1$'s as firm evidence of diffusion limited relaxation to

Fig. 8.4.1

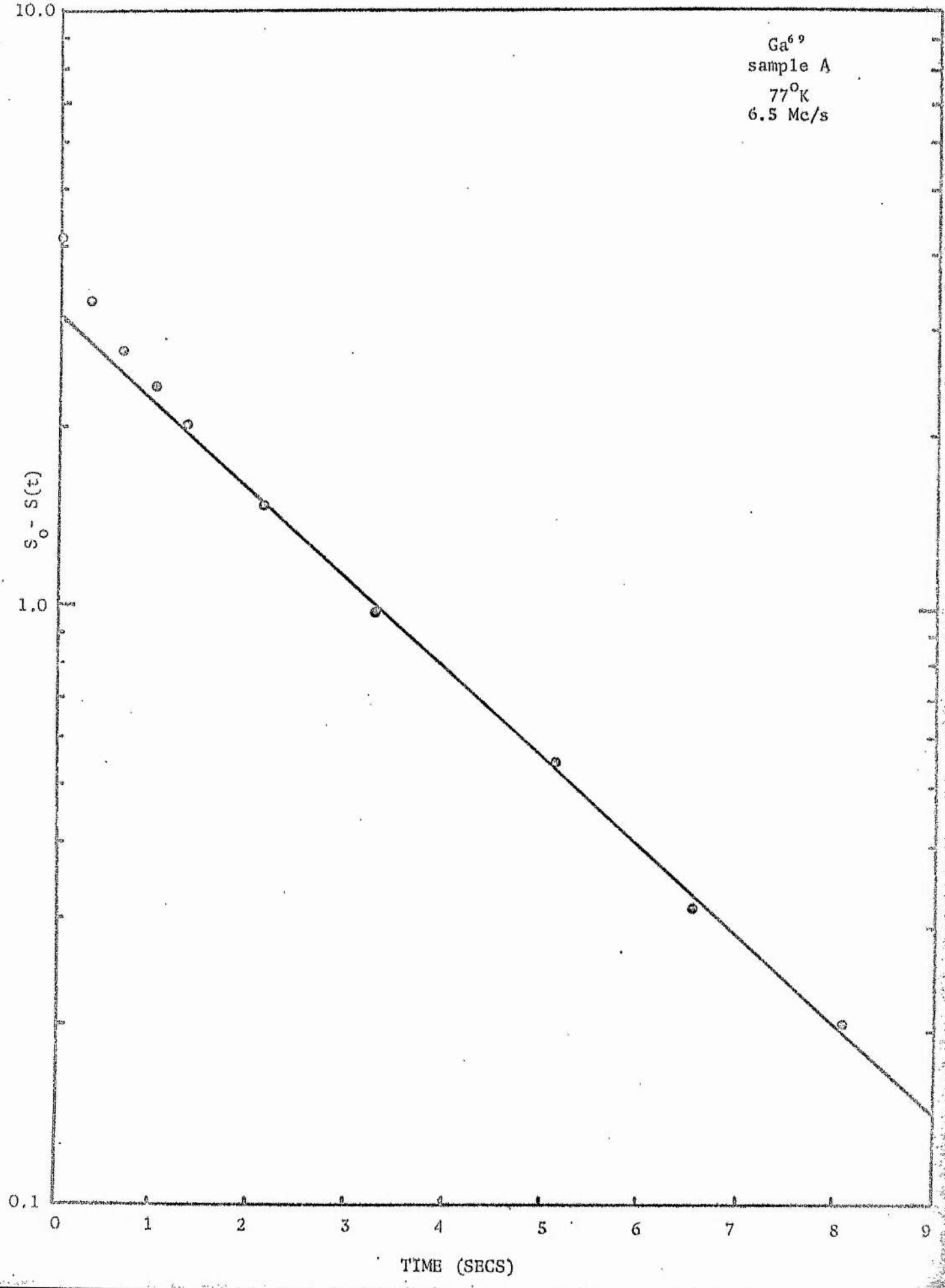

Fig. 8.4.2

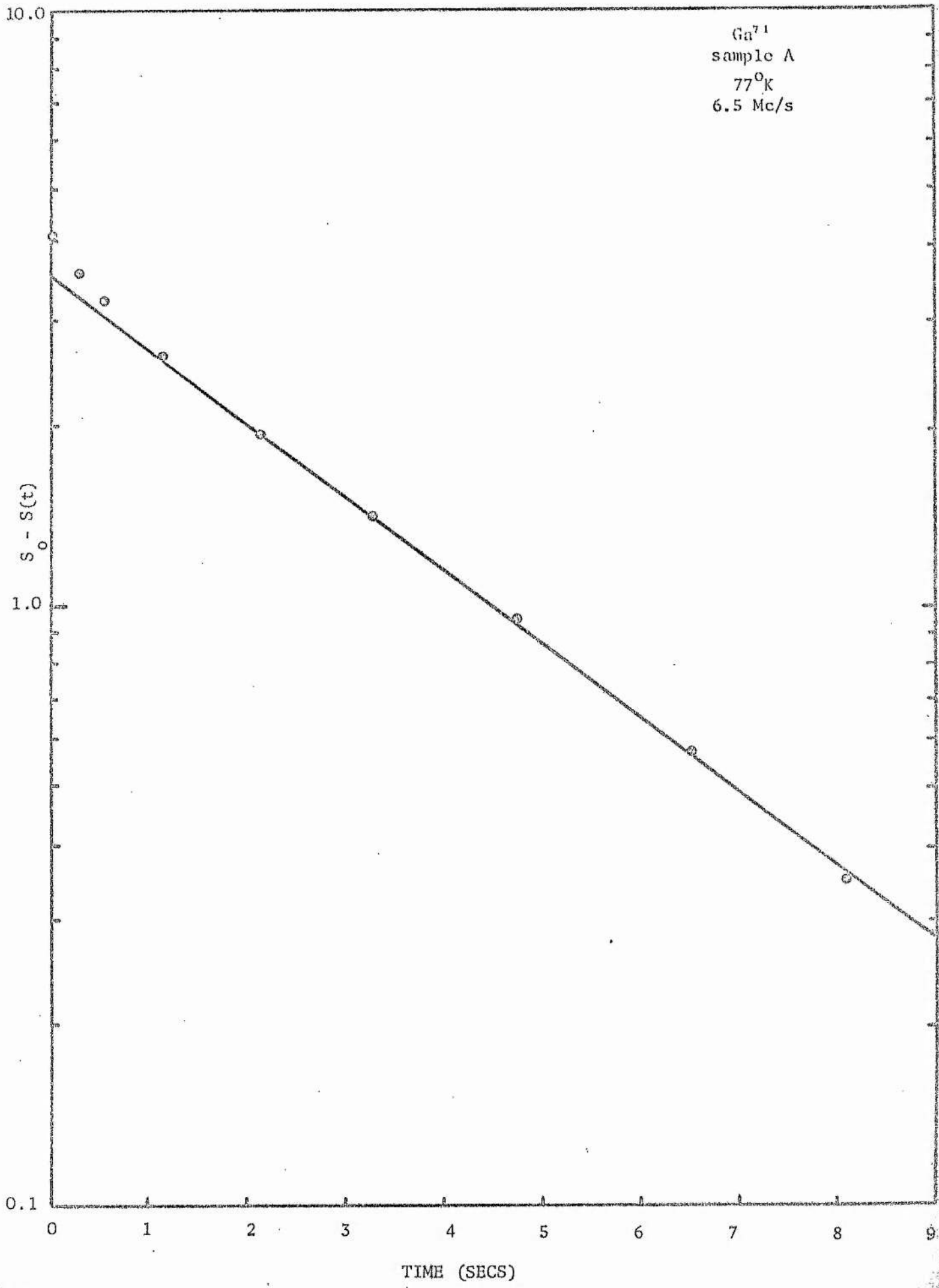

Fig. 8.4.3

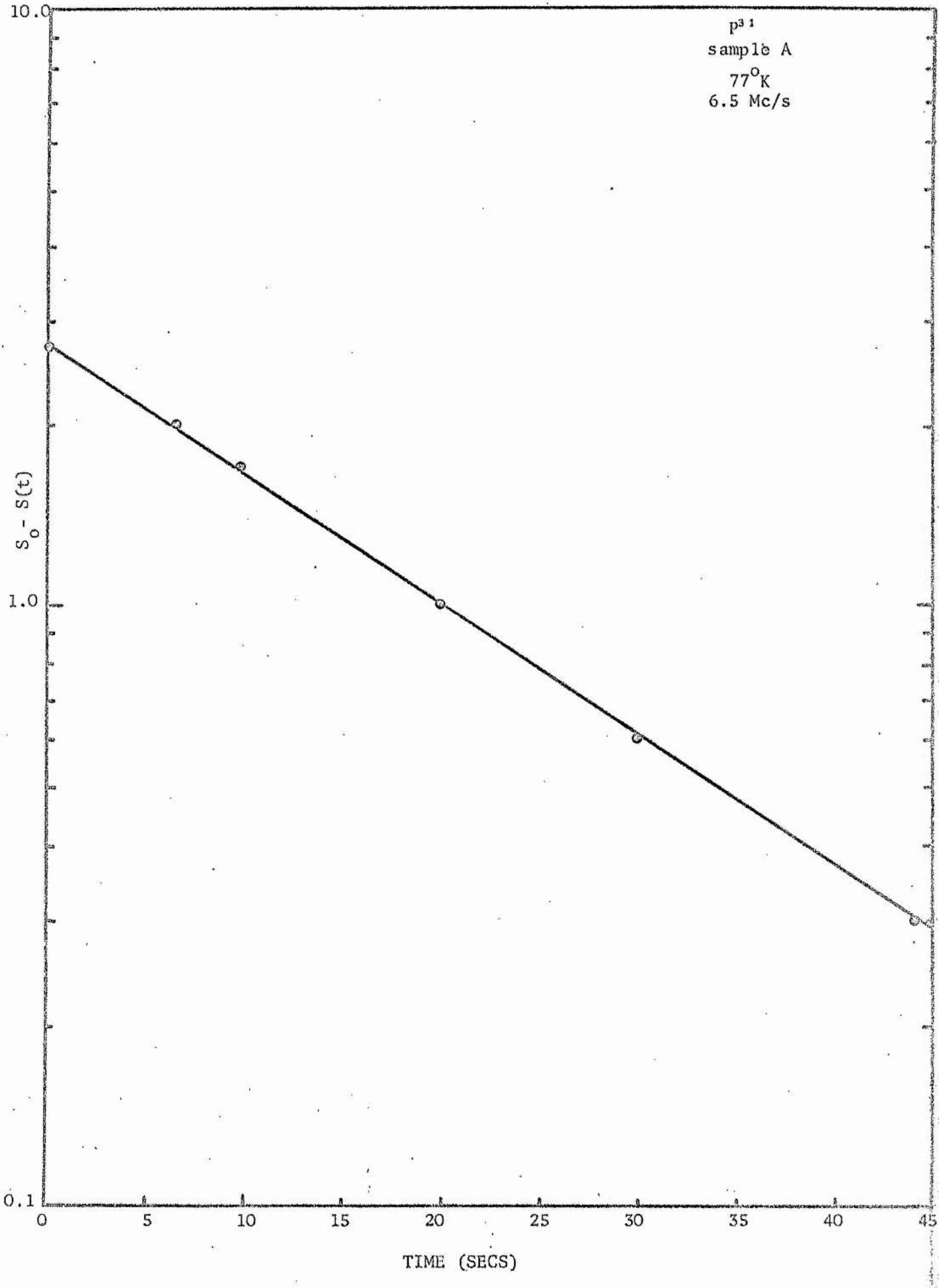
10.0
1.0
0.1
$S_o - S(t)$
$P^{31}$
sample A
77°K
6.5 Mc/s
0
5
10
15
20
25
30
35
40
45
TIME (SECS)

paramagnetic impurities. Expression 4.4.32 states that $t < C^{1/2}D^{-3/2}$, where t is the time interval over which the non-exponentiality lasts. Therefore using this expression, our theoretical values of C at the minimum and our measured values of t for the two Ga $T_1$'s, we can calculate minimum values for the spin diffusion coefficients for $Ga^{69}$ and $Ga^{71}$ in GaP. For $Ga^{69}$, $t \sim 0.5$ seconds and hence $D(Ga^{69}) = 6.0.10^{-14}$ $cm^2/sec$ while for $Ga^{71}$, $t \sim 1.0$ seconds and $D(Ga^{71}) = 4.4.10^{-14}$ $cm^2/sec$.

The approximate theoretical values of D can be obtained from equation 4.4.15 which states that $D = a^2/13.5\ T_2$. The values of $T_2$ for $Ga^{69}$ and $Ga^{71}$, deduced from equation 4.4.16 and Weber's[43] experimental values of their second moments, are 174 μsec and 136 μsec respectively. The lattice constant in GaP is 5.45 Å but, allowing for the fractional abundances of the two Ga isotopes and hence differing mean separation of like nuclei, the values of a substituted in equation 4.4.15 were 6.46 Å and 7.40 Å for $Ga^{69}$ and $Ga^{71}$ respectively. The resulting theoretical values of D obtained by this method are $1.8.10^{-12}$ $cm^2/sec$ for $Ga^{69}$ and $3.0.10^{-12}$ $cm^2/sec$ for $Ga^{71}$.

The large discrepancy between these values and the experimental values is similar to that observed by Blumberg[47] in Cr doped $NH_4HSO_4$ which he put down to restricted diffusion due to the non-uniform distribution of protons in this system. We can envisage a similar situation occurring for the two Ga systems in our samples, with the random distribution of impurities causing large quadrupole splittings in the energy levels of nearby nuclei thus inhibiting spin diffusion without actually prohibiting the setting up of a Boltzmann distribution amongst the spins. The differing abundances of the two spin species (60.2% for $Ga^{69}$, 39.8% for $Ga^{71}$) and their random distribution on the same face-centred cubic lattice would also restrict spin diffusion. The latter explanation might be more appropriate in our system since any quadrupolar effects would affect $Ga^{69}$ more than the $Ga^{71}$ nuclei

Fig. 8.4.4

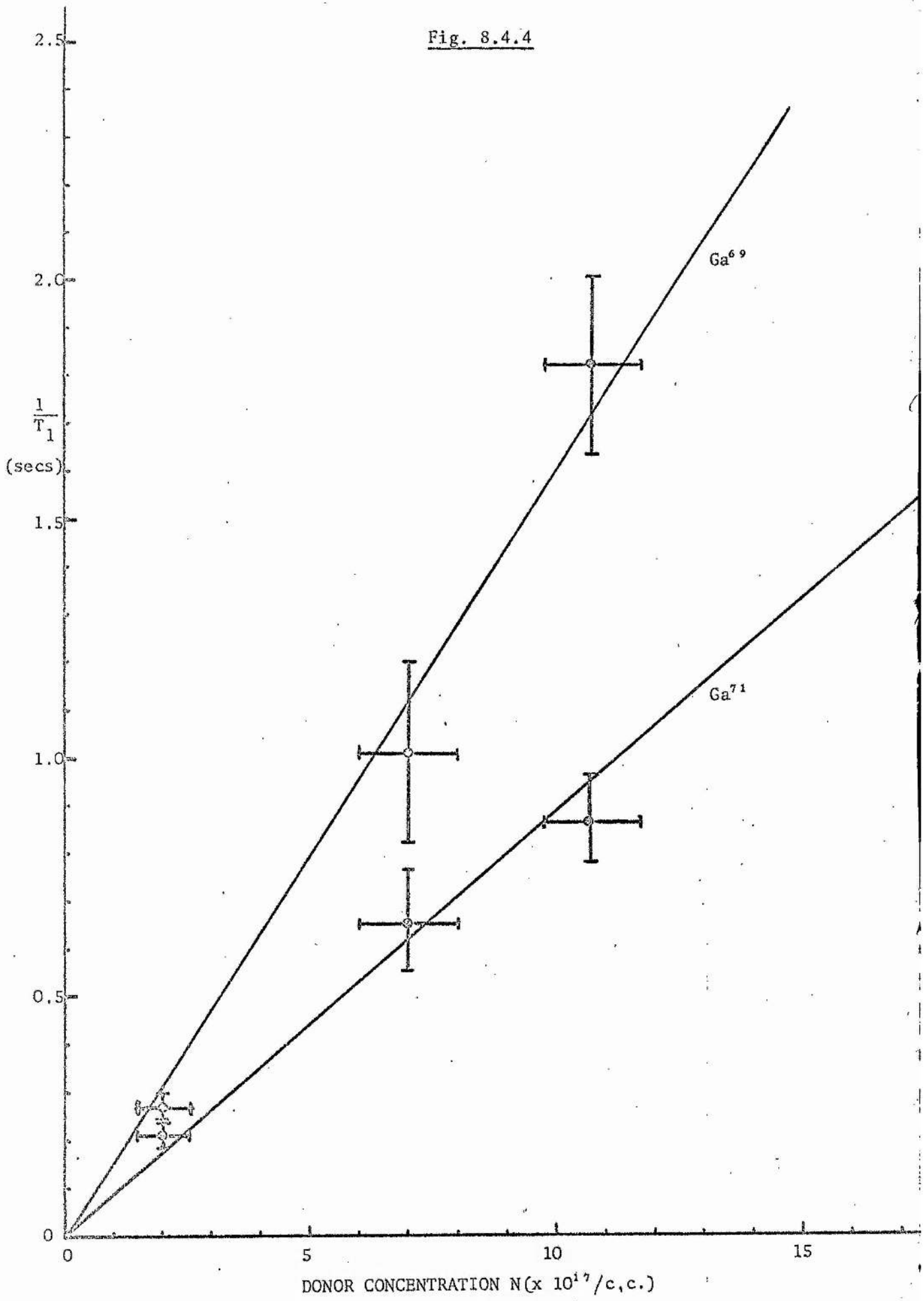
2.5
2.0
1.5
1.0
0.5
0
$\frac{1}{T_1}$
(secs)
$Ga^{69}$
$Ga^{71}$
0
5
10
15
DONOR CONCENTRATION N(x $10^{17}$/c.c.)

because of their large quadrupole moments.

If we calculate the theoretical values of the pseudopotential radii $\rho$ for the $Ga^{69}$ and $Ga^{71}$ nuclei around each impurity from equation 4.4.19, using the theoretical values of C and D, we obtain $\rho_{69} = 4.7$ Å and $\rho_{71} = 4.6$ Å respectively at the $T_1$ minimum. A calculation of the diffusion barrier radius b at the $T_1$ minima in samples A to C from equation 4.4.18 gives a value of $b = 10 \pm 1$ Å for both $Ga^{69}$ and $Ga^{71}$. Therefore the usual condition that $b < \rho$ for diffusion limited relaxation does not appear to hold. However using our experimental values of D, we obtain $\rho \simeq 20$ Å for $Ga^{69}$ and $Ga^{71}$ and hence $b < \rho$.

Another estimate of the $Ga^{69}$ and $Ga^{71}$ diffusion coefficients can be made from graphs of $1/T_{1min}$ against N for samples A, B and C. [Fig. 8.4.4]. Since equation 4.4.28 holds for diffusion limited relaxation the gradient of such a graph will equal $8.5\ C^{\frac{1}{4}}D^{\frac{3}{4}}$.

The values for $D(Ga^{69})$ and $D(Ga^{71})$ obtained from this analysis are $(2.8 \pm 1.0)10^{-12}$ $cm^2/sec$ and $(6.7 \pm 3.9)10^{-13}$ $cm^2/sec$ respectively. Despite the large errors inherent in this analysis the results do show that, at least around the $T_1$ minimum in samples A, B and C, the $Ga^{69}$ nuclei are relaxing faster than the $Ga^{71}$ nuclei due to the former's greater diffusion coefficient. The discrepancy between the two experimentally obtained values of D for each isotope is not understood.

## 8.5 Absence of non-exponentiality in $P^{31}$ nuclear relaxation

The lack of any observed non-exponentialities in the recovery of the $P^{31}$ nuclear magnetization suggests that if nuclear relaxation is dominated by the paramagnetic donors, then it must be the rapid diffusion case which applies. In order for this to be so theoretically, the barrier radius should be greater than the pseudopotential radius. A simple calculation of b and $\rho$ at the minimum in samples A, B and C, using a value of the spin diffusion coefficient of $2.75.10^{-12}$ $cm^2/sec$

obtained from equation 4.4.15, shows this to be true with $\rho$ = 5.9 Å and b = 11 to 12 Å. Experimentally, the values of b obtained from equation 4.4.34 by substituting for N, C and $T_1$ at the minimum for samples B and C are 13.6 ± 0.3 Å. Using this value to make an estimate of N in sample A by substituting again in equation 4.4.34 with $T_{1min}$ = 21 ± 1 sec, gives a value of $1.9.10^{17}$/c.c. which is in good agreement with the stated donor concentration in that sample. There is a small discrepancy between the theoretical value of b and the experimental value obtained from our $T_1$ results. An explanation for this and also possibly for the observation of diffusion limited relaxation in the Ga system can be deduced from some knowledge of the distribution of the donor electron wavefunction in GaP.

In providing an explanation for the discrepancy between the high radiative efficiency associated with group VI donors and group V isoelectronic centres and the low efficiency of group IV donors in GaP, Morgan[78] showed that band symmetry considerations led to the bound electron wavefunctions associated with impurities on either Ga or P sites having maxima at the P sites. For shallow donors in GaP the donor states are formed from states at the conduction band minima which, in GaP, are at the <100> points. The Bloch wavefunctions for an electron of wavevector $\underline{k}$ in a band may be written

$$\psi_{\underline{k}}(\underline{r}) = A\, U_k(\underline{r})\, \exp(i\underline{k}.\underline{r})$$

where $U_k(\underline{r})$ is a Bloch function with the lattice periodicity. At the edge of the Brillouin zone in the z direction, the wavevectors $\underline{k}_o$ and $-\underline{k}_o$ are coincident and so the proper eigenstates are even and odd combinations of the functions $\psi_{-\underline{k}_o}(r)$ and $\psi_{\underline{k}_o}(r)$, which are

$$\psi^{+}_{\underline{k}_o}(\underline{r}) = A\, U_{\underline{k}_o}(\underline{r})\, \cos k_o z$$

$$\psi^{-}_{\underline{k}_o}(r) = A\, U_{k_o}(\underline{r})\, \sin k_o z .$$

If we take the origin of the coordinates at a P site then the two states correspond to maxima in electron density at the P and Ga sites respectively. Similarly for the origin of coordinates on a Ga site the reverse is true. Which of these maxima has the lowest energy, and hence which corresponds to the conduction band minimum, depends on the difference in core potentials at the Ga and P sites. The P sites have the more attractive core potential and hence the bound electron wavefunction builds up preferentially on them. This will have a number of effects on the nuclear relaxation produced by such impurities in GaP.

Firstly, it will increase the probability of relaxation of the $P^{31}$ nuclei near the impurity via modulation of the hyperfine scalar contact interaction with the bound impurity electron. This would involve a mutual spin-flip of the electron and nucleus and hence would directly affect the electron correlation time $\tau$. If this were the dominant electron relaxation process it would have a very weak temperature dependence and could not be responsible for the sharp resonant dip in the $T_1$:T curve when $\omega\tau = 1$. However it could contribute substantially to the nuclear relaxation of these nuclei. Secondly, it will increase the effective magnetic field seen by the $P^{31}$ nuclei surrounding each Te impurity. This will have the effect of increasing the diffusion barrier radius for the $P^{31}$ nuclei and strengthen our argument for a rapid diffusion case in that spin system. A third possible result of this preferential distribution of the electron wavefunction is a reduction in the barrier radius of the two Ga isotopes. This would have the effect of taking the two Ga relaxations into the diffusion limited regime.

## 8.6 Impurity hopping

So far, in the analysis of the n.m.r. results for the lightly doped samples we have assumed that, around the $T_1$ minima, nuclear relaxation induced by magnetic fluctuations produced at nuclear sites by impurity hopping is negligible compared with that produced by bound electron-spin lattice interaction. One justification for this assumption is the rapid variation of $T_1$ with temperature around the minimum, which necessitates a rapidly varying $\tau$ not expected from an impurity hopping mechanism which shows only weak temperature dependence. Also, from the Hall data of Fig. 7.1.2, we can see that the conductivity in samples B to F at $77^{\circ}K$ is decreasing rapidly with decreasing temperature and is clearly dominated by electron excitation into the conduction band. At $4.2^{\circ}K$ on the other hand, excitation into the conduction band is negligible and impurity conduction should dominate. In samples B to F the conductivity was too low to measure on the system employed and only sample G had a measurable value.

Mott and Davis[86] have derived an expression for the conductivity $\sigma$ in terms of the hopping probability p, density of states at the Fermi level $N(E_F)$, and hopping distance R, for the situation in which impurity conduction dominates, and it has the form

$$\sigma = e^2 \, p \, R^2 \, N(E_F) \, . \qquad 8.6.1$$

We can use this expression to obtain an order of magnitude calculation of the impurity hopping time $\frac{1}{p}$, at $4.2^{\circ}K$ in sample G, assuming that at concentrations near the metallic transition we can treat the impurity electron system as a free electron gas.

$E_F$ and $N(E_F)$ are then given by

$$E_F = \frac{h^2}{2m} (3\pi^2 n)^{2/3} \qquad 8.6.2$$

and

$$N(E_F) = \frac{3n}{2E_F} \qquad 8.6.3$$

where n = donor electron density.

Taking $n \simeq 10^{19}$/c.c. in sample G we obtain that the Fermi temperature $T_F$ ($E_F = k_b T_F$) is 195°K and $N(E_F) \sim 5.6.10^{32}$/c.c. resulting in an impurity hopping time of $1.5.10^{-10}$ sec. at 4.2°K.

The number of electrons participating in this hopping mechanism is given by $N(E_F)$ kT and is equal to $\sim 3.3.10^{17}$/c.c. at 4.2°K. At 77°K, the number of electrons participating in the hopping process is $\sim 6.10^{18}$/c.c. We have assumed that only nearest neighbour hopping occurs but it is possible that at 4.2°K variable range hopping occurs resulting in an increased R and impurity hopping time.

The low conductivity of samples B to F at 4.2°K implies that the impurity hopping time is large compared with that in sample G and is probably much larger than the donor electron spin-lattice relaxation time at this temperature and above. Without measurements of the conductivity at 4.2°K in samples B to F it is not possible to assess the impurity hopping time at this temperature but, because of the rapid temperature variation of the bound electron spin-lattice relaxation time, it is possible that impurity hopping might be comparable with spin-lattice or spin-spin relaxation times and we shall discuss this further in sections 8.9 and 8.11.

## 8.7 Concentration dependence of $T_1$ minimum

We have already discussed the change in the magnitude of the $T_1$'s of the three isotopes around the minima in samples A, B and C in terms of the concentration dependence inherent in the two relaxation mechanisms thought responsible for the observed minima.

In order to understand the reasons for the movement of the minima to lower temperatures we must look again at the condition $\omega\tau = 1$ which holds at the minimum. A variation in the position of the $T_1$ minimum with concentration suggests that $\tau$ is both concentration and temperature dependent. Such concentration dependent electron

spin-lattice relaxation times have been observed in other doped semiconductors and have been discussed briefly in section 2.7.

The first main effect of an increase in donor concentration on the impurity electron system is a broadening and reduction of the donor ionization energy[3], as evidenced by the Hall and resistivity results. Therefore an electron relaxation mechanism which is dependent on $E_D$ might provide the $\tau$ behaviour observed in our samples.

A number of such mechanisms suggest themselves. One is the Orbach process suggested by Thomson and Lancaster[28] as a possible explanation of the concentration and temperature dependence of the e.s.r. linewidth in doped GaP in a similar concentration range. For such a process

$$\tau \propto e^{\Delta/kT} \qquad 8.7.1$$

where $\Delta$ is some donor excited state or, as they suggest, the donor ionization energy and as this decreases with increasing donor concentration, the variation in the temperature at which the resonant condition $\omega\tau = 1$ occurs decreases also. This mechanism agrees with the observed lack of any magnetic field dependence in $\tau$ as evidenced by the fact that the $T_1$ minima for all three isotopes in any one sample occur at the same temperature. The sharpness of the $T_1$ minima in samples A, B and C also fits in with the rapid temperature dependence predicted by equation 8.7.1. Further evidence to confirm the rapid variation of $\tau$ with temperature is provided from the frequency dependence of the $T_1$ minimum discussed in section 8.1.3.

However, for the Orbach process to be an effective electron relaxation mechanism, there has to be a sufficient number of phonons of energies greater than the energy required to excite electrons into the higher state. The usual condition placed on the process is that $\frac{\Delta}{k} \ll T_D$ where $T_D$ is the Debye temperature of the host lattice. Now

for GaP, $T_D$ is $400^{\circ}K$ [43] and taking $\Delta$ equal to 60 meV, so that $\frac{\Delta}{k} = 700^{\circ}K$, then this condition does not appear to be satisfied.

However in a system with a lattice as complex as that of GaP, the concept of a sharp Debye temperature is a bit misleading as there may still be phonons in optical bands capable of inducing an Orbach process. Alternatively, it is possible that an excited state other than the donor ionization energy might be involved, in which case the Orbach process could still be the most effective relaxation process despite the apparent non-fulfillment of the usual conditions.

A spin exchange or scattering mechanism involving conduction electrons interacting with the bound impurity electrons might produce a $\tau$ of a similar temperature dependence. Treating such a mechanism as a simple scattering problem[22], the relaxation rate $1/\tau$ is given by

$$\frac{1}{\tau} = \tfrac{1}{4} n \sigma v \qquad 8.7.2$$

where v is the thermal velocity of conduction electrons ($10^6$ cm/sec), $\sigma$ is the impurity capture cross section ($10^{-12}$ cm$^2$), and n is the density of conduction electrons.

A conduction electron density of $1.6.10^{14}$/c.c. would be required to produce the value of $\tau = 2.44.10^{-8}$ sec observed at the $T_1$ minima by this mechanism. Our Hall data indicates that carrier concentrations of this order of magntiude are present in our lightly doped samples around the $T_1$ minima.

Since $n << N_D - N_A$ in our lightly doped samples around the $T_1$ minima we can approximate equation 6.1.2 to obtain

$$n \propto T^{3/2} \exp(-\frac{E_D}{kT}) \qquad 8.7.3$$

and if the scattering mechanism is responsible for the observed electron relaxation then

$$\tau \propto T^{-3/2} \exp(\frac{E_D}{kT}) \ . \qquad 8.7.4$$

Although the temperature dependence of $\tau$ via this mechanism appears more complex than in the Orbach process, the $T^{-3/2}$ dependence is swamped by the exponential term at low temperatures resulting in $\tau$ again having an almost exponential dependence on $E_D$.

For reasons mentioned in the previous section, we do not expect impurity hopping to have a significant effect on nuclear relaxation around the $T_1$ minimum in our lightly doped samples and, similarly, it is unlikely that electron relaxation induced by interactions with other impurities would produce the observed temperature and concentration $T_1$ dependences.

## 8.8 Calculation of Donor Ionization Energy

If any one of the possible electron relaxation mechanisms is dominant in our samples around the $T_1$ minima it should be possible to make estimates of $\Delta$ in each sample and compare them with the values of $E_D$ expected from Hall data.

For diffusion limited relaxation on the high temperature side of the $T_1$ minimum $T_1 \propto \tau^{-\frac{1}{4}}$, while on the low temperature side $T_1 \propto \tau^{\frac{1}{4}}$. If we assume an Orbach process responsible for the electron relaxation then a plot of $\ell n\ T_1$ against $1/T$ will have gradients of $-\Delta/4k$ and $\frac{\Delta}{4k}$ on the high and low temperature sides respectively. Similarly, for rapid diffusion relaxation, a graph of $\ell n(T_1T)$ against $1/T$ will have a gradient of $-\Delta/k$ on the high temperature side and $\Delta/k$ on the low temperature side.

If the scattering mechanism is dominant then, for diffusion limited relaxation a graph of $\ell n(T_1T^{-3/8})$ against $1/T$ will have a gradient of $-E_D/4k$ on the high temperature side of the minimum, while on the low temperature side, a graph of $\ell n(T_1T^{3/8})$ against $1/T$ will have a gradient of $E_D/k$. For rapid diffusion relaxation a graph of $\ell n(T_1T^{-3/2})$ against $1/T$ will have a gradient of $-E_D/k$ on the high temperature side, while a graph of $\ell n(T_1T^{3/2})$ against $1/T$ will have a

gradient of $E_D/k$ for the low temperature side.

However we are hindered in a number of ways from calculating accurate values of $E_D$ from the experimental $T_1$ data around the various minima. For the two Ga isotopes, large errors are introduced into the corrected values of $T_1$ above the minima due to the uncertainty in determining the true quadrupolar contribution to the nuclear relaxation rate. Also, because of the variation of b and $\rho$ with temperature, nuclear relaxation may move from a diffusion limited to a rapid diffusion regime in a small temperature range on either side of the minimum. The decrease in the magnitude and duration of the short-time non-exponentialities in the magnetization recovery of the two Ga resonances, on both sides of the minima in samples A, B and C, is experimental evidence that this might be occurring. Thirdly, if more than one electron relaxation mechanism is significant around the minima, the above graphs will not be valid. Finally, because of the rapid variation of $\tau$ with temperature and the known presence of substantial quantities of other impurities it is possible that nuclear relaxation may become dominated by relaxation to these other centres away from the $T_1$ minimum.

Calculations of $\Delta$ from the $Ga^{69}$ and $Ga^{71}$ $T_1$ data in samples A, B, and C, assuming an Orbach process, give values of 82 ± 25 meV, 72 ± 40 meV, and 58 ± 40 meV respectively. Although the large uncertainties in each calculated value make detailed comparison between them difficult, the fact that they are of the expected magnitude for the Te donor ionization energy is encouraging.

The values of $\Delta$ obtained for samples A, B and C from the $P^{31}$ $T_1$ data around the $T_1$ minima are 22 ± 13 meV, 5.5 ± 1.5 meV, and 7.3 ± 2.3 meV respectively. These low values suggest that some additional relaxation mechanisms are present, or that the assumption of a rapid diffusion relaxation dominating the $P^{31}$ nuclei is incorrect. If diffusion limited relaxation were applicable in the $P^{31}$ system as well as in the

two Ga systems, the Δ values would be 88 ± 52 meV, 22 ± 6 meV, and 29.2 ± 9.2 meV respectively. Only the Δ value for sample A is consistent with the Ga values, the others still being much smaller, and so we can discount the possibility of a diffusion limited relaxation dominating in all three nuclear spin systems simultaneously.

It is possible that the enhanced scalar contact interaction between donor electron and $P^{31}$ nuclei around each impurity, caused by the heaping up of the electron wavefunction on $P^{31}$ sites, could contribute substantially to the $P^{31}$ nuclear relaxation rate while still enlarging the $P^{31}$ diffusion barrier radius. The resultant relaxation rate of the $P^{31}$ nuclei would then consist of two major components; one resulting from the dipolar interaction with the Te donor relaxing via an Orbach or scattering process and thus having a dependence on $E_D$, and the other, independent of $E_D$, but strongly dependent on the hyperfine interaction between donor electron and $P^{31}$ nucleus.

The nuclear relaxation rate might then be given by an expression of the form

$$\frac{1}{T_1} \propto \exp\left(\frac{E_D}{kT}\right) + f(\underline{I}.\underline{S}) \quad . \qquad 8.8.1$$

Therefore if the second term in 8.8.1 were comparable with or greater than the first term, the value of Δ obtained from the plot of $1/T_1$ against T could differ substantially from the true value of $E_D$, and this might explain the low values of Δ obtained from the $P^{31}$ $T_1$ data.

Furthermore, it should be noted that such an enhancement of the $P^{31}$ nuclear relaxation rate need not drastically alter the overall electron correlation time 'seen' by the Ga and P nuclei, since, around the $T_1$ minima, the donor electrons are already relaxing and exchanging energy with the lattice via the Orbach or scattering process. The component added to this relaxation rate due to the exchange of energy via the hyperfine interaction with $P^{31}$ nuclei need be only very small

in comparison. Therefore the sharpness of the two Ga $T_1$ minima, and the values of $\Delta$ calculated from the Ga data, remain unaffected.

Finally, it may be that relaxation by the hyperfine interaction with donor electron might be important in the $P^{31}$ system at temperatures above the minima and this, along with other possibilities, are discussed in section 8.10.

## 8.9 Weakening and disappearance of the $T_1$ minima in samples D and E

The weakening in the depth of the $T_1$ minima for the two Ga isotopes in samples D and E and the rapid movement of its position to lower temperatures in these samples (see table 8.9.1) is taken as evidence for the onset of impurity conduction and a reduction in the effectiveness of nuclear relaxation to the paramagnetic centres.

Table 8.9.1

| Sample | A | B | C | D | E |
|---|---|---|---|---|---|
| Temperature | $78^{o}K$ | $60^{o}K$ | $56^{o}K$ | $34^{o}K$ | $29^{o}K$ |

At temperatures around the $T_1$ minimum, nuclear relaxation by spin diffusion to the Te paramagnetic centres is at its most effective, and impurity hopping, by reducing the amount of time spent by any particular electron in a bound state, reduces the effective number of paramagnetic centres participating in this relaxation process. Nuclear relaxation induced by the magnetic fluctuations produced at nuclear sites by the hopping of the impurity electrons is unable to make up for the latter effect and this results in the observed weakening of the $T_1$ minimum. With increasing donor density and impurity hopping however, modulation of the coupling between nucleus and electron due to the hopping of electrons would begin to dominate the nuclear relaxation.

The theoretical calculation of the critical donor density for metallic conduction in Te doped GaP gives values between 2.3 and

$4.5.10^{19}$/c.c. depending on whether one uses 0.20 or 0.25 as the factor in equation 2.4.1. Therefore the donor densities in samples D and E are an order of magnitude below that expected for metallic conduction. However, remembering that samples B to G are L.E.C. grown, there will be substantial compensation present, and hence impurity hopping from occupied to unoccupied donor sites at low temperatures. This would effectively reduce the nuclear relaxation rate. Although it is thermally activated, the temperature dependence of this impurity hopping is much weaker than the electron spin-lattice relaxation processes and so, as it takes over as the dominant nuclear relaxation agent, the temperature dependence of the nuclear $T_1$'s weakens and this is observed in the low temperature $T_1$ data of samples D and E.

Nuclear relaxation to clusters of interacting impurities and bound electron spin-spin interactions might become important at low temperatures in this doping range, again resulting in an almost temperature independent electron correlation time. Under such conditions, the condition R >> (b and $\rho$) might not hold and the simple expressions for nuclear relaxation to bound paramagnetic impurities may have to be modified. The absence of any observed nonexponentialities in the two Ga magnetization recoveries around the $T_1$ minima in samples D and E is indicative of the much reduced role of spin diffusion in these samples. Lowe and Tse's[57] diffusion-vanishing theory of nuclear relaxation in the intermediate doping regime, where inter-impurity distances cannot be neglected in calculating $T_1$, may be more appropriate for samples D and E around the $T_1$ minima.

From equation 4.4.34, the dependence of $T_1$ on spin diffusion coefficient D and factor C is given by $T_1 \propto C^{-\frac{1}{2}} D^{-\frac{1}{2}}$ in the diffusion vanishing case, whereas $T_1 \propto C^{-\frac{1}{4}} D^{-\frac{3}{4}}$ in the standard diffusion limited case of equation 4.4.28. Given that $C(Ga^{69}) < C(Ga^{71})$, and that $D(Ga^{69}) > D(Ga^{71})$ at the $T_1$ minimum, the onset of diffusion vanishing relaxation with increasing donor concentration would result in a

reduction in the difference between the $T_1$ values of the two Ga isotopes around the minimum. As diffusion becomes negligible, $T_1(Ga^{71})$ becomes less than $T_1(Ga^{69})$, and this is observed in samples D and E.

The eventual disappearance of the minima in samples F and G and the much weaker $T_1$ temperature dependence in these samples is evidence of the strong electron interactions and motional effects in this doping regime. It was found in section 8.6 that an order of magnitude calculation of the impurity hopping time in sample G gave a value of $10^{-10}$ secs at $4.2^{\circ}K$. Thus the electron correlation time $\tau$ is much less than the inverse nuclear Larmor frequency $(1/\omega)$ at $4.2^{\circ}K$ and above. Hence the condition $\omega\tau \sim 1$, necessary for a $T_1$ minimum, does not occur at $4.2^{\circ}K$ and above, and no minima are observed. The corrected $T_1$'s in samples F and G do show an increase at high temperatures but, because of the large errors introduced in subtracting the high temperature quadrupolar component to the nuclear relaxation, no significance can be placed on them.

Given that we expect the $T_1$ minimum to be absent in samples F and G due to rapid electron correlation caused by impurity hopping or spin-spin effects both of which are relatively temperature independent, the increase in $T_1$ with decreasing temperature is rather surprising. There are several possible explanations for such behaviour and we shall outline them when discussing the $P^{31}$ results in the next section.

## 8.10 High temperature $P^{31}$ results

The almost temperature independent behaviour of the $P^{31}$ $T_1$'s in all our samples at high temperatures (Fig. 8.1.4) resembles Weber's[43] results in undoped gallium phosphide but with the $T_1$'s between one and two orders of magnitude shorter. This suggests nuclear relaxation dominated by a large background of paramagnetic centres which, because of their broad spectrum of correlation times, has an almost temperature independent effect on the nuclear relaxation time. However, assuming

such a process involves primarily centres other than the large concentrations of Te donors which are still unionized at room temperature, and whose electron relaxation times are so short as to have only a small effect on the bulk nuclear relaxation rate, it is difficult to explain the variation in the magnitude of the high temperature $P^{31}$ $T_1$'s in our samples.

Two possibilities suggest themselves; firstly nuclear relaxation dominated by a large background of paramagnetic centres which has a concentration dependence similar to that of the Te donors in our samples and secondly, nuclear relaxation dominated by a single paramagnetic species with a similar concentration dependence and exhibiting a diffusion limited type relaxation.

If the former possibility applied, one would expect $T_1$ to remain constant down to much lower temperatures than is observed in any of our samples, as the 'freeze out' of any one paramagnetic species would not be expected to have much effect on the overall nuclear relaxation rate. It is possible that inter-impurity interactions might have the effect of producing a net electron correlation time which displays the observed temperature dependence. So in samples A, B and C, we observe the temperature independent $T_1$'s down to approximately 150°K, below which a gradual weakening of the effectiveness of the background centres is evidenced by the increase in the $P^{31}$ $T_1$'s with decreasing temperature. Below 100°K, the rapidly varying correlation time of the Te donors begins to dominate and a dip is observed in the $P^{31}$ $T_1$:T curve. From the linewidth measurements of reference 28, the correlation time of the Te donors decreases from approximately $6.10^{-10}$ sec at 100°K to $3.10^{-8}$ sec at 60°K for a Te concentration similar to that in sample B.

In order to determine the true contribution to the nuclear relaxation rate due to the Te donors we would have to subtract the component due to the background centres in a manner similar to that used to remove the quadrupolar component from the two Ga relaxation rates in section 8.2.

Without detailed knowledge of the temperature dependence of the background component at low temperatures such a procedure would introduce large uncertainties into the values of $T_1$ around the minima and make any quantitative analysis of the resulting $T_1$ values extremely difficult. This would also introduce large errors into our analysis of the magnitudes of the $T_1$ minima in section 8.5.

If the second possibility were appropriate, i.e. that of a single paramagnetic species (in the diffusion limited regime being) responsible for the high temperature $P^{31}$ $T_1$'s, then the correlation time of the centre must have a very weak temperature dependence. As we have decided in section 8.5 that a rapid diffusion case is dominant around the minimum in the $P^{31}$ system, a cross-over to a diffusion limited regime must occur around $100^{\circ}K$.

It is possible that a combination of the two mechanisms occurs in which case analysis of the high temperature results remains impracticable, as so many different effects could contribute to the observed $T_1$ behaviour.

We can discount nuclear relaxation due to scalar contact with the conduction electron concentration, as the strength of this interaction depends strongly on electron concentration which is varying exponentially with temperature at these temperatures. However, as mentioned in section 8.8, it is possible that scalar contact interaction between the bound donor electron and the $P^{31}$ nuclei around each impurity might be responsible for the weakness of the $P^{31}$ $T_1$ minimum compared with the two Ga minima. Now although we expect dipolar interactions between the bound electron and $P^{31}$ nuclei to dominate nuclear relaxation at the $T_1$ minimum and below, the scalar contact interaction might be of greater importance at higher temperatures. With the temperature independence of the basic interaction and the weak temperature dependence of the unionized Te concentration below $300^{\circ}K$, this process could result in nuclear relaxation by spin diffusion to the Te centres displaying the observed high temperature behaviour. Therefore this is a third possible

explanation for our high temperature $P^{31}$ results.

The existence of this additional relaxation mechanism for the $P^{31}$ nuclei might also explain the absence of any observed minima in samples D and E. Whereas the onset of impurity hopping only weakens the minima for the two Ga spin systems in these samples by reducing the effective number of paramagnetic centres, it might permit the scalar contact interaction to gain dominance in the $P^{31}$ spin system and so wash out the minima completely in the same samples.

The strong temperature dependence of $T_1$ observed in samples D to G at low temperatures could be due to exchange effects in the bound impurity system as the metallic transition is approached. Quirt and Marko[85] have suggested that, in Si:P at concentrations approaching the metallic transition, the donor electron system aligns itself into an amorphous antiferromagnetic array due to strong exchange interactions between nearest neighbours. Low temperature measurements of the spin susceptibility $\chi_s$ confirm this, with $\chi_s$ obeying a Curie-Weiss law on the low concentration side of the metallic transition. As the temperature and concentration increase, $\chi_s$ deviates from the Curie-Weiss law, and Quirt and Marko have associated this with the Pauli spin susceptibility of thermally excited conduction electrons.

Furthermore, Hall measurements in Si:P indicate that, above $77^{o}K$, there is a rapid increase in the number of free carriers up to a concentration almost equal to the total uncompensated donor concentration. This behaviour prompted Quirt and Marko to postulate the existence of a metal-semiconductor transition induced by the critical shielding of unionized donors by thermally excited conduction electrons. Above the critical temperature at which this transition occurs, the Pauli spin susceptibility dwarfs the Curie-Weiss component and this is observed in their results.

Such an antiferromagnetic array in GaP:Te would have a number of effects on the relaxation rates of the host nuclei. Previously rapidly

Fig. 8.11.1

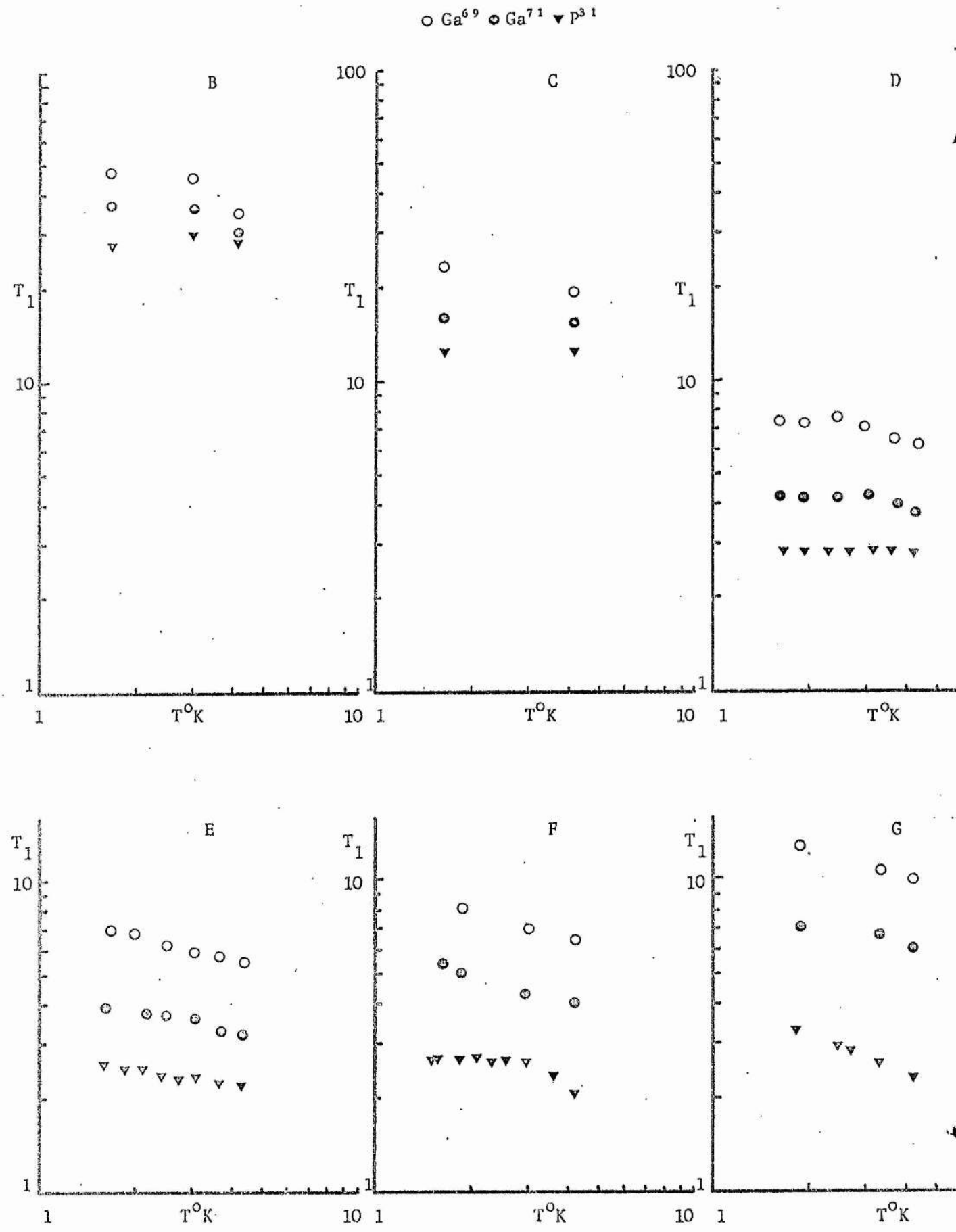

fluctuating electron magnetic moments would be obliged to spend more time in a particular spin orientation, thus increasing the average local magnetic field experienced by neighbouring nuclei. The enlarged barrier radius so produced around each impurity by these moments, and the existence of non-magnetic pairs of localized moments due to their oppositively directed magnetic fields, would cause a general reduction of the nuclear relaxation rate.

The strength of the ordering of magnetic moments would be inversely proportional to temperature below that temperature at which either a metallic transition occurred or the magnetic ordering broke down due to thermal effects. This would correspond to the Neel temperature of crystalline antiferromagnets. The increase in the $T_1$'s of all three isotopes in samples F and G at low temperatures is consistent with this mechanism.

The temperature at which the antiferromagnetic ordering breaks down will be strongly dependent on carrier concentration and hence donor concentration. Therefore we would expect our $T_1$'s to begin to display the above temperature dependence at progressively lower temperatures as the donor concentration increases in our samples. Thus the marked change in the $T_1$:T curves of all three isotopes in samples F and G at low temperatures is explained.

## 8.11 6.5 Mc/s $T_1$ results between 1.8°K and 4.2°K

$T_1$ results below 4.2°K for the three isotopes in samples B to G are presented in fig. 8.11.1. No $T_1$ measurements were made below 4.2°K in sample A.

The weak temperature dependence of the two Ga $T_1$'s in all the samples in this temperature range contrasts strongly with the observed $T_1$ behaviour above 25°K. Similar results are obtained in the $P^{31}$ $T_1$'s except for samples D and E for which the weak temperature dependence exists at higher temperatures also. The fact that $T_1(Ga^{71}) < T_1(Ga^{69})$

in all samples indicates that magnetic interactions are dominant, with spin diffusion taking a minor role.

We have explained the occurrence of the $T_1$ minimum in our samples in terms of the resonant condition latent in the expressions for nuclear relaxation to paramagnetic Te donors when $\omega\tau = 1$. In the samples where this minimum exists therefore, we expect that $\omega\tau >> 1$ at $4.2^{o}K$ and below. Considering the differing dependences of $\rho$ and b on temperature, we would expect that the rapid diffusion or diffusion vanishing cases to be appropriate for all three isotopes at these temperatures. Under these conditions we can deduce from equation 4.4.34 that $T_1 \propto \tau$.

The results of Feher[22] and others in Si:P indicate that $\tau$ can display a range of temperature dependences in this temperature region, the weakest of these being $\tau \propto T^{-1}$ resulting from a one-phonon process. None of the $T_1$'s in our lightly doped samples reflect such a large temperature dependence, suggesting that their interpretation in terms of the single electron relaxation mechanisms discussed by Feher is not possible.

Nuclear relaxation to background paramagnetic centres would produce such $T_1$ temperature dependences but such an explanation suffers from the same weakness as it did in interpreting the $P^{31}$ results i.e. the background paramagnetic impurity concentration must vary in a similar manner to the Te concentration in order to explain the spread of $T_1$ values at $4.2^{o}K$ in our samples.

A more plausible explanation is one in which spin-spin interactions between Te donors provide the dominant electron relaxation and hence nuclear relaxation mechanism. As spin-spin interactions are almost temperature independent but strongly concentration dependent, the general $T_1$:T behaviour in our samples can be explained. In order to determine whether spin-spin interactions are indeed dominant at low temperatures, an order of magnitude calculation of values of $\tau$ expected by the various spin-lattice and spin-spin mechanisms described previously

must be made.

Using the fact that at the $T_1$ minimum $\tau \approx 2.44.10^{-8}$ sec, we can deduce that, at $4.2^{\circ}K$, the Orbach or scattering processes would result in $\tau$ values of several hours, while other mechanisms, such as two-phonon processes, for which $\tau \propto T^{-7}$ or $T^{-9}$, would produce values of tens of seconds at this temperature. Such long electron relaxation times are ineffective in producing the relatively short $T_1$'s observed in even our most lightly doped samples.

An order of magnitude expression for the electron spin-spin relaxation time $\tau_s$ has the form

$$\tau_s = \frac{6\hbar}{\pi N \beta^2} \qquad 8.11.1$$

where $\beta$ is the Bohr magneton and N is the donor concentration.

Substituting in this expression the calculated Te donor concentrations in our samples, we obtain $\tau_s$ values between $10^{-4}$ to $10^{-5}$ seconds which are much shorter than the values predicted for the other mechanisms.

As discussed in section 8.6 the small conductivity at $4.2^{\circ}K$ in samples B to F indicate that the impurity hopping time is long and only a small fraction of the donor electrons participate in the process. As the donor concentration increases in our samples this situation will gradually change and, although we have no conductivity measurements from which to calculate the hopping time, it is possible that it becomes of the same order as the spin-spin relaxation in the more heavily doped samples at low temperatures.

Calculations of the $T_1$'s expected in the three different relaxation regimes described in chapter 4 given an electron correlation time of $10^{-4}$ seconds and donor concentration of $10^{18}$/c.c., reveal the feasibility of electron spin-spin interactions producing the observed $T_1$'s in our lightly doped samples at $4.2^{\circ}K$. For a rapid diffusion case we expect $T_1$'s of over 100 seconds, whereas for diffusion-limited and diffusion

vanishing cases we expect $T_1$'s of about 3 seconds and 30 seconds respectively. Of these, the diffusion vanishing value fits the observed data best but the diffusion limited case cannot be ruled out solely on the basis of the results of this rough calculation.

The expressions for $T_1$ derived by Lowe and Tse[57] for nuclear relaxation under such conditions give overall concentration dependences varying from $N^{-11/6}$, to $N^{-5/4}$, to $N^{-2}$, as relaxation shifts from the diffusion vanishing case, to the diffusion limited case, and onto the rapid diffusion case. As they point out however, verification of the existence of these concentration dependences in various temperature and concentration regimes requires such strenuous experimental conditions as to make it almost impossible.

In Fig. 8.11.2 is plotted $\ln T_1$ against estimated total uncompensated donor concentration N at $4.2^{\circ}K$ for the $Ga^{69}$, $Ga^{71}$, and $P^{31}$ nuclei in samples A to G. For samples A to E, the data fit the following expressions,

$$\text{For } Ga^{69}, \quad T_1 \propto N^{-(1.46 \pm 0.05)}$$
$$\text{For } Ga^{71}, \quad T_1 \propto N^{-(1.59 \pm 0.10)}$$
$$\text{For } P^{31}, \quad T_1 \propto N^{-(1.85 \pm 0.10)} .$$

The additional concentration dependences evident in these results lend support to the theory that spin-spin interactions are important in the lightly doped samples at low temperatures. The observed differences in concentration dependences of the three isotopes could be due to restricted spin diffusion in the two Ga spin systems caused by large inhomogeneous quadrupolar splitting of the nuclear energy levels around impurities. This has the effect of taking the two Ga systems into the diffusion limited or diffusion vanishing regimes. Assuming diffusion limited relaxation is important at helium temperatures in the two Ga systems, the reason for the lack of any observed non-exponentiality in the magnetization recoveries could be due to the time

Fig. 8.11.2

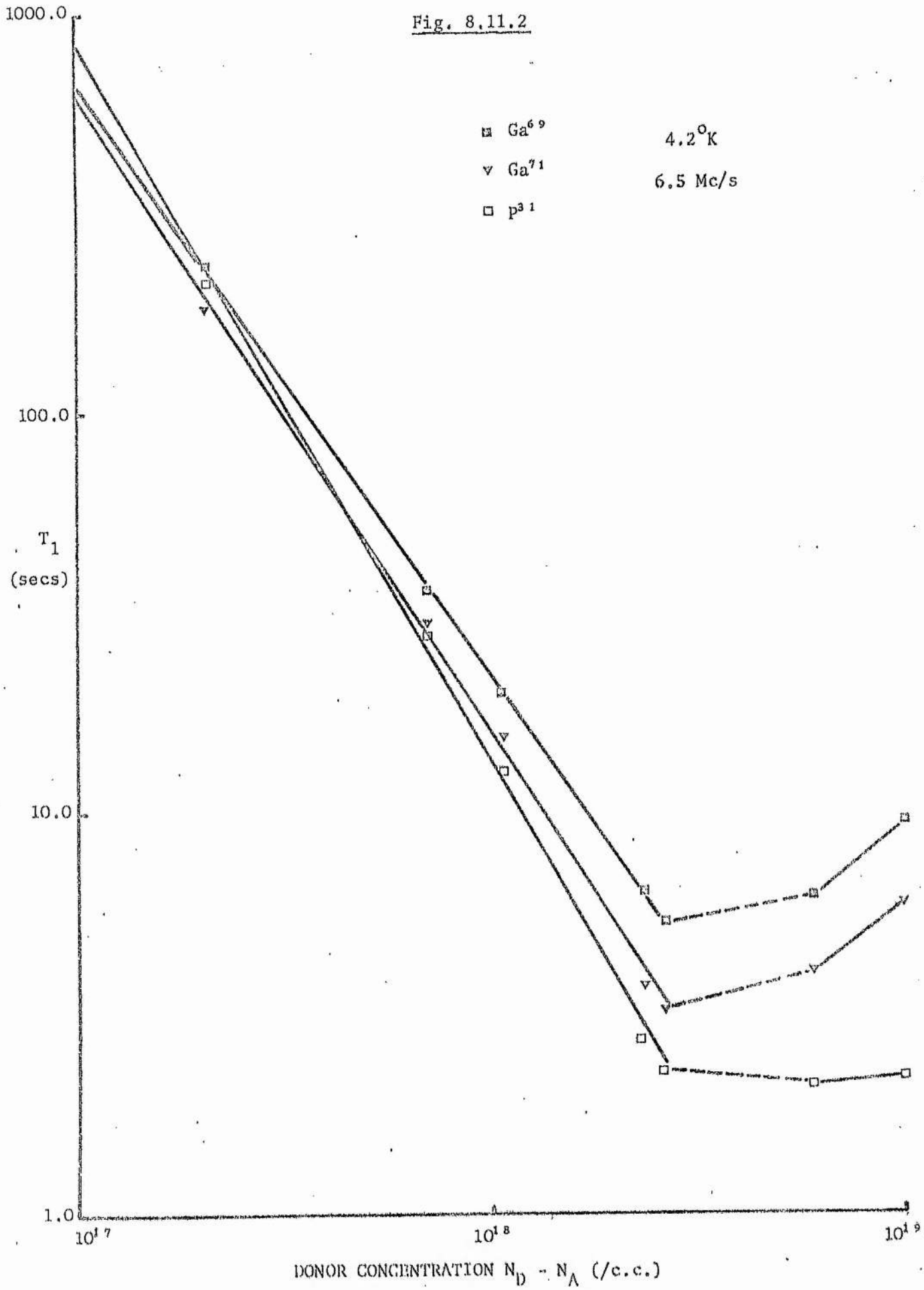
1000.0
100.0
10.0
1.0
$T_1$ (secs)
$Ga^{69}$
$Ga^{71}$
$P^{31}$
4.2°K
6.5 Mc/s
$10^{17}$
$10^{18}$
$10^{19}$
DONOR CONCENTRATION $N_D - N_A$ (/c.c.)

over which this non-exponentiality extends being extremely short because of the small value of the factor C at these temperatures.

The larger concentration dependence of the $P^{31}$ $T_1$'s in samples A to E would be due to diffusion vanishing or rapid diffusion relaxation. Certainly the $P^{31}$ diffusion barrier radius at $4.2^{o}K$, calculated from equation 4.4.18, gives a value of 25 Å which, if it was isotropic, would envelope all of the nuclei in samples D and E and a large percentage of the nuclei in samples A, B and C. Under such conditions observation of the nuclear resonances would be extremely difficult as most of the nuclei would be field shifted by differing amounts. As this is patently not the case, we can deduce that either equation 4.4.18 does not hold at such low temperatures, or that the angular dependence of b, so far neglected, is of importance.

Equation 4.4.18 holds if $\tau << T_2$. At $4.2^{o}K$, $\tau \simeq \tau_s$ and, as $T_2 \approx 10^{-4}$ seconds, $\tau \simeq T_2$. Treating the magnetic moment of the paramagnetic donor as a stationary magnetic dipole aligned along the applied magnetic field direction, the magnetic field perpendicular to the applied field will extend much further than that parallel to the applied field. Similarly the barrier radius perpendicular to the applied field will be much greater than that parallel to it, and we can imagine a situation in which spin diffusion is greatly restricted in one direction and not in another. This situation could arise for the $P^{31}$ nuclei in samples A to E and result in the diffusion vanishing case being applicable. Certainly the concentration dependence and observed $T_1$'s are in good agreement with theoretical predictions of such a relaxation process.

The slight increase in the $T_1$'s of all three isotopes in samples F and G relative to those in sample E in evidence of the incomplete delocalization of the electron system in the doping region immediately preceding the transition. This has been observed previously in Si:P[81] and SiC:N[82] and put down to the relative ineffectiveness of the

delocalized electrons compared with localized electrons in relaxing the host nuclei. A similar explanation was put forward to explain the weakening of the $T_1$ minima in samples D and E at high temperatures.

The temperature dependence of the $T_1$'s in sample G below $4.2^{\circ}K$ is greater than in the other samples, and could be further evidence of nuclear relaxation not totally dominated by spin-spin interactions. For the $P^{31}$ nuclei, $T_1 \propto T^{-0.51}$ which coincides with the temperature dependence expected for nuclear relaxation by nondegenerate electrons. This is unlikely at such low temperatures and it is probably due to some temperature dependence associated with the antiferromagnetic ordering discussed in section 8.10.

## 8.12 Relative magnitudes of the $Ga^{69}$ and $Ga^{71}$ $T_1$'s

The changes which are observed in the relative magnitudes of the $T_1$'s of the two Ga isotopes with temperature and concentration in our samples can be understood in terms of the relative differences in their spin diffusion coefficients, gyromagnetic ratios, and electric quadrupole moments, and a knowledge of the conditions under which each plays a dominant role in determining the bulk nuclear relaxation rate.

As discussed in section 8.2, at high temperatures nuclear relaxation is dominated by quadrupolar interactions between the nuclear quadrupole moments and fluctuating electric field gradients produced by distortions of the crystal lattice by defects, impurities and phonons. Because of this, $Ga^{69}$ nuclei, having the larger quadrupole moments, results in $T_1(Ga^{69}) < T_1(Ga^{71})$ at room temperature in all samples. As the temperature is lowered, magnetic interactions with the electron system begin to dominate and, since the strength of this interaction is proportional to $\gamma_n^2$, one would expect the $Ga^{71}$ relaxation rate to become greater than that of the $Ga^{69}$ nuclei. In fact, in samples A, B and C $T_1(Ga^{69}) < T_1(Ga^{71})$ down to $25^{\circ}K$, and this can be explained in terms of the dominance of diffusion limited relaxation to paramagnetic

Te donors in these samples around the $T_1$ minima. $D(Ga^{69}) > D(Ga^{71})$ and hence $T_1(Ga^{69}) < T_1(Ga^{71})$ despite the latter's greater $\gamma_n$.

At helium temperatures in samples A, B and C, the dominance of spin-spin interactions over spin-lattice interactions in the electron system and the greater values of b and ρ have the effect of reducing the importance of spin diffusion in determining $T_1$ and as a result $T_1(Ga^{71}) < T_1(Ga^{69})$. With increasing donor concentration spin diffusion becomes of secondary importance at progressively higher temperatures and in sample D, $T_1(Ga^{69}) < T_1(Ga^{71})$ at the $T_1$ minimum only in the non-quadrupolar regime. Again the diffusion vanishing theory might be more applicable around the $T_1$ minimum in samples D and E.

The dominance of magnetic interactions with free or strongly interacting bound electrons in samples F and G below 150°K is evidenced by the fact that $T_1(Ga^{71}) < T_1(Ga^{69})$ and no minima are observed in the $T_1$:T curves of both Ga nuclei below this temperature.

From equations 4.3.3 and 4.3.4 we can deduce that if nuclear relaxation is dominated by scalar contact with free electrons, then $T_1 \propto \gamma_n^{-2}$. Neglecting differences in diffusion coefficients, for rapid diffusion relaxation we have that $T_1 \propto \gamma_n^{-7/3}$ while for diffusion limited relaxation $T_1 \propto \gamma_n^{-\frac{1}{2}}$. For a diffusion vanishing case $T_1 \propto \gamma_n^{-1}$.

The ratios $\frac{T_1(Ga^{69})}{T_1(Ga^{71})}$ at 4.2°K for all samples are presented in table 8.12.1.

Table 8.12.1

| Sample | A | B | C | D | E | F | G |
|---|---|---|---|---|---|---|---|
| $\frac{T_1(69)}{T_1(71)}$ | 1.28 ±0.13 | 1.17 ±0.14 | 1.26 ±0.14 | 1.66 ±0.17 | 1.67 ±0.18 | 1.58 ±0.10 | 1.60 ±0.10 |

$$\frac{\gamma_n(Ga^{71})}{\gamma_n(Ga^{69})} = 1.27 , \qquad \left(\frac{\gamma_n(Ga^{71})}{\gamma_n(Ga^{69})}\right)^2 = 1.62 .$$

Therefore we can see that at 4.2°K, in samples A, B, and C, the two Ga isotopes have $T_1$'s whose ratios correspond approximately with those expected from a diffusion vanishing case of nuclear relaxation to paramagnetic centres. In samples D, E, F, and G however, the $T_1$ ratios are more in line with rapid diffusion or scalar contact relaxation.

These results fit in well with the $T_1$ behaviour below 4.2°K in our samples. As expected in the diffusion vanishing regime, $T_1$ is only weakly temperature dependent. In the rapid diffusion or scalar contact dominating relaxations, $T_1$ has a temperature dependence inherent in the expressions for b, the barrier radius, and $T_1 \propto T^{-1}$ or $T^{-\frac{1}{2}}$ respectively.

Jerome et al[83] have proposed a model for nuclear relaxation in doped semiconductors near the metallic transition in which they assume the system to be made up of regions of semiconducting and impurity-banded tunnel regions produced by macroscopic doping inhomogeneities. They assume that nuclear spins in or near the impurity band tunnels are strongly relaxed by conduction electrons, while the remaining spins are relaxed by rapid diffusion to localized paramagnetic centres.

Spin diffusion away from the impurity banded regions is restricted due to the large local magnetic field shifts produced at nuclear sites by the polarized quasi-free electron system in such regions, and this results in an enhancement of the size of the barrier radius around localized paramagnetic centres. The size of the barrier radius depends directly on the polarization of the conduction electrons and this has a Curie-law dependence.

Therefore, as $T \propto b^{-3}$ in the rapid diffusion case and $b \propto \left(\frac{H}{T}\right)^{1/3}$, the increasing temperature dependence and the observed $T_1$ ratios of the $Ga^{69}$ and $Ga^{71}$ nuclei as the doping densities in our samples approach the metallic transition is qualitatively explained.

## 8.13 16 Mc/s $T_1$ measurements

$T_1$ measurements were made at liquid nitrogen temperatures in samples B and C at 16 Mc/s in an attempt to determine the frequency dependence of the position and depth of the $T_1$ minima in our samples. The cryostat used during this part of the project did not have the variable temperature facilities incorporated in the 6.5 Mc/s equipment, and so measurements were limited to the temperature range 77°K to 63.5°K. This range could be attained by pumping on liquid nitrogen. Samples B and C were studied as they were the only samples whose $T_1$ minima were likely to lie in this temperature range. The $T_1$ measurements for both samples are shown in Figs. 8.13.1, 8.13.2, and 8.13.3 along with $T_1$ results at 6.5 Mc/s and 10 Mc/s.

In sample B, the $Ga^{69}$ and $Ga^{71}$ $T_1$ results between 77°K and 63.5°K are almost identical to those obtained at 6.5 Mc/s except for a small high temperature shift at the $T_1$ minimum to $(6.5 \pm 1)$°K. Similar results were obtained for sample C but no distinct minima observed.

The lack of any substantial temperature variation in the position of the $T_1$ minimum with frequency is strong evidence for a field independence, and large temperature dependence, in the electron spin-lattice relaxation process for our lightly doped samples. As the $T_1$ minimum $\omega\tau = 1$, and hence we can say that,

$$\text{at the minimum} \quad \frac{\tau(6.5 \text{ Mc/s})}{\tau(16 \text{ Mc/s})} = 2.46 \ .$$

Therefore in sample B, the electron spin-lattice relaxation time varies by a factor of 2.46 between $60 \pm 1$°K and $65 \pm 1$°K. Because of the $\pm 1$°K error in measuring both these temperatures, the exact magnitude of the temperature dependence cannot be deduced accurately but it roughly corresponds to $\tau \propto T^{12\pm4}$. Such a temperature dependence has been observed in other doped semiconductors, and it is in good agreement with the $\tau \propto T^{11}$ dependence deduced from the e.s.r. linewidths

Fig. 8.13.1 $Ga^{69}$

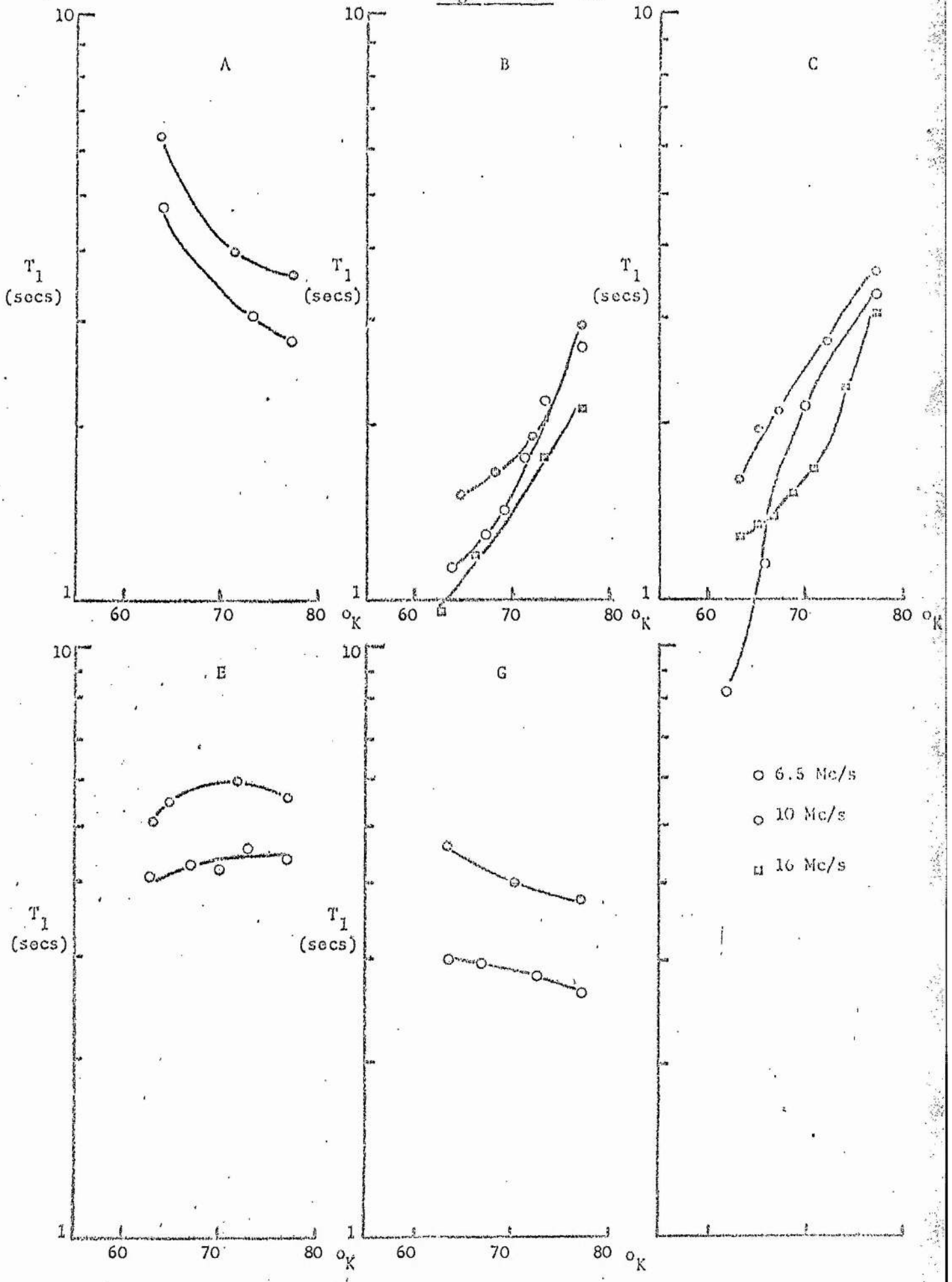

Fig. 8.13.2 $Ga^{71}$

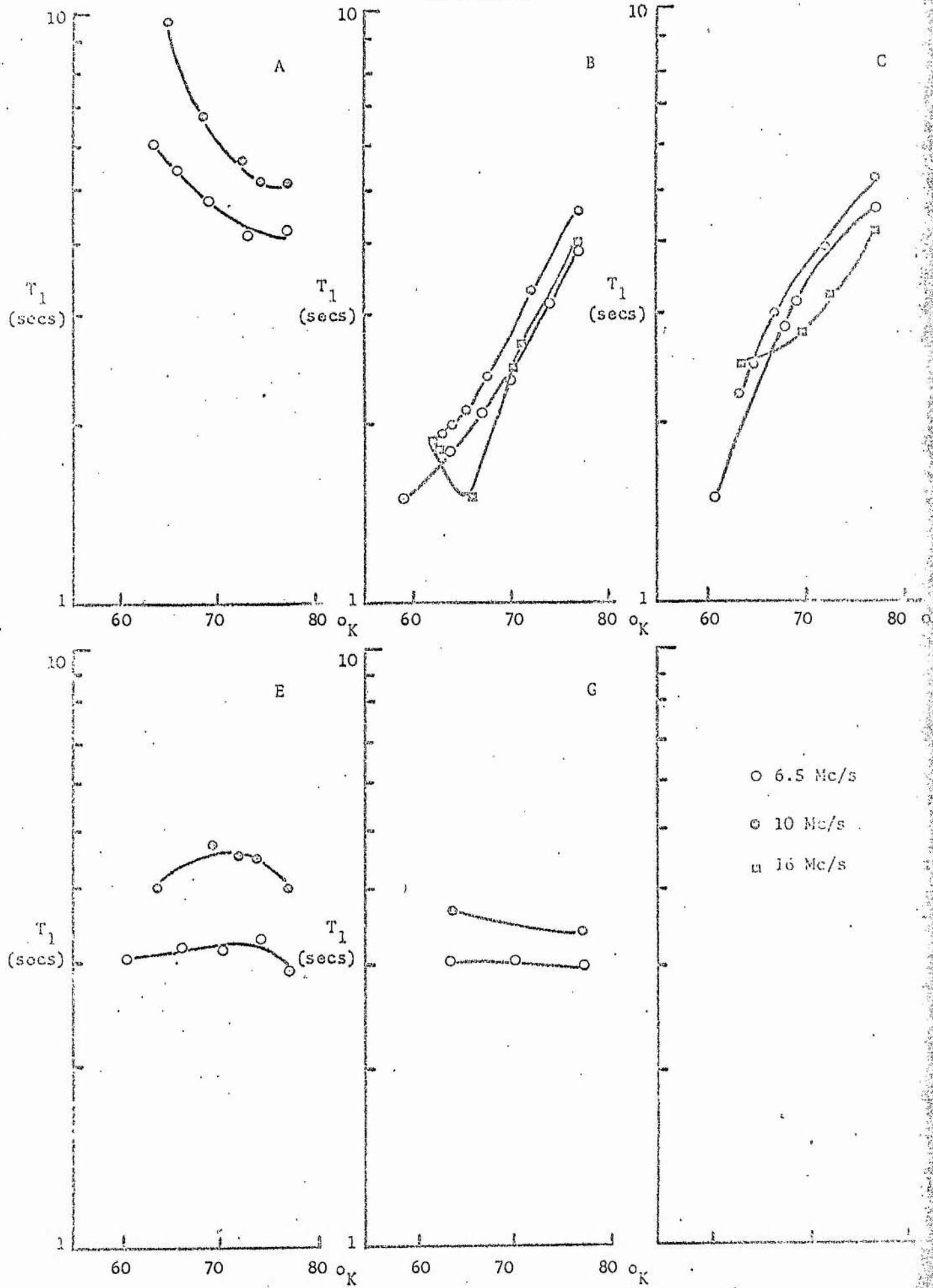

Fig. 8.13.3 P31

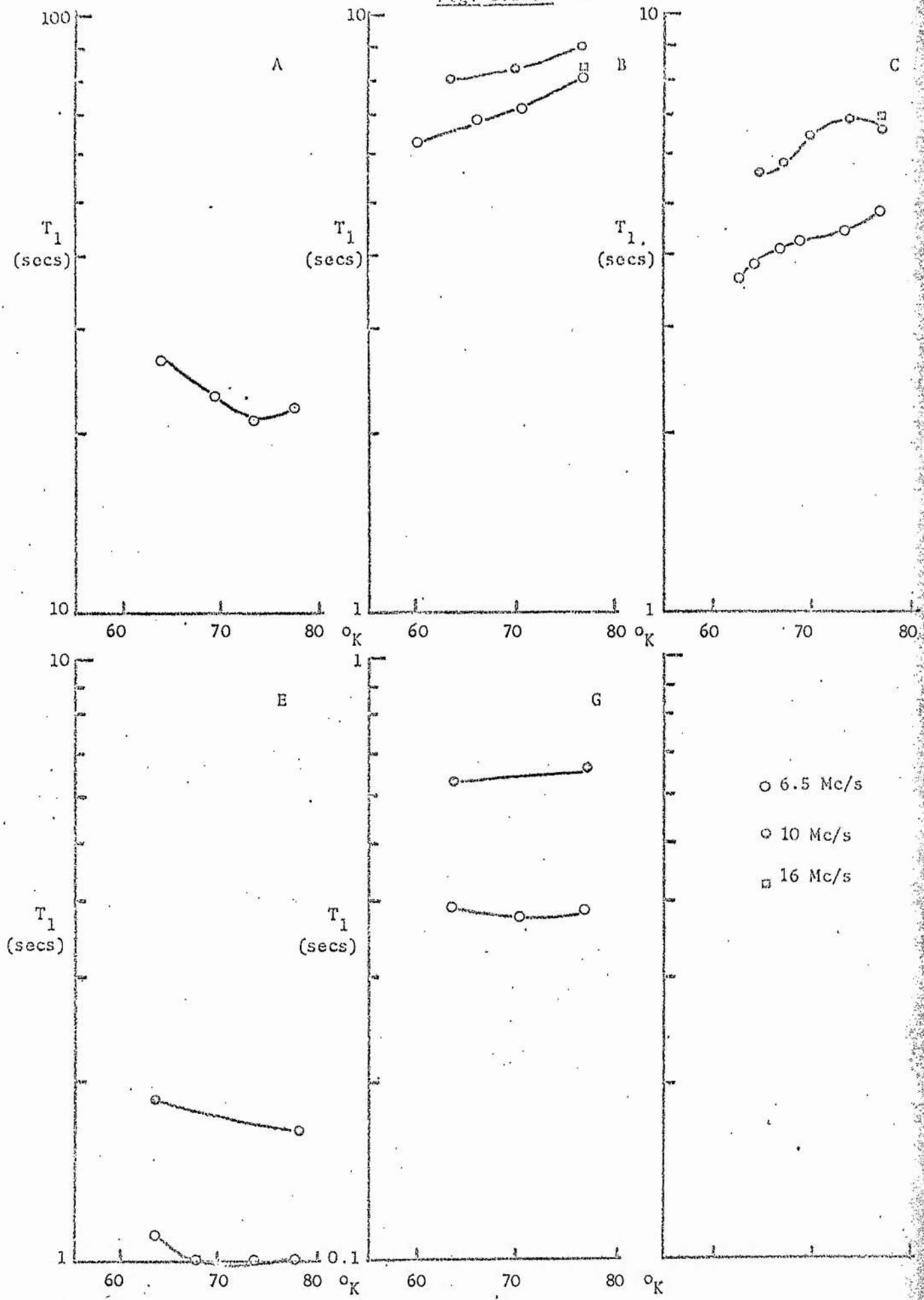

of Thomson and Lancaster[28] in GaP:Te.

We have suggested an Orbach process as a possible electron relaxation mechanism in these samples, and for such a process

$$\frac{\tau_1}{\tau_2} = \frac{e^{\Delta/kT_1}}{e^{\Delta/kT_2}} = e^{\frac{\Delta}{k}(\frac{1}{T_1} - \frac{1}{T_2})} \quad . \qquad 8.13.1$$

Assuming $\Delta$ is field independent, we can use equation 8.13.1 to obtain a value of $\Delta$ from the positions of the $T_1$ minima at 6.5 Mc/s and 16 Mc/s in sample B. Substituting for $\tau$ and T in this equation, we deduce that $\Delta = 57 \pm 22$ meV which is approximately equal to the ionization energy of the Te donor level in our lightly doped samples.

The absence of any appreciable frequency dependence in the Ga $T_1$'s on the high temperature side of the $T_1$ minimum in samples B and C is further evidence for a diffusion limited process for which $T_1 \propto H^0$ above, $T_1 \propto H^{\frac{1}{4}}$ at, and $T_1 \propto H^{\frac{1}{2}}$ below the $T_1$ minimum. One $P^{31}$ $T_1$ measurement was made at 77°K in sample C and it was found that its value was appreciably larger than that obtained at 6.5 Mc/s indicating that some mechanism other than diffusion-limited relaxation was effective. As a similar $P^{31}$ $T_1$ measurement at 77°K in sample B did not reveal a similar increase over the 6.5 Mc/s value it would be unwise to attempt an interpretation of these two conflicting results without first repeating the measurements. Unfortunately, as the main reason for undertaking these high temperature 16 Mc/s measurements was to study the variation of the position of the minimum in the Ga $T_1$'s, no time was available to do this.

## 8.14 16 Mc/s $T_1$ measurements at 4.2°K

$T_1$ measurements were made at 4.2°K at 16 Mc/s in samples B to G and the results are presented in Fig. 8.14.1. The concentration dependences of the three isotopes in samples B to E were found to be the following,

Fig. 8.14.1

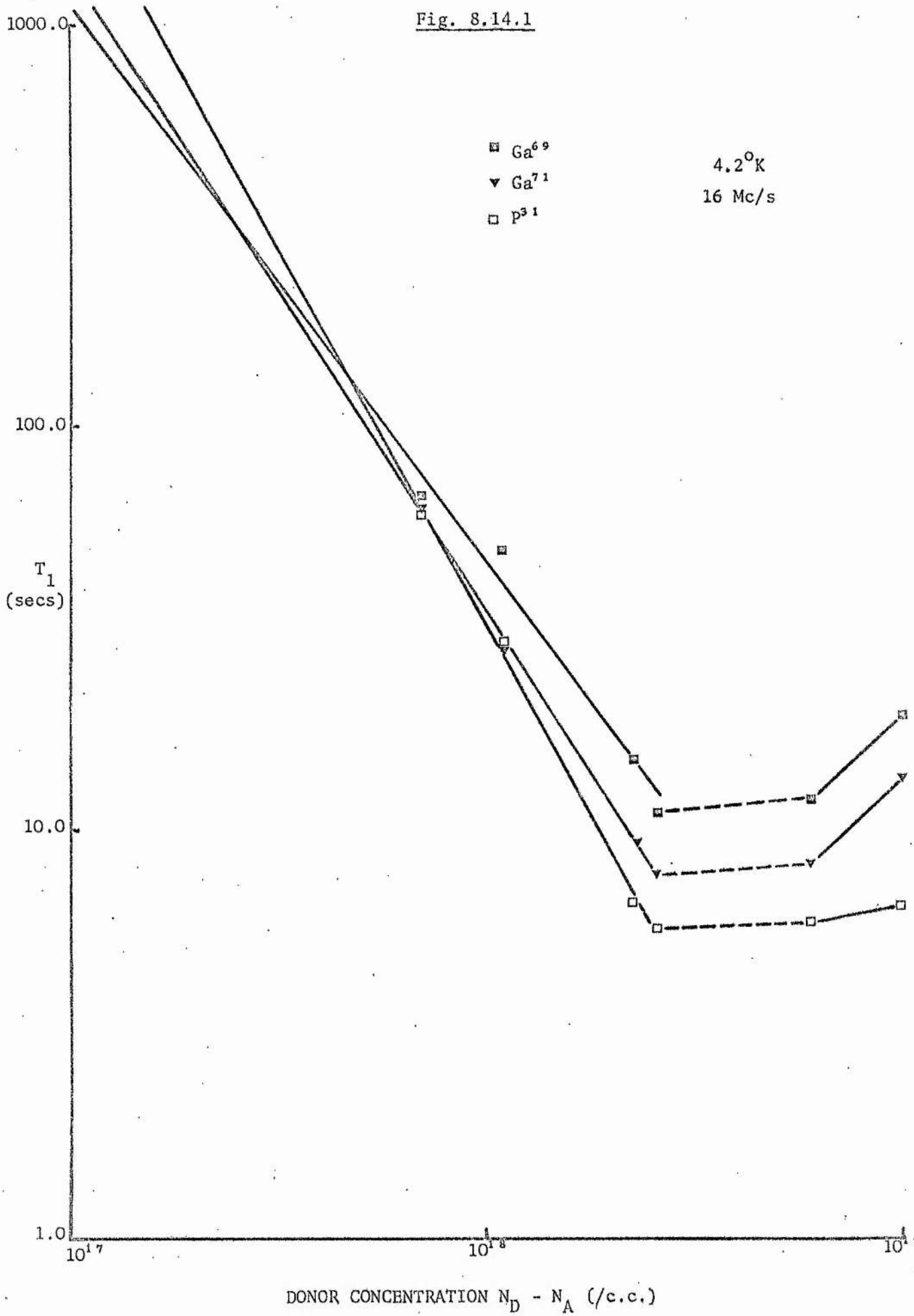
1000.0
100.0
10.0
1.0
$T_1$ (secs)
$Ga^{69}$
$Ga^{71}$
$P^{31}$
4.2°K
16 Mc/s
$10^{17}$
$10^{18}$
$10^{19}$
DONOR CONCENTRATION $N_D - N_A$ (/c.c.)

$$\text{For } Ga^{69}, \quad T_1 \propto N^{-(1.43 \pm 10)}$$

$$\text{For } Ga^{71}, \quad T_1 \propto N^{-(1.62 \pm 0.10)}$$

$$\text{For } P^{31}, \quad T_1 \propto N^{-(1.89 \pm 0.10)}$$

which are in good agreement with the concentration dependences observed at 6.5 Mc/s and discussed in section 8.11. The ratios of the $T_1$'s at 6.5 Mc/s and 16 Mc/s for all three isotopes in samples B to G at 4.2°K are presented in table 8.14.1.

Table 8.14.1

| Sample | B | C | D | E | F | G |
|---|---|---|---|---|---|---|
| $\frac{T_1(16)}{T_1(6.5)}_{P^{31}}$ | 2.20 ±0.22 | 2.36 ±0.23 | 2.40 ±0.12 | 2.60 ±0.13 | 2.86 ±0.14 | 2.89 ±0.15 |
| $\frac{T_1(16)}{T_1(6.5)}_{Ga^{69}}$ | 1.89 ±0.19 | 2.51 ±0.32 | 2.45 ±0.24 | 2.04 ±0.21 | 1.91 ±0.19 | 2.03 ±0.20 |
| $\frac{T_1(16)}{T_1(6.5)}_{Ga^{71}}$ | 2.07 ±0.21 | 1.80 ±0.30 | 2.50 ±0.25 | 2.33 ±0.23 | 2.08 ±0.21 | 2.08 ±0.21 |

Only the $P^{31}$ $T_1$'s display an increasing magnetic field dependence with increasing impurity concentration expected as a result of the polarization of the quasi-free electron system around paramagnetic centres discussed in section 8.12. For the $Ga^{69}$ and $Ga^{71}$ $T_1$'s, the field dependence does not display such a simple variation with concentration and the experimental errors forbid any detailed analysis of the observed ratios. However, of all the theoretical field dependences discussed in section 8.12, the diffusion vanishing case, for which $T_1 \propto H^1$, appears to be in best agreement with our results at 4.2°K.

## 8.15 10 Mc/s $T_1$ measurements

$T_1$ measurements were made at 10 Mc/s on all three isotopes in samples A, B, C, E, and G between 63.5°K and 77°K. These measurements

Fig. 8.16.1

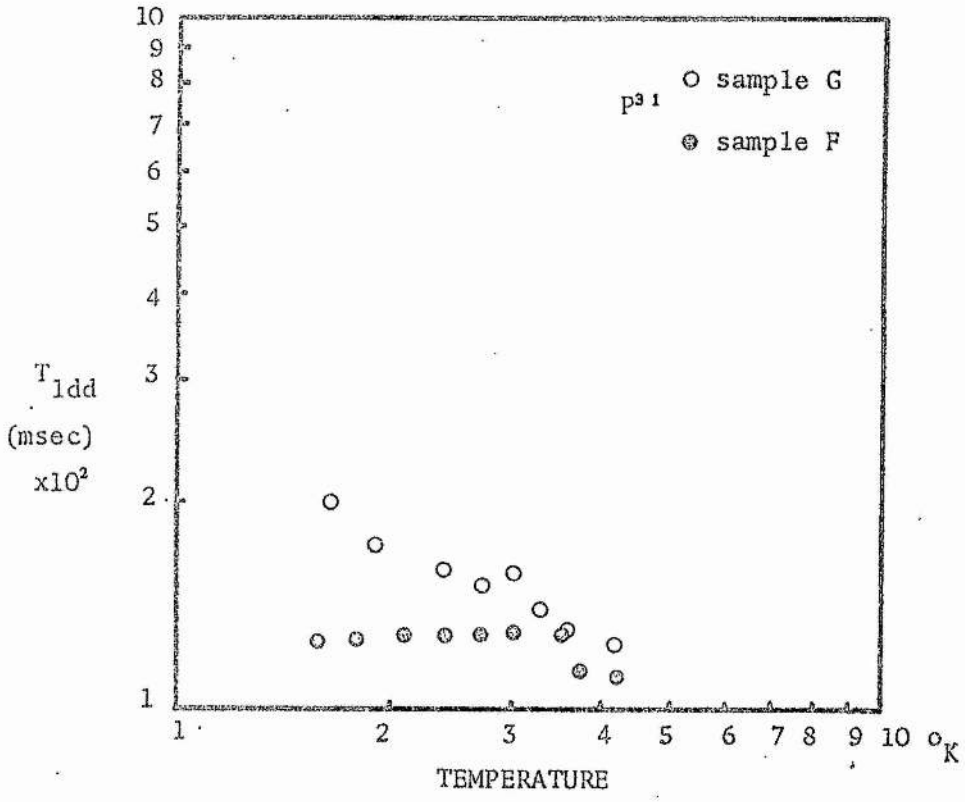
10
9
8
7
6
5
4
3
2
1
$T_{1dd}$
(msec)
x10²
p³₁
sample G
sample F
1
2
3
4
5
6
7
8
9
10
°K
TEMPERATURE

were made before samples D and F were obtained whilst samples B and C were in the form of small discs stacked on top of each other. It was later found that anisotropic effects would be present, resulting in the $T_1$ measurements from the disc like samples being larger by as much as 20% than the true isotropic $T_1$ obtained from a powdered specimen. No time was available to repeat these measurements but the original $T_1$ values plus the $T_1$'s for the other, crushed samples are presented here in Figs. 8.13.1, 8.13.2, and 8.13.3.

In sample A, the two Ga $T_1$'s differ appreciably from the data obtained at 6.5 Mc/s but do display similar short time non-exponentialities whose size diminish away from the minimum. The data at 6.5 Mc/s and 10 Mc/s are in good agreement with the $T_1 \propto H^{\frac{1}{4}}$ behaviour expected for a diffusion limited process below the $T_1$ minimum.

Despite the systematic error introduced into the 10 Mc/s data for samples B and C it can be seen that the $Ga^{69}$ and $Ga^{71}$ $T_1$ data at 6.5 Mc/s, 10 Mc/s, and 16 Mc/s in this small temperature range, correspond well with the field independent relaxation expected for a diffusion limited process above the minimum. Again non-exponentialities were observed in the $T_1$ decays.

The $P^{31}$ $T_1$ data in samples C, E and G and the $Ga^{69}$ and $Ga^{71}$ data in samples E and G lend strong support to the theory of nuclear relaxation becoming dominated by a field dependent mechanism as the doping density increases. The onset of this field dependent mechanism coincides with the crossing of the $Ga^{69}$ and $Ga^{71}$ curves above the $T_1$ minimum and could be due to the polarization of free electrons around paramagnetic impurities as described in section 8.12.

## 8.16 Dipolar Relaxation Times

The dipolar relaxation times, $T_{1dd}$, of the $P^{31}$ nuclei in samples F and G were measured between 4.2°K and 1.8°K at 6.5 Mc/s using the Jeener[69] technique and the results are presented in Fig. 8.16.1.

Measurements were also made in sample G at 27°K, 47°K and 77°K, and in sample E at 4.2°K. The values of $T_{1z}/T_{1dd}$ in these samples at the various temperatures are presented in table 8.16.1.

Table 8.16.1

| Sample | 1.8°K | 4.2°K | 27°K | 47°K | 77°K |
|---|---|---|---|---|---|
| E | | 18±1 | | | |
| F | 21±1 | 19±1 | | | |
| G | 18±1 | 18±1 | 16±3 | 13±3 | 10±1 |

Large non-exponentialities were observed in the $T_{1dd}$ magnetization decay at all temperatures.

It was originally thought that a study of the $T_{1z}/T_{1dd}$ ratios in samples F and G might reveal information about correlation effects in the non-localized electron system in these samples. For a degenerate electron system relaxing spin ½ nuclei by scalar contact interaction, $T_{1z}/T_{1dd}$ lies between 2 and 3 depending on the amount of electron correlation.

However the observation of large ratios experimentally in samples E, F and G suggest two possibilities. Firstly, in these samples nuclear relaxation to single or clusters of paramagnetic centres is still important. We have deduced that this is so for nuclear relaxation in the Zeeman reservoir, and the fact that the observed $T_{1dd}$'s display a similar temperature dependence to the $T_1$'s suggests that both relaxations occur via the same mechanism.

Secondly, in the dipolar reservoir the $P^{31}$ spin system and the two Ga spin systems are intrinsically mixed. The observed dipolar relaxation rate is therefore a combination of the relaxation rates of all three spin systems with the one with the largest relaxation rate dominating the others. Therefore, if the dipolar relaxation rate in either or both of the Ga spin systems is more rapid than in the $P^{31}$

system, the observed $T_{1dd}$ for the $P^{31}$ system is artificially shortened. Considering the large $T_{1z}/T_{1dd}$ ratios still observed in sample G, at $77^{o}K$ where most of the paramagnetic centres will be ionized, it is most probable that this latter explanation provides the main reason for the large $T_{1z}/T_{1dd}$ ratios observed in samples E, F and G.

## 8.17 Knight Shift, K

No Knight shift was observed at 16 Mc/s for the $P^{31}$ nuclei in sample G relative to sample A at $4.2^{o}K$ and $77^{o}K$. Given that the experimental uncertainty was 0.25 gauss, the Knight shift must be less than $2.7.10^{-5}$. This is an order of magnitude smaller than the value expected for a degenerate electron system at the metallic transition, as calculated from the Korringa relation. This relation links $T_1$, T and K such that

$$T_1 \, T \, K^2 = \frac{\hbar \gamma_e^2}{4\pi k \gamma_n^2} . \qquad 8.17.1$$

In order to obtain the rough estimate of K at the metallic transition mentioned above, the measured $T_1$'s of the $P^{31}$ nuclei in sample G at $4.2^{o}K$ and $77^{o}K$ were substituted into equation 8.17.1. The very small Knight shift found experimentally implies that even in sample G, at low temperatures there is only a small density of electrons sufficiently delocalized to influence the resonant field of the bulk nuclei.

## 8.18 Summary

In this chapter, the n.m.r. measurements made in samples A to G have been discussed, and analysed, in terms of the various mechanisms thought responsible for nuclear relaxation in GaP:Te over the ranges of temperature, magnetic field, and impurity concentration studied during this work.

It was found that the temperature variation of the nuclear relaxation times $T_1$ of the $Ga^{69}$ and $Ga^{71}$ isotopes in all samples at

high temperatures agreed well with those expected from nuclear relaxation dominated by quadrupolar interactions. The observed average ratio of the $Ga^{69}$ to $Ga^{71}$ $T_1$'s at 300°K was 2.41 ± 0.14, which is in good agreement with the theoretical value of 2.52, that being the value of the ratio of the squares of the $Ga^{69}$ and $Ga^{71}$ quadrupole moments.

Additional low temperature structure was observed in the $T_1$:T curves of all samples and this was associated with nuclear relaxation by spin diffusion to the paramagnetic donor impurities in our samples. The $T_1$ minima observed in samples A to E were associated with a resonant coupling between the magnetic moments of the Te donor centres and those of the host nuclei when $\omega\tau = 1$. The existence of short-time non-exponentialities in the magnetization recovery of the two Ga isotopes after initial saturation suggested the dominance of diffusion-limited relaxation in these two spin systems around the $T_1$ minima.

Values of the nuclear spin diffusion coefficients of $2.8 \pm 1.0.10^{-12}$ $cm^2/sec$ for $Ga^{69}$, and $6.7 \pm 3.9.10^{-13}$ $cm^2/sec$ for $Ga^{71}$, were calculated from the variation of $T_1$ at the minimum with donor concentration in samples A, B and C. The values obtained from the simple theoretical expression, $D = a^2/13.5\ T_2$, were $1.8.10^{-12}$ $cm^2/sec$ for $Ga^{69}$, and $3.0.10^{-12}$ $cm^2/sec$ for $Ga^{71}$. The observed discrepancies between the theoretical and experimental values suggest some weakness in spin diffusion theory applied to systems containing more than one abundant spin species.

Calculations of the spin diffusion barrier radii and pseudopotential radii for all three isotopes around the $T_1$ minima were made, and shown to agree with the values expected for diffusion limited relaxation in the two Ga systems, and rapid diffusion in the $P^{31}$ system. It was suggested that an enhancement of the barrier radius for $P^{31}$ nuclei around each Te donor should occur due to the preferential distribution of the donor wavefunction on $P^{31}$ sites.

The movement of the $T_1$ minima to lower temperatures with increasing donor concentration was taken as indirect evidence of a reduction in the Te donor ionization energy $E_D$, with increasing donor concentration. As the resonant condition $\omega\tau = 1$ held at the minimum, and various possible donor electron relaxation processes displayed an exponential dependence on $E_D$, the movement of the $T_1$ minima to lower temperatures reflected the variation in $E_D$. Assuming an Orbach or scattering process to be the dominant donor electron relaxation mechanism, estimates of $E_D$ were made from the variation of $T_1$ with temperature on both sides of the minima in samples A, B and C. The values obtained from the two sets of Ga data were 82 ± 25 meV, 72 ± 40 meV, and 58 ± 40 meV respectively, which are in reasonable agreement with the values of the Te donor ionization energy observed by other authors in this concentration range.

Consistently low values of $E_D$ were obtained from analysis of the $P^{31}$ data and this suggested the existence of an additional relaxation mechanism for the $P^{31}$ nuclei. Enhanced scalar contact interaction between the donor electron and the $P^{31}$ nuclei around each impurity was put forward as an explanation for this discrepancy, and also as a possible reason for the almost temperature independent $P^{31}$ $T_1$'s observed at high temperatures in all samples.

The weakening of the $T_1$ minima and its rapid movement to lower temperatures in samples D and E was taken as evidence of the onset of impurity hopping and a reduction in the effectiveness of nuclear relaxation to single paramagnetic Te donors. The cross-over of the $Ga^{69}$ and $Ga^{71}$ $T_1$'s in these samples near the minima was consistent with the existence of diffusion-vanishing relaxation while the absence of any observable $P^{31}$ $T_1$ minima was interpreted as being a result of the dominance of scalar contact interactions over dipolar interactions for $P^{31}$ nuclei near the Te donors.

The washing out of the $T_1$ minima of all three isotopes in samples F and G was taken as firm evidence of the strong electron correlation

and hopping effects expected at donor concentrations of $10^{19}$/c.c. and above. Furthermore, the impurity hopping time of $10^{-10}$ seconds, calculated from the single conductivity measurement made at 4.2°K in sample G, confirms the failure to observe any minima to be due the resonant condition $\omega\tau = 1$ not being satisfied.

In order to explain the temperature dependent $T_1$'s observed at low temperatures in samples E to G, Quirt and Marko's model of an amorphous antiferromagnet phase in the donor electron system preceding the metallic transition was discussed in terms of the effects it would have on nuclear relaxation. It was decided that the preferential alignment of electron magnetic moments, resulting from such a model, would provide a qualitative explanation for the observed low temperature behaviour in samples E to G.

$T_1$ results in all samples below 4.2°K displayed very weak temperature dependences and the concentration dependence of the $Ga^{69}$, $Ga^{71}$, and $P^{31}$ $T_1$'s of samples A to E at 4.2°K were $T_1 \propto N^{-(1.46\pm0.05)}$, $T_1 \propto N^{-(1.59\pm0.10)}$, and $T_1 \propto N^{-(1.85\pm0.10)}$ respectively.

The differences in concentration dependence of the three isotopes was taken as tentative evidence for restricted spin diffusion in the two Ga systems taking them into the diffusion limited regime, while the anisotropic barrier radius in the $P^{31}$ system took it into the diffusion vanishing regime. A theoretical calculation of the $T_1$'s expected in a system in which spin-spin interactions between donor electrons were important was made, and found to be in good agreement with the $T_1$'s observed in our samples. The increase in $T_1$ in samples F and G relative to samples D and E at 4.2°K reflected the incomplete delocalization of the electron system near the metallic transition.

From comparison of the temperature of the $T_1$ minimum in sample C at 16 Mc/s with that at 6.5 Mc/s, a further estimate of the donor ionization energy in this sample was obtained. The value of 57 ± 22 meV so obtained was in good agreement with that obtained from analysis of

the $T_1$:T curves on both sides of the minima. Comparison of the $T_1$'s obtained at 6.5 Mc/s, 10 Mc/s and 16 Mc/s around the $T_1$ minima in samples A, B, and C lends support to our description of nuclear relaxation dominated by diffusion limited and rapid diffusion processes in the Ga and P systems respectively.

The concentration dependences of the $T_1$'s in samples A to E at $4.2^{\circ}K$ at 16 Mc/s were as follows; $T_1 \propto N^{-(1.43\pm0.10)}$ for $Ga^{69}$, $T_1 \propto N^{-(1.62\pm0.10)}$ for $Ga^{71}$, and $T_1 \propto N^{-(1.89\pm0.10)}$. These are in excellent agreement with the dependences observed at 6.5 Mc/s and, along with the magnetic field dependences calculated from the two sets of data, lend strong support to our previous description of nuclear relaxation in these samples. In samples F and G a stronger magnetic field dependence of $T_1$ was observed and this was discussed in terms of Jerome's model of nuclear relaxation in heavily doped semiconductors. In this model, $T_1$ is dependent on the polarization of the conduction electron cloud formed around clusters of paramagnetic centres to which nuclear energy diffuse.

Finally, the absence of any measurable Knight shift in sample G relative to sample A at $4.2^{\circ}K$ and the existence of large $T_{1z}/T_{1dd}$ ratios at low temperatures in samples F and G, was taken as further evidence of the importance of the presence of paramagnetic impurities on nuclear relaxation in even the most heavily doped samples.

# CHAPTER IX

## CONCLUSION

A study has been made of seven, L.E.C. grown, tellurium doped gallium phosphide samples using pulsed n.m.r., Hall effect, and related measurements. From analysis of the results obtained by these techniques, and their correlation with n.m.r., e.s.r., electron susceptibility, and transport measurements made in similar systems, the changes which occur in the donor electron system in the intermediate doping region preceding the metallic transition have been studied. The effects which these changes have on the nuclear relaxation times of the host nuclei have been discussed in terms of the various stages of nuclear relaxation by spin diffusion to paramagnetic impurities.

In the lightly doped samples, rapid diffusion and diffusion limited relaxation processes have been identified around the minima in the $T_1$:T curves of the $P^{31}$, and two Ga isotopes respectively. In discussing differences in the relaxation behaviour of the $P^{31}$ and two Ga spin systems in the same samples, reference has been made to the effect on nuclear relaxation of the preferential distribution of the Te donor wavefunction on $P^{31}$ sites. Experimental calculations of the spin diffusion coefficients in the $Ga^{69}$ and $Ga^{71}$ spin systems have been made and compared with theoretical values derived from spin diffusion theory. The $T_1$ results from the more heavily doped samples have been discussed in terms of the various models of the state of the electron system in the intermediate doping region. Evidence of the increasing importance of electron spin-spin interactions and diffusion vanishing relaxation processes have been obtained from the concentration, magnetic field, and temperature dependences of the $T_1$'s of all three isotopes at low temperatures.

Hall and conductivity measurements reflected the reduction in donor ionization energy with increasing donor concentration in the intermediate doping region preceding the metallic transition, and the observed movement of the position of the $T_1$ minima to lower temperatures

in the same samples has been taken as further evidence of this effect. Calculations of the donor ionization energy have been made from analysis of the temperature dependence of the $Ga^{69}$ and $Ga^{71}$ $T_1$'s around the $T_1$ minima, and from the variation of the position of the minimum with frequency. The weakening and eventual disappearance of the $T_1$ minima in the most heavily doped samples have been discussed in terms of the reduction in the effectiveness of nuclear relaxation to single paramagnetic impurities as impurity hopping and spin-spin effects increase. Finally the enhanced magnetic field dependence and increase in $T_1$ observed, in the most heavily doped samples at low temperatures have been taken as evidence for the incomplete delocalization of the donor electron system in these samples.

## REFERENCES


[1]W. KOHN and J.M. LUTTINGER, (1955), Phys. Rev. 97, 883.

[2]J. HUBBARD, (1964), Proc. R. Soc. A. 277, 237.

[3]T.N. MORGAN, (1965), Phys. Rev. 139, A343.

[4]E.A. DAVIS and W. DALE COMPTON, (1965), Phys. Rev. 140, A2183.

[5]F.R. ALLEN and C.J. ADKINS, (1972), Phil. Mag. 26, 1027.

[6]H.C. CASEY, F. ERMANIS, and R.B. WOLFSTIRN, (1969), J. Appl. Phys. 40, 2945.

[7]N.F. MOTT, (1949), Proc. Phys. Soc. 62, 416.

[8]N.F. MOTT, (1972), Adv. Phys. 21, 785.

[9]P.W. ANDERSON, (1958), Phys. Rev. 109, 1492.

[10]FLETCHER, YAGER, PEARSON, HOLDEN, READ, and MERRITT, (1954), Phys. Rev. 94, 1392.

[11]G. FEHER, (1959), Phys. Rev. 114, 1219.

[12]S. MAEKAWA and N. KINOSHITA, (1965), J. Phys. Soc. Jap. 20, 1447.

[13]K. MORIGAKI and S. MAEKAWA, (1972), J. Phys. Soc. Jap. 32, 462.

[14]C.P. SLICHTER, (1955), Phys. Rev. 99, 479.

[15]A. HONIG, (1954), Phys. Rev. 96, 234.

[16]A. HONIG and J. COMBRISSON, (1956), Phys. Rev. 102, 917.

[17]A. ABRAGAM and J. COMBRISSON, (1956), Compt. Rend. 243, 576.

[18]G. FEHER, R.C. FLETCHER, and E.A. GERE, (1955), Phys. Rev. 100, 1784.

[19]L.M. ROTH, (1960), Phys. Rev. 118, 1534.

[20]H. HASEGAWA, (1960), Phys. Rev. 118, 1523.

[21]A. HONIG, (1959), Quantum Electronics Conference, Columbia University, New York.

[22]G. FEHER and E.A. GERE, (1959), Phys. Rev. 114, 1245.

[23]T.G. CASTNER Jr., (1963), Phys. Rev. 130, 58.

[24]D. PINES, J. BARDEEN, and C.P. SLICHTER, (1957), Phys. Rev. 106, 489.

[25]C.B. FINN, R. ORBACH, and W.P. WOLF, (1961), Proc. Phys. Soc. 77, 261.

[26]R.S. TITLE, (1967), Phys. Rev. 154, 668.

[27]S. HAROLDSON and C.G. RIBBING, (1969), J. Phys. Chem. Sols. 30, 2419.

[28]F. THOMSON and G. LANCASTER, (1970), B.R.S.G. Conference, Nottingham.

[29]S.J. BASS and P.E. OLIVER, (1968), J. Crys. Growth. 3, 286.

[30]E.P.A. METZ, R.C. MILLER, and R. MAZELSKY, (1962), J. Appl. Phys. 33, 2016.

[31]M.L. YOUNG and S.J. BASS, (1972), J. Appl. Phys. D. 4, 995.

[32]S.F. NYGREN, C.M. RINGEL, and H.W. VERLEUR, (1971), J. Elec. Chem. Soc. 118, 306.

[33]F. BLOCH, W.W. HANSON, and M.E. PACKARD, (1946), Phys. Rev. 69, 127.

[34]E.M. PURCELL, H.C. TORREY, and R.V. POUND, (1946), Phys. Rev. 69, 37.

[35]N. BLOEMBERGEN, (1949), Physica, 15, 386.

[36]A. ABRAGAM, (1961), Principles of Nuclear Magnetism, Clarendon Press, Oxford

[37]C.P. SLICHTER, Magnetic Resonance, Harper and Row, New York.

[38]M.A. RUDERMAN and C. KITTEL, (1953), Phys. Rev. 96, 99.

[39]N. BLOEMBERGEN, (1955), Report of the Bristol Conference on Defects in Crystalline Solids, Physical Society, London.

[40]R.V. POUND, (1950), Phys. Rev. 79, 685.

[41]J. van KRANENDONK, (1954), Physica, 20, 781.

[42]R.L. MIEHER, (1960), Phys. Rev. Lett. 4, 57.

[43]M.J. WEBER, (1961), J. Phys. Chem. Sols. 21, 210.

[44]N. BLOEMBERGEN, (1954), Physica, 11, 1130.

[45]B.V. ROLLIN, (1947), Nature, 160, 436.

[46]G.R. KHUTSISHVILI, (1957), Sov. Phys. - J.E.T.P. 4, 382.

[47]W.E. BLUMBERG, (1960), Phys. Rev. 119, 79.

[48]D. TSE and S.R. HARTMANN, (1968), Phys. Rev. Lett. 21, 511.

[49]G.R. KHUTSISHVILI, (1962), Sov. Phys. - J.E.T.P. 15, 909.

[50]A.G. RORSCHACH Jr., (1964), Physica, 30, 38.

[51]E.P. HORVITZ, (1971), Phys. Rev. B. 3, 2868.

[52]G.R. KHUTSISHVILI, (1966), Sov. Phys. - Uspekhi, 8, 743.

[53]J.H. van VLECK, (1948), Phys. Rev. 74, 1168.

[54]I.J. LOWE and S. GADE, (1967), Phys. Rev. 156, 817.

[55]G.R. KHUTSISHVILI, (1956), Proc. Inst. Phys. Acad. Sci. Georgia (SSR) 4, 3.

[56]P.G. de GENNES, (1958), J. Phys. Chem. Sols. 7, 345.

[57]I.J. LOWE and D. TSE, (1968), Phys. Rev. 166, 279.

[58]W.G. CLARK, (1964), Rev. Sci. Instr. 32, 554.

[59]D. BROWN, (1970), Ph.D. Thesis, (unpublished).

[60]I.J. LOWE and C.E. TARR, (1968), J. Phys. E. 1, 320.

[61]I.J. LOWE and C.E. TARR, (1968), J. Phys. E. 1, 604.

[62]E.H. PUTLEY, The Hall Effect and Related Phenomena, Semiconductor Monographs, London (1960).

[63]L.J. van der PAUW, (1958), Philips Research Reports. 13, 1.

[64]W. SCHOTTKY, (1942), Z. Phys. 118, 539.

[65]A.M. GOLDMAN, (1963), J. Appl. Phys. 34, 329.

[66]D. WIGHT, S.E.R.L. - Private Communication (1973).

[67]A. NARATH and D.W. ALDERMAN, (1966), Phys. Rev. 143, 328.

[68]E.R. ANDREW and D.P. TUNSTALL, (1961), Proc. Phys. Soc. 78, 1.

[69]J. JEENER and P. BROEKHART, (1961), Phys. Rev. 157, 232.

[70]B.C. JOHNSON and W.I. GOLDBURG, (1966), Phys. Rev. 145, 380.

[71]H.C. MONTGOMERY and W.L. FELDMANN, (1965), J. Appl. Phys. 36, 3228.

[72]H.C. MONTGOMERY, (1968), J. Appl. Phys. 39, 2002.

[73]A.S. EPSTEIN, (1966), J. Phys. Chem. Sols. 27, 1611.

[74]P.J. DEAN, J.D. CUTHBERT, D.G. THOMAS, and R.T. LYNCH, (1967), Phys. Rev. Lett. 18, 122.

[75]G.F. NEUMARK, (1972), Phys. Rev. B. 2, 408.

[76]A. ONTON and R.C. TAYLOR, (1970), Phys. Rev. B. 1, 2587.

[77]Y.L. YARNELL, J.L. WARREN, R.G. WENZEL, and P.J. DEAN, (1968), Proc. Conf. on Neutron Scattering.

[78]T.N. MORGAN, (1968), Phys. Rev. Letters, 21, 819.

[79]G.W. LEPPELMEIER and J. JEENER, (1968), Phys. Rev. 175, 498.

[80]C. YAMANOUCHI, K. MIZUGUCHI, and W. SASAKI, (1967), J. Phys. Soc. Jap. 22, 859.

[81]R.K. SUNDFORS and D.F. HOLCOMB, (1964), Phys. Rev. 136, A810.

[82]M.N. ALEXANDER, (1968), Phys. Rev. 172, 331.

[83]D. JEROME, C. RYTER, and J.M. WINTER, (1965), Physics, 2, 81.

[84]M.N. ALEXANDER and D.F. HOLCOMB, (1968), Rev. Mod. Phys. 40, 815.

[85]J.D. QUIRT and J.R. MARKO, (1973), Phys. Rev. B, 7, 3842.

[86]N.F. MOTT and E.A. DAVIS, Electronic Processes in Non-Crystalline Materials, Clarendon Press, London, 1971.

## APPENDIX I - MASS SPECTROGRAPHIC DATA

| CRYSTAL PULL | B | C | N | O | Al | Si | Cl | Cr | Mn | Fe | Zn | As | S |
|---|---|---|---|---|---|---|---|---|---|---|---|---|---|
| 172 | 0.1 | 10 | 1 | 2.5 | 0.2 | 2.8 | 0.5 | <0.01 | <0.01 | 0.07 | <0.02 | 0.04 | 2.2 |
| 175 | 2.0 | 9 | 5 | 2,5 | 10 | 95 | 0.8 | <0.01 | <0.01 | 0.04 | ≤0.05 | 0.2 | <0.3 |

APPENDIX II - D.C. ARC EXCITATION ANALYSIS

| Sample No. | Te | B | Hg | Mn | Pb | Fe | Bi |
|---|---|---|---|---|---|---|---|
| A | $<6.10^{18}$ | $1.4.10^{20}$ | $7.5.10^{19}$ | $<1.2.10^{18}$ | $3.5.10^{18}$ | $1.3.10^{19}$ | $7.3.10^{17}$ |
| B | $<6.10^{18}$ | $<7.10^{18}$ | $<7.5.10^{17}$ | $<1.2.10^{18}$ | $<3.5.10^{17}$ | $1.3.10^{19}$ | $3.6.10^{17}$ |
| C | $<6.10^{18}$ | $1.4.10^{19}$ | $<7.5.10^{17}$ | $2.4.10^{18}$ | $1.4.10^{19}$ | $2.6.10^{18}$ | $<3.6.10^{17}$ |
| D | $<6.10^{18}$ | $1.4.10^{19}$ | $<7.5.10^{17}$ | $1.2.10^{18}$ | $3.5.10^{18}$ | $2.6.10^{18}$ | $<3.6.10^{17}$ |
| E | $<6.10^{18}$ | $<7.10^{18}$ | $<7.5.10^{17}$ | $1.2.10^{18}$ | $3.5.10^{18}$ | $1.3.10^{18}$ | $<3.6.10^{17}$ |
| F | $1.2.10^{19}$ | $<7.10^{18}$ | $<7.5.10^{17}$ | $<1.2.10^{18}$ | $3.5.10^{18}$ | $2.6.10^{18}$ | $3.6.10^{17}$ |
| G | $2.4.10^{19}$ | $<7.10^{18}$ | $<7.5.10^{17}$ | $<1.2.10^{18}$ | $<3.5.10^{17}$ | $1.3.10^{18}$ | $<3.6.10^{17}$ |
| Periodic Table | VIA | IIIA | IIB | VIIB | IVA | VIII | VA |

< sign indicates that the concentration was below the limit of detectability of that particular element.

APPENDIX II - D.C. ARC EXCITATION ANALYSIS

| Sample No. | Al | Cu | Na | Zn | Ca | In | Cr | Sn |
|---|---|---|---|---|---|---|---|---|
| A | $5.6.10^{19}$ | $2.3.10^{19}$ | $1.3.10^{20}$ | $4.6.10^{18}$ | $7.5.10^{18}$ | $<6.10^{17}$ | $<1.4.10^{18}$ | $1.2.10^{19}$ |
| B | $<2.8.10^{18}$ | $2.3.10^{18}$ | $3.10^{19}$ | $1.1.10^{18}$ | $1.9.10^{19}$ | $2.6.10^{19}$ | $2.8.10^{18}$ | $<6.10^{17}$ |
| C | $5.6.10^{18}$ | $4.7.10^{19}$ | $6.10^{19}$ | $2.3.10^{18}$ | $3.8.10^{18}$ | $6.10^{18}$ | $<1.4.10^{18}$ | $2.5.10^{19}$ |
| D | $5.6.10^{18}$ | $1.1.10^{19}$ | $6.10^{19}$ | $4.6.10^{18}$ | $3.8.10^{18}$ | $6.10^{18}$ | $<1.4.10^{18}$ | $6.10^{18}$ |
| E | $1.1.10^{19}$ | $2.3.10^{18}$ | $6.10^{19}$ | $1.1.10^{18}$ | $1.9.10^{19}$ | $2.6.10^{18}$ | $2.8.10^{18}$ | $<6.10^{17}$ |
| F | $5.6.10^{18}$ | $2.3.10^{18}$ | $6.10^{19}$ | $1.1.10^{18}$ | $7.5.10^{19}$ | $6.10^{18}$ | $<1.4.10^{18}$ | $6.10^{18}$ |
| G | $5.6.10^{18}$ | $2.3.10^{18}$ | $6.10^{19}$ | $1.1.10^{18}$ | $1.9.10^{18}$ | $1.3.10^{18}$ | $<1.4.10^{18}$ | $<6.10^{17}$ |
| Periodic Table | IIIA | IB | IA | IIB | IIA | IIIA | VIB | IVA |

< sign indicates that the concentration was below the limit of detectability of that particular element